PRE-CHAMBER CHARGE STRATIFICATION OF A SPARK IGNITED INTERNAL COMBUSTION ENGINE

A thesis

submitted in fulfilment

of the requirements for the degree

of

MASTER OF ENGINEERING (MECHANICAL)

in the

University of Canterbury

by

IAN CALVERT

Department of Mechanical Engineering

University of Canterbury

Christchurch

NEW ZEALAND

February 1994

TO MUM AND DAD

ABSTRACT

This thesis details and reviews the development of a Pre-Chamber Stratified Charge Combustion System developed on a Ricardo E6/Mk6 single cylinder, variable compression, spark ignition research engine in the Thermodynamics Laboratory of the Mechanical Engineering Department at the University of Canterbury.

Operating a spark ignition engine on an overall lean charge has the potential to simultaneously reduce exhaust emissions and maintain good thermal efficiency. However, problems associated with ignition of the lean mixture to increased exhaust emissions and reduced thermal efficiency. Stratified charge engines offer the potential to overcome these ignition problems, and restore thermal efficiency and reduce exhaust emissions.

The stratified charge combustion process developed was centred around the separate injection of methane and air into a pre-chamber, located in an auxiliary spark plug hole in the cylinder head, to form an easily ignitable mixture which would establish a flame which would propagate through a lean mixture located in the main combustion chamber. Timing and duration of the injected methane was controlled electronically, whereas the air introduced into the pre-chamber was controlled by a metering valve and a check valve connected to the pre-chamber. The main charge to the engine was formed by using a gas carburettor.

ACKNOWLEDGEMENTS

First and foremost I would like to thank my project supervisor Dr Roger Green for providing me with a most interesting and rewarding project, as well as for much needed technical, administrative and personal guidance throughout the project duration.

To Messrs Ron Tinker and Eric Cox, many thanks for their practical advice and help in developing and debugging the test apparatus.

Thanks must also go to Mr O. Bolt for the use of the Departmental workshop and for the manufacture of equipment, Mr G.Leathwick for obtaining materials used in the project, and Mr J.Murphy for help with matters electronic.

A great deal of gratitude must be expressed towards my post-graduate colleagues, of whom there are too many to name, for much needed insight into problems relating to the project, as well as in not so formal matters.

Finally to Karin for all her support throughout the last few years, thank you.

The work undertaken led to the following conclusions:-

1, The equipment lean limit of combustion is extended by the charge stratification system.

2, The equipment lean limit of combustion for the charge stratification system is related to the flame propagation mechanisms, whereas the baseline engine equipment lean limit of combustion is related to the ignition and flame development mechanisms.

3, Combustion duration is reduced for the charge stratification system.

4, Brake thermal efficiency is reduced relative to the baseline system around the stoichiometric region, but is higher at leaner air/fuel ratios.

5, Hydrocarbon emissions for the charge stratification system are higher than baseline tests, but lower than the results of Zavier.[122]

6, Part load tests show similar improvements in combustion stability as in the wide open throttle tests, but also show the same reductions in brake thermal efficiency near stoichiometric operation, and increased hydrocarbon emissions.

TABLE OF CONTENTS

LIST OF TABLES vi

LIST OF FIGURES vii

LIST OF PLATES xii

NOMENCLATURE xiii

CHAPTER 1 AIR POLLUTION 1

1.1 INTRODUCTION 1

1.2 AIR POLLUTION 1

1.3 AUTOMOTIVE POLLUTION 3

1.3.1 Present emission standards. 4

1.3.2 Exhaust emission sources. 5

1.3.3 Pollutant Effects. 11

1.3.4 Initial Reduction Efforts. 15

CHAPTER 2 ALTERNATIVE ENGINE COMBUSTION TYPES. 19

2.1 INTRODUCTION. 19

2.2 LEAN BURN ENGINES. 19

2.3 STRATIFIED CHARGE ENGINES 23
2.3.1 Ford PROCO 23
2.3.2 Texaco TCCS 25
2.3.3 MAN FM 26
2.3.4 Porsche SKS 27
2.3.5 Volkswagen PCI 29
2.3.6 Honda CVCC 30
2.3.7 LAG Process 32
2.3.8 Pre-chamber Variations 35
2.4 PREVIOUS WORK AT THIS DEPARTMENT 38

CHAPTER 3 TURBULENCE AND COMBUSTION. 41
3.1 INTRODUCTION 41
3.2 TURBULENCE, SWIRL AND SQUISH. 41
3.2.1 Turbulence. 41
3.2.2 Swirl and tumble. 45
3.2.3 Squish. 47
3.3 FLOWS INSIDE THE CYLINDER. 48
3.4 COMBUSTION. 51
3.4.1 Flame Structure 51
3.4.2 Flame Propagation. 55
3.4.3 Bulk Quenching of the Flame. 63
3.4.4 Flame Structure inside the Engine. 65
3.4.5 Combustion within the Engine. 67

3.5 HYDROCARBON OXIDATION 70

3.5.1 Introduction 70

3.5.2 Chemical pathways 71

3.5.3 Reaction Regimes. 74

3.5.4 Methane oxidation 75

3.5.5 Methane as an automotive fuel. 77

CHAPTER 4 EXPERIMENTAL APPARATUS 81

4.1 INTRODUCTION 81

4.2 DESIGN PHILOSOPHY 81

4.3 ENGINE APPARATUS. 84

4.3.1 Pre-chamber Design 84

4.3.2 Test Engine. 85

4.3.3 Auxiliary Equipment 88

4.3.4 Fuel Supply System. 96

4.4 EXHAUST GAS ANALYSIS 99

4.4.1 Exhaust Gas Analysers. 99

4.4.2 Span Gas Mixtures 103

4.5 ENGINE DATA ACQUISITION 105

4.5.1 System inputs 105

4.5.2 Pressure Data 106

4.5.3 Pressure Trace Reference Point 107

CHAPTER 5 EXPERIMENTAL PROCEDURES 113

5.1 INTRODUCTION 113

5.2 CALIBRATION OF ROTAMETERS 113

5.3 CALIBRATION OF PRESSURE TRANSDUCER 117

5.4 CALIBRATION and USE of EXHAUST GAS ANALYSERS . 118

5.4.1 HORIBA MEXA-534 GE :- CO, CO_2, UHC,O_2 119

5.4.2 BECKMAN 951A NO/NOx Analyser. 121

5.5 PREPARATION OF NO/N_2 MIXTURES. 123

5.6 TEST ENGINE PREPARATION. 125

5.7 ENGINE TEST PROCEDURE 126

5.7.1 Baseline tests 127

5.7.2 Charge Stratification tests. 127

5.8 TEST DATA RECORDED 129

CHAPTER 6 DISCUSSION OF EXPERIMENTAL RESULTS 132

6.1 INTRODUCTION 132

6.2 INITIAL TRIALS 133

6.2.1 Air system trials. 133

6.2.2 System durability. 134

6.2.3 Errors associated with the system. 137

6.3 COMBUSTION SYSTEM OPTIMISATION. 138

6.3.1 Air System Optimisation. 140

6.3.2 Methane Injection Duration Optimisation. 144

6.3.3 Methane Injection Timing Optimisation. 148

6.4 ENGINE PERFORMANCE. 152

6.4.1 Extension of the equipment lean limit. 152

6.4.2 Emissions. 157

6.4.3 Performance. 163

6.4.4 IMEP Variations. 166

6.4.5 Part Load Operation. 167

6.4.5 Pre-chamber Combustion Characteristics. 170

CHAPTER 7 CONCLUSIONS 175

CHAPTER 8 RECOMMENDATIONS FOR FUTURE WORK 180

REFERENCES 181

APPENDICIES 203

A1 COMPUTER PROGRAMS 204

PRESANAL.BAS 205

RICPC.BAS 212

A2 NOx METER, GAS SYSTEM OPERATING INSTRUCTIONS. . . 217

A3 EQUATIONS OF STATE FOR ACCURATE GAS MIXTURES . . 219

A4 NO/N_2 GAS MIXTURE PREPARATION PROCEDURE 222

LIST OF TABLES

Table 1.1 Total man made and natural air pollution emissions. 3

Table 1.2 Selected present emission standards for spark ignition engines. 4

Table 1.3 Lead Content of Fuel. 5

Table 1.4 Engine design and operating variables affecting HC emissions. 18

Table 3.1 Thermodynamic properties of Methane. 78

LIST OF FIGURES

Figure 1,1 Pollution Concentrations vs Equivalence Ratio 12

Figure 2,1 Ford PROCO engine. 24

Figure 2,2 Texaco TCCS system. 26

Figure 2,3 MAN-FM system. 27

Figure 2,4 Porsche SKS system. 28

Figure 2,5 Volkswagen PCI system. 29

Figure 2,6 Honda CVCC system. 31

Figure 2,7 Honda Branched Conduit CVCC head. 32

Figure 2,8 LAG-process engine. 33

Figure 2,9 Pre-chamber excess air coefficient vs Temperature, Flame speed and Combustion delay time. (dP is the pressure differential across the torch passage) 34

Figure 3,1 Turbulent structure visualisation. 42

Figure 3,2 Intake flow visualisation. 47

Figure 3,3 Scheme of a Plane Combustion Wave. 52

Figure 3,4 Chomiak's turbulent flame visualisation. 62

Figure 3,5 Mass fraction burned as a function of crank angle. 68

Figure 3,6 Methane reaction path schematic. 77

Figure 3,7 Flame speeds of methane and various fuels. 80

Figure 4,1 Methane Injector Non-Return Valve. 89

Figure 4,2 Injector driver circuit. 92

Figure 4,3 Injector over-voltage protection circuit. 94

Figure 4,4 Fuel supply system. 96

Figure 4,5 NOx Meter gas supply system. 101

Figure 4,6 Span Gas Mixing system. 104

Figure 4,7 Pressure signal and spike generator signals. 109

Figure 5,1 Rotameter Calibration Rig 114

Figure 5,2 Gas Injector calibration curve. 115

Figure 5,3 Gas Carburettor calibration curve. 116

Figure 5,4 Piezo-electric Pressure Transducer Calibration Curve. . . 117

Figure 6,1 Pre-chamber air induction ratio vs throttle position. 133

Figure 6,2 Brake Thermal Efficiency vs Main Chamber Relative Air/fuel Ratio for pre-chamber air optimisation tests. 1000 RPM, WOT, MBT. 141

Figure 6,3 Hydrocarbon emissions vs Main Chamber Relative Air/fuel Ratio for pre-chamber air optimisation tests. 1000 RPM, WOT, MBT. 142

Figure 6,4 NOx Emissions vs Main Chamber Relative Air/fuel Ratio for the pre-chamber air optimisation tests. 1000 RPM, WOT, MBT. 143

Figure 6,5 Brake Thermal Efficiency vs Main Chamber Relative Air/fuel Ratio for the methane injection rate optimisation tests. 1000 RPM, WOT, MBT 100%IR. 144

Figure 6,6 Corrected Power vs Main Chamber Relative Air/fuel Ratio for methane injection rate optimisation tests. 1000RPM, WOT, MBT, 100%IR. 145

Figure 6,7 Hydrocarbon emissions vs Main Chamber Relative Air/fuel Ratio for methane injection rate optimisation tests.1000RPM, WOT, MBT, 100%IR 146

Figure 6,8 NOx emissions vs Main Chamber Relative Air/fuel Ratio for methane injection timing optimisation tests. 1000RPM, WOT, MBT, 100%IR. 147

Figure 6,9 Brake Thermal Efficiency vs Main Chamber Relative Air/fuel Ratio for methane injection timing optimisation tests. 1000RPM,WOT, MBT 100%IR. 148

Figure 6,10 Hydrocarbon Emissions vs Main Chamber Relative Air/fuel Ratio for methane injection timing optimisation tests. 1000RPM, WOT, MBT, 100%IR. 150

Figure 6,11 Brake Thermal Efficiency vs Main Chamber Relative Air/Fuel Ratio for various methane injection angles and baseline tests. 2000RPM, WOT, MBT, 100%IR, 0.07076kg/h. 153

Figure 6,12 Brake Thermal Efficiency vs Main Chamber Relative Air/Fuel Ratio for various methane injection angles and baseline tests. 1500RPM, WOT, MBT 100%IR, 0.0537kg/h. 153

Figure 6,13 Brake Thermal Efficiency vs Main Chamber Relative Air/Fuel Ratio for various injection angles and baseline tests. 1000RPM, WOT, MBT, 0.0367kg/h, 100%IR. 154

Figure 6,14 Hydrocarbon Emissions vs Main Chamber Relative Air/Fuel Ratio for various methane injection angles and baseline tests. 1500RPM, WOT, MBT, 100%IR, 0.0537kg/h. 158

Figure 6,15 Carbon Monoxide emissions vs Main Chamber Relative Air/Fuel Ratio for various methane injection rates and baseline tests. 1500RPM. WOT, MBT, 100%IR, 0.0537kg/h. 161

Figure 6,16 NOx Emissions vs Main Chamber Relative Air/Fuel Ratio for various methane injection angles and baseline tests. 1500RPM, WOT, MBT, 100%IR, 0.0537kg/h. 162

Figure 6,17 Specific NOx Emissions vs Main Chamber Relative Air/Fuel Ratio for various methane injection angles and baseline tests. 1500RPM, WOT, MBT, 100%IR, 0.0537kg/h. 162

Figure 6,18 Corrected Brake Power vs Main Chamber Relative Air/Fuel Ratio for various methane injection angles and baseline tests. 1500RPM, WOT, MBT, 100%IR, 0.0537kg/h. 164

Figure 6,19 MBT Ignition Angle vs Main Chamber Relative Air/Fuel Ratio. 1500RPM, WOT, 100%IR, 0.0537kg/h 165

Figure 6,20 Exhaust Temperature vs Main Chamber Relative Air/Fuel Ratio. 1500RPM, MBT, WOT, 100%IR, 0.0537kg/h. 165

Figure 6,21 IMEP vs Main Chamber Relative Air/Fuel Ratio for baseline and charge stratification systems. 1000RPM, WOT, MBT. 166

Figure 6,22 Brake Thermal Efficiency vs Main Chamber Relative Air/Fuel ratio for 1500RPM, 1/2 and 1/4 part load conditions. MBT, 100%IR 0.0537kg/h. 168

Figure 6,23 Hydrocarbon Emissions vs Main Chamber Relative Air/Fuel Ratio for 1/2 and 1/4 part load tests. 1500 RPM, MBT, 100%IR, 0.0537kg/h. 169

Figure 6,24 NOx Emissions vs Main Chamber Relative Air/Fuel Ratio for 1/4 and 1/2 part load tests. 1500RPM, MBT, 100%IR, 0.0537kg/h. 169

Figure 6,25 Pressure Volume diagram for baseline test. 1500RPM, WOT, MBT. 171

Figure 6,26 Pressure Volume diagram for the Pre-Chamber Stratified Charge Combustion engine. 1500RPM, WOT, MBT, 100%IR, 0.0537kg/h. 173

Figure 6,27 Pressure fluctuations on the crest of a pressure trace for the charge stratification process. 174

LIST OF PLATES

Plate 4,1 Pre-chamber location in cylinder head. 82

Plate 4,2 Methane Injector assembly. 110

Plate 4,3 Rotameters and plenum chambers. 110

Plate 4,4 Beckman 951A NO/NOx analyser and associated equipment. 111

Plate 4,5 NO/N_2 span gas mixing system. 112

Plate 5,1 HORIBA MEXA 534GE Exhaust gas analyser. 120

Plate 5,2 BECKMAN 951A NO/NOx Exhaust gas analyser front panel. 122

Plate 6,1 Failed check valve. 136

NOMENCLATURE

ABBREVIATIONS

ATDC	After Top Dead Centre
A/D	Analogue to Digital conversion.
A/F	Air/Fuel ratio
barg	bar gauge
BDC	Bottom Dead Centre
BMEP	Brake Mean Effective Pressure
BP	Brake Power
BSFC	Brake Specific Fuel Consumption
BTDC	Before Top Dead Centre
BTE	Brake Thermal Efficiency
CNG	Compressed Natural Gas
D.C	Direct Current
DMA	Direct Memory Access
EGR	Exhaust Gas Recirculation
ELLC	Equipment Lean Limit of Combustion
EMF	Electro-Motive Force
Ford PROCO	Ford PROgrammable COmbustion
HC	Hydrocarbon
Honda CVCC	Honda Controlled Vortex Controlled Combustion system

IP	Indicated Power
IR	Induction Ratio
MAN	Maschinenfabrik Augsburg Nurnberg
MBT	Minimum advance for Best Torque
MCAFR	Main Chamber relative Air Fuel Ratio
MOSFET	Metal Oxide Semiconductor Field Effect Transistor
NOx	Oxides of Nitrogen
NRV	Non-Return Valve (check valve)
OFN	Oxygen Free Nitrogen
OPIR	Optimised Pre-chamber Induction Ratio
Porsche SKS	Porsche Stratified Charging System (Translation)
ppm	parts per million
pphm	parts per hundred million
psig	pounds per square inch gauge
PTFE	PolyTetraFluoroEthylene (Teflon)
RON	Research Octane Number
RPM	Revolutions Per Minute
SCE	Stratified Charge Engine
SOS	Slotted Optical Switch
SOx	Oxides of Sulphur
S/V	Surface Area to Volume ratio at TDC
TCCS	Texacos Controlled Combustion System
TDC	Top Dead Centre
UHC	Unburned Hydrocarbons

VW PCI	VolksWagen Pre-chamber Injection system
WOT	Wide Open Throttle

SYMBOLS

b	burned
D	Diode
Da	Damkohler number
K	Kelvin / reaction rate constant
kHz	kiloHertz
kW	kiloWatt
L	Integral Length Scale
P	Pressure
R	Resistor / Gas constant
Re	Reynolds number
S_t	Turbulent flame speed
S_l	Laminar flame speed
s	second
T	Temperature
u	unburned
$\bar{u}$	mean velocity component
ú	fluctuating velocity component
V	Volume

v	volts
Z	Zener Diode
%vol	Percentage volume

CHEMICAL SYMBOLS

CO	Carbon monoxide
CO_2	Carbon dioxide
H	Hydrogen radical
H_2S	Hydrogen Sulphide
N_2	Nitrogen
N_2O	Nitrous oxide
NO	Nitric oxide
NO_2	Nitrogen dioxide
O	Oxygen radical
O_2	Oxygen
O_3	Ozone
OH	Hydroxyl radical
SO_2	Sulphur dioxide

GREEK SYMBOLS

γ	ratio of specific heats
ε	eddy energy dissipation rate per unit mass
η	Kolomogorov length scale
θ	crank-angle rotation
λ	relative air/fuel ratio / Taylor micro scale
ν	kinematic viscosity
τ	eddy turn over time scale
υ	specific volume

CHAPTER 1

AIR POLLUTION

1.1 INTRODUCTION

In today's society man has become highly dependent upon the automobile. It has opened up the world, making distances which would have once taken days to travel attainable in a fraction of the time. The personal automobile is commonly powered by a spark ignited internal combustion engine, utilizing the four stroke cycle. As technology has developed the price of the vehicle has been reduced to such a level that almost anybody in western society can afford to own one. Data for the USA[1] shows that the vehicles per person ratio has increased from 0.005 in 1910 to 0.51 in 1970, and vehicle numbers have swelled from 468,000 to 104,702,000 over the same time period. However, with the increase in vehicle numbers has come an increase in the associated air pollution generated by them. The evidence of which is easily seen in large urban centres, e.g Los Angeles (U.S.A), Christchurch (New Zealand).

1.2 AIR POLLUTION

Perkins[1] defines air pollution as:

> *"the presence in the outdoor atmosphere of one or more air contaminants, such as dust, gas, mist, odour, smoke, or vapour*

in quantities, of characteristics, and of duration, such as to be injurious to human, plant, or animal life or to property, or which unreasonably interferes with the comfortable enjoyment of life and property."

The major sources of air pollution can be categorized into three distinct groups, namely transport, stationary power generation and industrial processes. The types of pollutant emitted by these sources can be categorized into five main groups; particulate matter, carbon monoxide (CO), oxides of sulphur (SO_x), oxides of nitrogen (NO_x) and hydrocarbons (HC). Carbon dioxide (CO_2) is gaining higher status as a pollutant due to its role in the green-house effect.

Strauss[24] estimated that the total man made emissions were significantly less than the natural emission sources with the exception of sulphur dioxide (SO_2). This is associated with power generation, which upon reaction with water forms both sulphurous (H_2SO_3) and sulphuric (H_2SO_4) acid, synonymous with acid rain.

Table 1.1 gives the estimated values of total man made and natural emissions for 1984. Perkins[1] estimated that 95% of the total man made emissions were emitted in the northern hemisphere.

TABLE 1.1 Total man made and natural air pollution emissions.[24]

Pollutant	Man made emissions (*10^{tonnes}/year)	Natural emissions (*10^{tonnes}/year)	Automotive % of total man made.
CO	304	>3000	59.2%
HC	90	170	32.0%
NO_x	53	370-795	47.5%
†SO_x	100-140	220	2.4%
Particles	28.3 (US)	unknown	¥4.3%

† includes H_2S which ultimately forms SO_2. ¥ From spark ignition engines.

Although the man made emissions at this time were significantly lower than the natural emissions the fact that the majority of the emission sources are concentrated in urban areas makes the problem substantial.

1.3 AUTOMOTIVE POLLUTION

The automotive contribution to air pollution comes in the form of carbon monoxide, hydrocarbons (both unburned and partially burned), oxides of nitrogen (NO, NO_2 and small quantities of N_2O) and particulate matter, especially lead halides for spark ignition engines[2]. The role that each plays in the photochemical smog process, or more direct health problems has been postulated for some time, and it is these factors that have mainly prompted the introduction of stringent emission laws throughout the world. Table 1.1 also shows the role that automotive emissions play with regards to the total man made emissions.

1.3.1 Present emission standards.

Until 1970 the United States of America had no federal vehicle emission standards. However over the past two decades standards have been introduced and continually reviewed to meet the demands of an increasing automobile population. The majority of the rest of the world has also introduced legislation depending upon their own location and circumstances. Table 1.2 summarizes the present status of some countries with respect to their emission standards and Table 1.3 gives the present lead content in petrol for selected countries.

TABLE 1.2 Selected present emission standards for spark ignition engines.[3]

Country	HC	NO_x	CO	EVAP
USA (1981-1994) g/mile	.41	1.0	3.4	2.0
USA (1994-1998) "	0.25	0.4	3.4	0.2
USA (2001-) "	0.125	0.2	1.7	0.2
Europe ECE 83	($HC+NO_x$)			
>2000cc (g/test)	6.5	3.5	25	-
1400-2000cc	8	-	30	-
<1400cc	8	6	45	-
Japan (10.15 mode)	0.39	0.48	2.7	-
11 mode, g/test	6.0	9.5	85.0	-

Table 1.3 Lead Content of Fuel.[3]

gPb/litre	Leaded Premium	Leaded Regular	Unleaded super 98 RON	Unleaded premium 95 RON	Unleaded regular <95 RON
EC	.15 -.4	.15 -.4	.013	.013	.013
USA "	.026	.026	.013	.013	.013
Canada "	.026	.026	.013	.013	.013
NZ	.45	P	N/A	W	.013
South Australia "	.65	P	N/A	W	W
Japan "	N/A	N/A	N/A	W	W

P-Prohibited. W-Widespread. N/A-Not Available.

1.3.2 Exhaust emission sources.

a, Carbon monoxide.(CO)

The formation of CO in a premixed hydrocarbon flame is one of the principle reaction paths responsible for the combustion of the hydrocarbon fuel. The mechanism may be represented schematically by;[4]

$$RH \rightarrow R \rightarrow RO_2 \rightarrow RCHO \rightarrow RCO \rightarrow CO \qquad (1.1)$$

The final step of the reaction which produces the CO is believed to be due to thermal decomposition of the RCO radical.[4,5]

$$RCO \rightarrow CO + R \qquad (1.2)$$

Other reactions do occur involving O_2, OH, O and H, but the temperature of the combustion chamber favours the above reaction making it the principle CO formation reaction.

The rate of oxidation of $CO \rightarrow CO_2$ is relatively slow compared to the formation of CO, hence high CO concentration values are initially found in the combustion chamber.

Reaction kinetics have shown that direct oxidation of CO in the form of:

$$CO + O_2 \rightarrow CO_2 + O \qquad (1.3)$$

is very slow, whereas the reaction:

$$CO + OH \leftrightharpoons CO_2 + H \qquad (1.4)$$

is the principle reaction involved in the oxidation of CO. During the early stages of expansion the CO is oxidised at a rate which satisfies the overall equilibrium values, however as the expansion continues the rate of oxidation reduces, ie. the process is temperature dependent.

However, The above reaction is equilibrated throughout the expansion process, so that the relative levels of CO and CO_2 are controlled by the levels of OH and H.

i.e

$$\frac{[CO]}{[CO_2]} = \frac{1}{K}\frac{[H]}{[OH]} \qquad (1.5)$$

The levels of H and OH are controlled by various other reactions,[7] and it is these reactions at the lower temperatures associated with the expansion process which favour a disproportionately large amount of H relative to OH. Hence the partial equilibrium state dictates that the ratio of CO and CO_2 must be greater than that for total equilibrium.

The variation of air/fuel ratio effects the CO concentration in the manner described above. For a rich mixture, the formation of excess H occurs and the reverse direction reaction is favoured which results in higher CO levels, whereas lean mixtures favour the formation of excess OH which favours the forward reaction resulting in reduced CO. This trend is illustrated in figure 1.1.

b, Oxides of Nitrogen.(NO_x)

The majority of NO_x is comprised of NO. The formation of NO is governed by the reactions proposed by Zeldovich.[4,5,6,7,8,9,10,12]

$$N + NO \rightarrow N_2 + O \qquad (1.6)$$

$$N + O_2 \rightarrow NO + O \qquad (1.7)$$

$$N + OH \rightarrow NO + H \qquad (1.8)$$

The first two reactions have large activation energies[6] which result in the necessity for high temperatures for the formation of the pollutant. The thermal formation rate of NO is generally much slower than the combustion rate, hence the majority of NO is formed in the post flame gases for near stoichiometric mixtures. For slightly rich or lean mixtures increased rates of formation in the flame have been reported.[4,5,10] This was believed to be due to an overshoot of radical concentrations of O and OH above equilibrium values for lean mixtures and partially for rich mixtures. For the rich mixtures there is experimental evidence that reactions between hydrocarbon species and molecular nitrogen are another important factor in the formation of NO.

After the formation of NO the concentration "freezes" well above the equilibrium values predicted for the exhaust conditions. The reason for this discrepancy is that the rate of NO destruction associated with the Zeldovich reactions is not sufficiently rapid to achieve good decomposition as the temperature decreases rapidly due to the expansion process.

The levels of NO emitted from the exhaust can be effected by several engine design and operating variables including compression ratio, ignition timing, A/F ratio, combustion chamber shape, engine speed, inlet pressure and temperature, charge dilution (from both residual gases and/or EGR), number of spark plugs and air humidity.[6,8,10,11,12]

c, Unburned Hydrocarbons (UHC)

Hydrocarbon emissions, unlike CO and NO_x, are the consequence of incomplete combustion of the hydrocarbon fuel. Most hydrocarbon species found in the exhaust gases are the result of the low temperature regions of the combustion chamber. These species consist of fuel hydrocarbons and non-fuel hydrocarbons including paraffins, olefins, aromatics, alcohols and aldehydes, depending upon the fuel used.[4,5,6,13] The non fuel hydrocarbons are generally formed due to decomposition/pyrolysis and partial oxidation of the original fuel hydrocarbons.

The main classical reasons for the presence of the "low temperature" regions within the combustion chamber is due to the high thermal gradient between the combustion chamber surfaces and the hot burning gases. This thermal gradient s to quenching of the flame near the surfaces of the combustion chamber.[1,4,5,6,10,12,14,15,16] In this process the heat from the flame is transferred into the surfaces away from the unburned fuel/air mixture adjacent to the chamber surfaces at a rate which exceeds the requirements of the flame propagation, extinguishing the flame and preventing oxidation of the remaining fuel. The non fuel hydrocarbons were believed to be formed in the intermediate region between the cold unburned fuel/air mixture the hot combustion gases, as the flame is extinguished. Here the temperature is still high enough for some of the partial decomposition/oxidation mechanisms to occur. Some of the unburned gases are believed to be oxidised after the flame is extinguished as a result of mixing between the hot and cold gases, termed

post-flame reactions. The amounts which react in this manner are dependent upon the mixing rates (ie turbulence), gas temperatures and concentrations of oxygen and hydrocarbons as well as other active species remaining from the burned flame regions. This post flame oxidation can continue throughout expansion and exhaust strokes, and even into the exhaust system if the environment is suitable.

More recent investigations are pointing away from wall quenching as the only source of UHC's and towards crevice quenching and absorbtion/desorption of hydrocarbons into lubricating oil as another major sources of hydrocarbons.[17,18,19,20] Daniel[14] had initially seen the presence of crevices as a hydrocarbon source, but placed a smaller value on their contribution compared to more recent investigations. The main processes for crevice quench occur during compression of the air/fuel mixture. Here the mixture is forced into crevices such as those around valve seats, head gasket, spark plug threads and between the piston, cylinder wall and the first piston ring. The latter being the major source. These spaces are generally too small to permit flame travel, ie. smaller than the quench distance associated with the flame, and so the hydrocarbons remain unburned. During expansion the gases are released back into the main chamber where some are oxidised and others are subjected to partial decomposition\pyrolysis due to the mixing with the hot post flame gases discussed earlier. Good design could eliminate many of the crevices, but for obvious reasons the region around the top of the piston and top ring cannot be totally eradicated.

Oil absorbtion/desorption occurs due to the ability of the thin layer of lubricating oil on the walls of the cylinder barrel and combustion chamber, to dissolve the hydrocarbon fuel. Combustion studies have shown that of the hydrocarbons remaining in a combustion bomb coated with lubricating oil after ignition, 97% were original fuel hydrocarbons.[17] The ability of the oil to absorb the fuel is primarily effected by temperature. Increased temperature reduces the amount of fuel absorbed by the oil.[21,22] This would indicate that increasing the cylinder wall temperature would reduce the hydrocarbon emissions from this source.

Gas phase quenching is a process by which the fluid motions inside the combustion chamber cause the premature extinction of the propagating flame. Hence the occurrence of this process would increase the hydrocarbon levels. Theories of this phenomenon will be discussed in more detail in chapter 3.

1.3.3 Pollutant Effects.

Carbon monoxide is a highly toxic substance. The formation of Carboxyhaemoglobin reduces the oxygen carrying capability of the blood.[24] The haemoglobin has a higher affinity for carbon monoxide than for oxygen. Toxicity is both concentration and time dependent, and can cause death within a very short time period with a sufficiently high concentration.

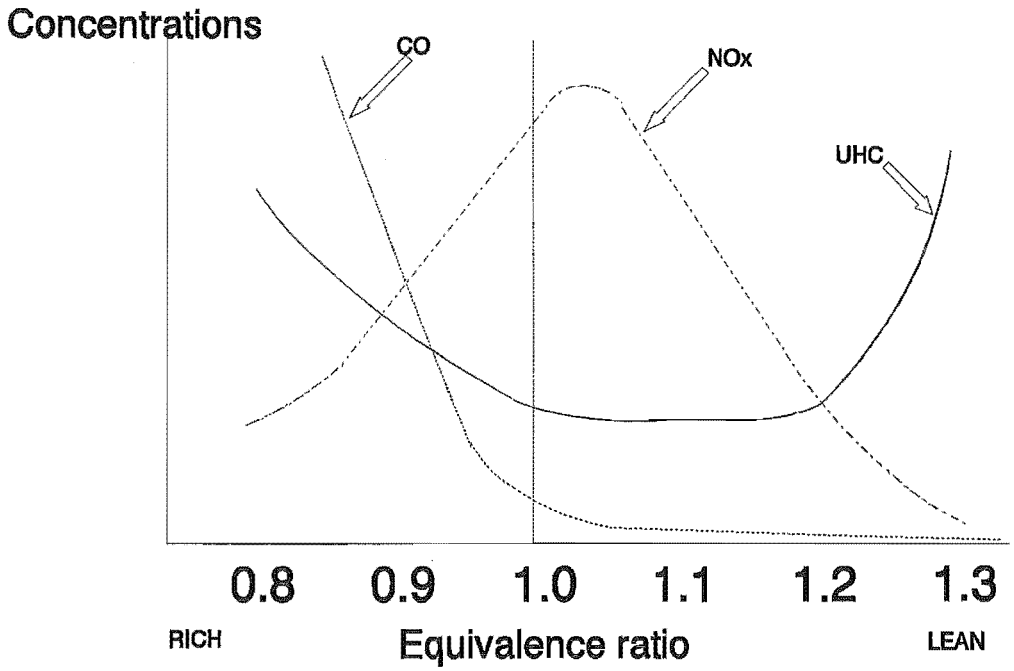

Figure 1,1 Pollution Concentrations vs Equivalence Ratio

The oxides of nitrogen and certain hydrocarbon species, both in the presence of Ultra-Violet light form **Photochemical Smog**. The components of the smog have detrimental effects on health, vegetation, materials and general welfare. Health problems include eye irritation, respiratory distress and reduced visibility. Certain aromatic hydrocarbons are also carcinogenic.

The photochemical reactivity of the hydrocarbons depends upon the size and structure of the molecule.[1,15,24] (Photochemical reactivity refers to the Nitric oxide photo-oxidation rate, i.e the rate at which the hydrocarbon causes the NO to be oxidised to NO_2.) Saturated hydrocarbons are generally non-reactive, aromatics are intermediate and olefinic materials are very reactive.

The photolytic cycle begins with the photolysis of NO_2,

$$\text{ie,} \quad NO_2 + h\nu \rightarrow NO + O \qquad (1.9)$$

Ozone is quickly formed,

$$O + O_2 + M \rightarrow O_3 + M \qquad (1.10)$$

where M is a third body which is required to absorb the energy of the reaction, Mainly N_2 or O_2 as they are the most abundant. The final reaction in the cycle is;

$$O_3 + NO \rightarrow NO_2 + O_2 \qquad (1.11)$$

These reactions would remain in chemical equilibrium with an ozone concentration of approximately 2.7pphm[¥] for a 10pphm concentration of NO_2. However for the same NO_2 concentration ozone levels have been measured in Los Angeles at levels of 50pphm for one hour peak averages.[(1)] This ozone build up is caused by the presence of the reactive hydrocarbons which oxidise NO without the destruction of the ozone.

$$O + \text{OLEFIN} \rightarrow R + R'O \qquad (1.12)$$

¥ pphm-Parts Per Hundred Million

These organic radicals react with O_2 to form peroxy radicals.

$$R + O_2 \rightarrow RO_2 \quad (ROO) \qquad (1.13)$$

These yield an oxygen atom to NO,

$$RO_2 + NO \rightarrow RO + NO_2 \qquad (1.14)$$

The NO_2 in turn releases an oxygen atom into the photolytic cycle, which in turn produces the higher levels of ozone.

The other radical formed in reaction 1.12 may be an aldehyde, which is an eye irritant. A side effect of the peroxy radical is the formation of peroxyacetylnitrate, or PAN. This is also an eye irritant which also causes damage to plants.

The increasing levels of automotive pollution especially in urban areas have to the stringent emission standards listed in section 1.3.1.

Increased levels of carbon dioxide (CO_2) in the atmosphere are believed to be contributing to the increase in global temperature, known as the green-house effect. Here the CO_2 absorbs the infra red radiation emitted from the earth. The result is that the thermal energy cannot be expelled from the atmosphere into space and so the temperature of the atmosphere increases.

1.3.4 Initial Reduction Efforts.

Early attempts to reduce the exhaust emissions were focused around optimisation of existing conventional engines. Inlet manifolds were redesigned to deliver more homogeneous mixtures with as small as possible variation in A/F ratios between cylinders. Various centrifugal and vacuum advance systems were implemented to reduce CO and NO_x emissions at idle, deceleration, etc.[23] Hydrocarbon emissions were initially reduced substantially by recycling of the crankcase blow by fumes into the inlet manifold so that they may be burned. Also evaporative recycling systems were installed into the fuel tank and carburettor.[1,15,23,24] As well as these measures, new engines were designed with minimised surface to volume (S/V) ratios to reduce flame quenching and some crevice volumes were reduced in order to further reduce the hydrocarbon emissions. These modifications went some way to reduce the exhaust emissions, but further reduction was necessary. Post treatment of the gases was investigated.

Thermal Reactors.

These are basically enlarged exhaust manifolds which are designed to promote rapid mixing of exhaust gases with secondary air so that further oxidation of the UHC's and CO may occur. This also requires the reactor to increase residence time of the gases in the reactor at a sufficiently high temperature.

The main problems with thermal reactors are that they require sufficient time

to warm up to their operating temperatures from start up, and they do not address the reduction of NO_x. During the initial stages of start up the engine temperatures are lower and the choke generally is used, hence this phase of the drive cycle produces the highest levels of UHC's and CO. Hence the reactors are generally useless during this time.

Catalytic Convertors.

These consist of an active catalytic material such as a noble metal, or a combination of transition and non transition metals deposited on thermally stable support materials, such as alumina. The exhaust gases flow through the catalytic material where they are converted into non reactive species. There are two basic types of convertor available, the dual catalytic convertor and the three-way catalytic convertor.

Dual convertor.

In a dual convertor the exhaust gases first pass through a reducing catalyst so that the NO_x may be reduced. From here the gases pass into a secondary convertor which oxidises the hydrocarbons and the remaining CO.

Again the convertors require high temperatures to sufficiently oxidise the CO and hydrocarbons, Hence they are less effective during warm up. Another problem is that the reducing catalyst may reduce the $NO \rightarrow NH_3$ which can be readily oxidised back into NO. The use of Ruthenium or metallic Ni-Cu

catalysts have overcome this problem.

Another major problem is the poisoning of the catalyst by lead, Phosphorous and sulphur. To overcome this the vehicle must be operated on unleaded high quality petrol.

3-Way Convertor.

In a 3-way convertor all three pollutants are simultaneously converted to CO_2 and N_2 etc in the same chamber. However their operation is severely influenced by air-fuel ratio and the engine is restricted to operate in a very fine band around stoichiometric. Useful conversion therefore requires careful control of the air-fuel ratio throughout the drive cycle. One way of doing this is by the use of feedback control using Lambda sensors in the exhaust. Lambda sensors detect the relative oxygen content between the exhaust gases and the atmosphere. The difference produces a voltage across the sensor which can be used as the feedback signal for a controller. The voltage changes steeply as the air-fuel ratio passes through stoichiometric. Again the sensors require the use of uned petrol for satisfactory performance.

Whilst the use of catalytic convertors can help meet present emission standards they generally incur a fuel penalty. Also it is viewed that the use of convertors is simply avoiding the problem of pollution reduction within the combustion chamber.

Table 1.4 Engine design and operating variables affecting HC emissions. [6]

1.Formation of HC quench regions.	2.Post-quench oxidation in combustion chamber	3.Fraction HC leaving combustion chamber.	4.Oxidation in exhaust system.
a. Effective S/V ratio. i, Compression ratio ii, Combustion chamber design iii, Spark timing iv, Burn rate	a. Mixing with bulk gases. i, Speed ii, Induction system design iii, Combustion chamber design	a, Engine geometry. i, Compression ratio ii, Combustion chamber design iii, Valve overlap	a, Oxygen conc. i, Mixture ratio ii, Air injection in exhaust port
b. Quench thickness. i, Mixture ratio/EGR ii, Load iii, Wall temperature iv, Wall roughness v, Deposits	b. Oxygen concentration i, Mixture ratio	b, Operating parameters i, Load ii, Exhaust pressure iii, Speed	b, Exhaust gas temp. i, Compression ratio ii, Spark timing iii, Load iv, Mixture ratio /EGR v, burn rate vi, Heat losses
c. Quench crevice. i, Combustion chamber design ii, Mixture ratio/EGR iii, Load iv, Deposits	c, Bulk gas temp. during expansion i, Compression ratio ii, Spark timing iii, load iv, Mixture ratio/EGR v, Burn rate		c. Residence time. i, Volume of exhaust system ii, Exhaust flow rate
	d. Wall temperature.		d. Exhaust reactors i, Thermal reactor ii, Catalytic reactor

CHAPTER 2

ALTERNATIVE ENGINE COMBUSTION TYPES.

2.1 INTRODUCTION.

From figure 1,1 it can clearly be seen that if the air/fuel ratio of a combustible mixture to an engine is made leaner than stoichiometric, then all the emissions will begin to reduce, with the exception of NOx which rises to a maximum just past stoichiometric and then drops off dramatically. The question under consideration is how far could the air/fuel ratio be leaned, minimising emission levels and still maintaining good fuel economy? It has been found that the operation of an engine under lean conditions is limited by certain ignition and combustion characteristics which result in poor emission levels and a decrease in fuel economy. This chapter will deal with the initial investigations into lean burn engines, followed by a look at a stratified charge engines, which are believed to overcome some of the problems of the lean burn engine.

2.2 LEAN BURN ENGINES.

In an attempt to reduce simultaneously all major exhaust emissions while

retaining acceptable brake thermal efficiency and performance, manufacturers and researchers have investigated lean burn engines. Initial efforts were centred around the modification of existing engines, but this immediately exposed certain problems associated with burning lean mixtures in an engine. The most significant of which is excessive cycle-to-cycle variation.

Cyclic variation can be divided into two broad categories;

Inter-cylinder variations,

In-cylinder variations.

Patterson[29] showed that the air fuel/ratio between cylinders varied by a standard deviation of 1.45 for an average air/fuel ratio 16.6 for a conventional carburetted engine. Variations of this type are caused by poor manifold and/or carburation design. Modern multi-point injection engines with symmetrical "tuned" intake systems have minimised this problem.[26,112]

In-cylinder cyclic variation has a very different cause. Peters[26] defined 3 types of combustion event which could occur within the cylinder.

1, Normal cycle,

2, Slow burn cycle,

3, Incomplete burn cycle.

He defined a normal, or complete, burn cycle to occur when 85% of the fuel

mass was burned before the exhaust valve opened. He found for a relative air fuel ratio‡ of 1.72 that 32.5% of all cycles were slow burning and only 1.5% were incomplete cycles.

From this type of result it was concluded by Peters, and other researchers[26,28,29,30,32,36,37] that the major source of this slow burn lay in the flame initiation process. This to a slow initial burn rate, and hence an overall slow burn rate. It has been shown that a reduction in the ignition delay will reduce the amount of cyclic variation in a given engine.[27,33,34,35,36,37] A reduction in the main burn time has also been shown to decrease cyclic variation, but only upon good flame initiation. These two approaches to the problem have been summarised by Quader[27] as follows;

Decrease flame propagation time:-	Decrease charge dilution,
	Decrease flame path length,
	Increase the mixture temperature,
	INCREASE mixture turbulence.
Decrease flame initiation time:-	Prevent quenching at ignition,
	Decrease charge dilution,
	Increase compression ratio,

‡ defined as the actual air/fuel ratio divided by the stoichiometric air/fuel ratio.

Increase ignition energy,
DECREASE mixture turbulence around the spark plug.

It is interesting to note that the mixture turbulence which promotes the flame propagation may inhibit the flame initiation. Kalghatgi[28] et al claim that the minimum ignition energy requirements increase with an increase in turbulence intensity. They also claim that the initial straining of the flamelet can slow down the flame speed due to the low amounts of energy being released from the flamelet. Bolt[30] stated that the ignition system is only able to ignite mixtures whose minimum energy requirements are less than the energy available from the ignition system. This claim was made with both air/fuel ratio and turbulence effects in mind.

The In-cylinder cyclic variation can be effected by various engine variables, such as mixture turbulence and bulk motion,[29,30,3944,45,53] air/fuel ratio,[29,39,44,47,48] mixture homogeneity,[29,39] spark timing,[29,32,48,55] number and location of spark plugs,[44,55,56] residual exhaust gases,[39,44,51] type of fuel[30,44] and compression ratio.[41,44]

It was the conclusion that a decrease in the ignition delay period would increase the overall burn rate that to an investigation into stratified charge engines.

2.3 STRATIFIED CHARGE ENGINES

Charge stratification within an internal combustion engine refers to a process by which a relatively rich fuel mixture is present in the vicinity of the spark electrodes at the time of ignition and this is used to ignite the remaining leaner mixture which forms the majority of the combustion charge.

The idea of stratified charge engines dates back to 1866 where Otto[59] used a 3 layer combustion system to prevent knock occurring. Its first use in igniting lean mixtures was under taken by Ricardo[59] in 1918, and again by Summers in 1926. Their commercial application were not realised as conventional engines became cheaper to manufacture, and developments within the conventional engine reduced the need for stratified charge engines. A resurgence in interest began in the mid 1960,s with the need to reduce exhaust emissions and the need to improve fuel economy in the mid 1970's. Since then a vast array of stratified charge engines has been developed. Only a few of the more successful one's shall be discussed.

2.3.1 Ford PROCO

This is a direct injection stratified charge engine which is dependent upon a combination of swirl and injection timing to facilitate the charge stratification process.[59,60,61] The swirl is generated during the induction stroke and is

intensified into the piston cup near TDC to an angular swirl speed of 3-5 times the engine speed.

At high load the injection is early in the compression stroke, so that a virtual homogeneous mixture is obtained,ing to almost full air utilisation and good BMEP. A reduction in the load is achieved by retarding the injection timing. The reduction in mixing time produces a relatively rich mixture near the spark plug at the point of ignition. Throttling of the intake air under part load is used to maintain an air fuel ratio less than 22:1.

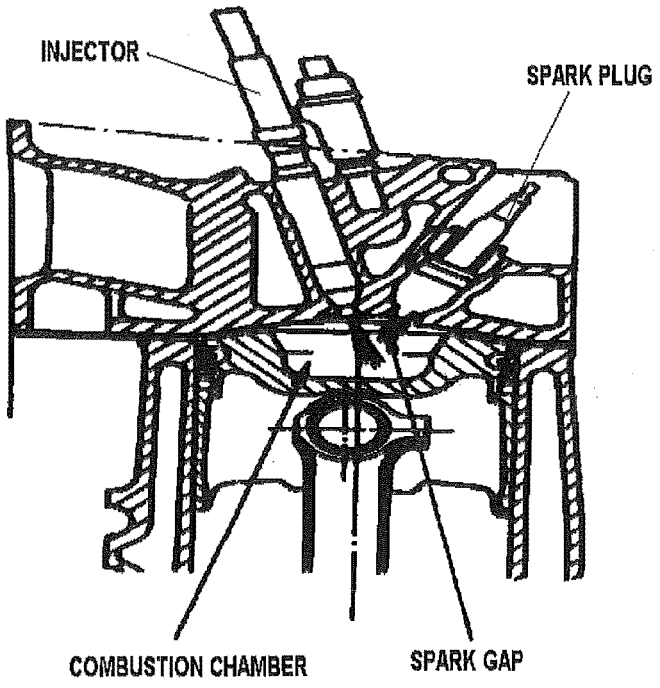

Figure 2,1 Ford PROCO engine.

A slight reduction in specific fuel consumption and NOx levels are observed relative to a standard carburetted engine, especially at part load. However CO

and UHC levels were found to be higher. Thermal reactors or catalysts were used to oxidise the CO and UHC's, and exhaust gas recirculation (EGR) was used to further reduce NOx formation.

2.3.2 Texaco TCCS

The Texaco Controlled Combustion System engines is another direct injection stratified charge engine which is dependent upon the air swirl to provide mixture formation.[60,61,62] The design is similar to that of the Ford PROCO, but instead of varying the injection timing the injection rate alone is varied to give the required power. The injection angle/direction is also different. Fuel injection begins around TDC, just before ignition. The initial fuel injection becomes the centre of ignition for the remaining fuel injected.

The combustion process is similarto that of diesel engines in that the rate of combustion becomes dependent upon the rate at which the air and fuel can mix, ie a diffusional process. Due to the heterogeneous nature of the combustion, smoke levels limit the output of the engine.

Exhaust emission targets were able to be met with the use of exhaust catalysts for CO and UHC's, and high levels of EGR for NOx reduction. However a fuel consumption penalty of 50% resulted. The system has the advantage of multi-fuel capability.

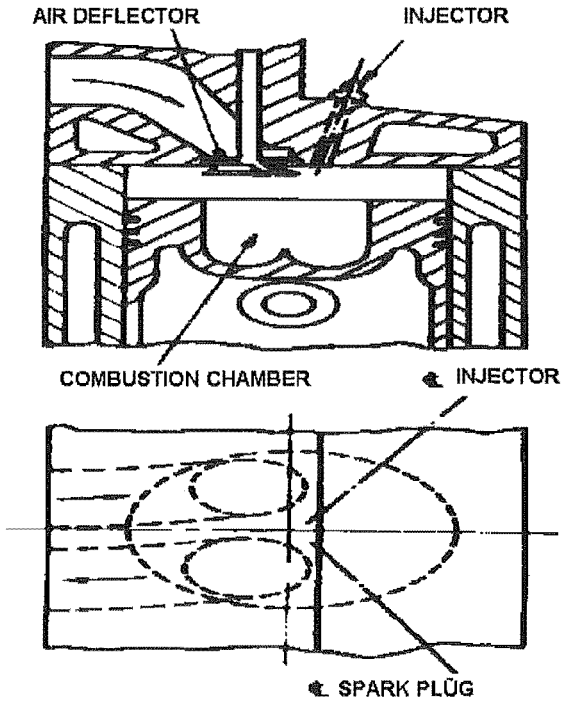

Figure 2,2 Texaco TCCS system.

2.3.3 MAN FM

The MAN FM engine is another example of a direct injection stratified charge engine utilising swirl.[60,63,64] This system operates by injecting the fuel onto the piston bowl surface. Ignition is accomplished by a modified spark plug which protrudes into the piston bowl cavity. The combustion rate is controlled by the rate of evaporation of the fuel from the piston bowl.

Again this heterogeneous combustion process limits the output because of smoke formation. Exhaust emissions are reduced by the use of exhaust catalysts. The engine also possesses multi-fuel capability, even being operated on methanol and ethanol.[63]

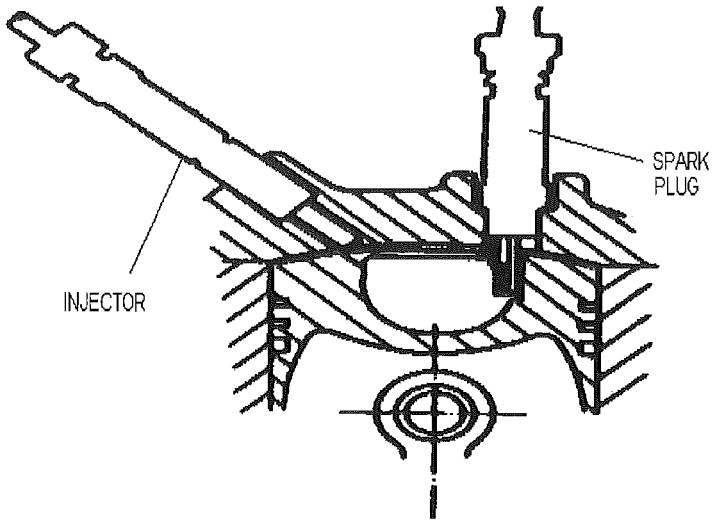

Figure 2,3 MAN-FM system.

Dual chamber S.C engines are by far the largest category since many attempts have been made to develop such an engine.

2.3.4 Porsche SKS

This pre-chamber engine utilises fuel injection into both the pre-chamber and main chamber for mixture formation.[59,65] The main mixture injection occurs in the inlet manifold whereas the pre-chamber injection is direct. The pre-chamber mixture has an approximate relative air/fuel ratio between λ=0.4-0.8, and a very lean mixture of λ=1.5-3.0 in the main chamber. These together produce an overall relative air/fuel ratio of $\lambda \geq 1.0$.

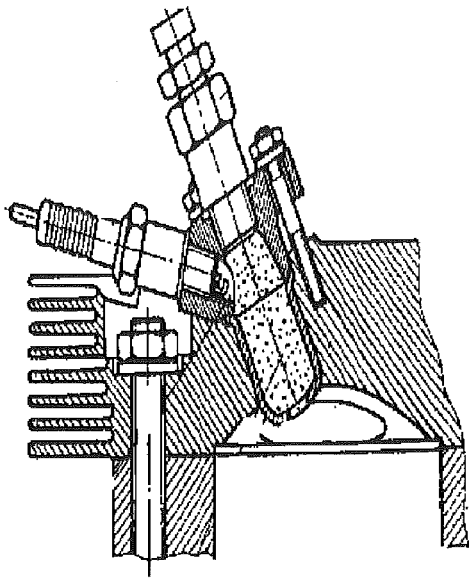

Figure 2,4 Porsche SKS system.

The ignition kernel is formed in a part of the pre-chamber known as the ignition chamber. Here the mixture is relatively quiescent, allowing good flame initiation. The flame spreads into the pre-chamber where intense turbulence promotes the spread of the flame. During the expansion stroke the flame emerges from the pre-chamber and propagates through the main "lean" chamber.

Emission levels relative to a standard 911 engine were reduced with the specific fuel consumption remaining at acceptable levels. However hydrocarbon levels were still above those required by legislation. These were believed to be due to a small amount of injected fuel not evaporating off the pre-chamber walls during combustion.

2.3.5 Volkswagen PCI

The VW Pre-Chamber Injection system[59,60,66,67,68] is similar to the Porsche in that fuel is directly injected to the pre-chamber and the main charge is formed externally. However where the Porsche system used turbulence to increase the burn rate, the VW system uses swirl generated by the incoming charge from the main chamber which passes through an offset connecting passage. The flow enters the spherical pre-chamber and hence creates a level of swirl during compression. The fuel is injected early in the compression stroke to take advantage of this.

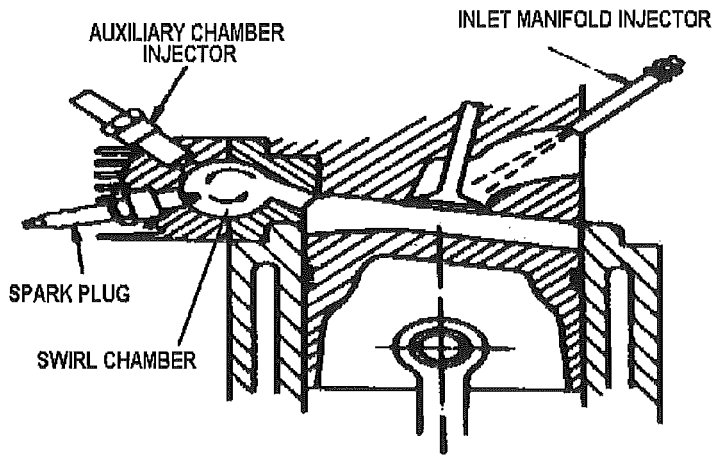

Figure 2,5 Volkswagen PCI system.

Hydrocarbon and CO exhaust emission legislation levels could not be achieved without post combustion treatment. The production of smoke also

became a problem. A large reduction in NOx was achievable due to both the pre-chamber and main chambers having air/fuel ratios which did not support the formation of NOx.

2.3.6 Honda CVCC

The Honda Compound Vortex Controlled Combustion system[59,60,69,70,71] uses a secondary carburettor to supply a relatively rich mixture to the pre-chamber through a secondary inlet valve. Its operation is based upon a three zone stratification system, whereby during the induction stroke a proportion of the rich mixture leaves the pre-chamber and mixes with a proportion of the lean charge in the main combustion chamber. During compression this intermediate charge is compressed into the connecting passage between the pre-chamber and the main chamber.

The rich mixture is easily ignited in the pre-chamber. This rich charge forces a torch of burning gas across the main combustion chamber. The torch is maintained by the intermediate charge and causes the lean mixture to burn at a faster rate than it would normally. The burning speed is controlled so that further combustion of most UHC occurs during the expansion stroke. Because of the extended burning time the maximum temperatures and pressures occurring in the engine are unfavourable to the formation of NO_x. Also the overall lean mixture reduces the emission of CO. By this controlled process

Honda has reduced all three emissions simultaneously. With the addition of branch conduits into the torch passage the hydrocarbon emissions were reduced even further. These conduits allowed burnt and unburned gases to recirculate back into the main combustion chamber for a secondary combustion event.[70]

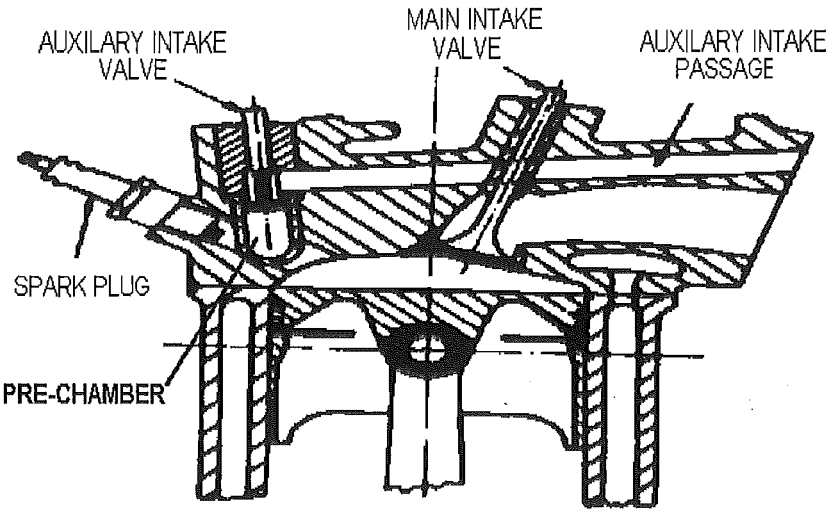

Figure 2,6 Honda CVCC system.

It was also noted by Yagi[71] et al that the increased combustion rate of the combustion process increased the anti-knock quality, thereby allowing an increase in the compression ratio relative to the baseline engine and hence a decrease in the specific fuel consumption.

Emission levels experienced by the CVCC, especially the branched conduit system, were able to meet the primary emission targets of that time with no detrimental effects to specific fuel consumption, and secondary emission targets with a large increase in specific fuel consumption.

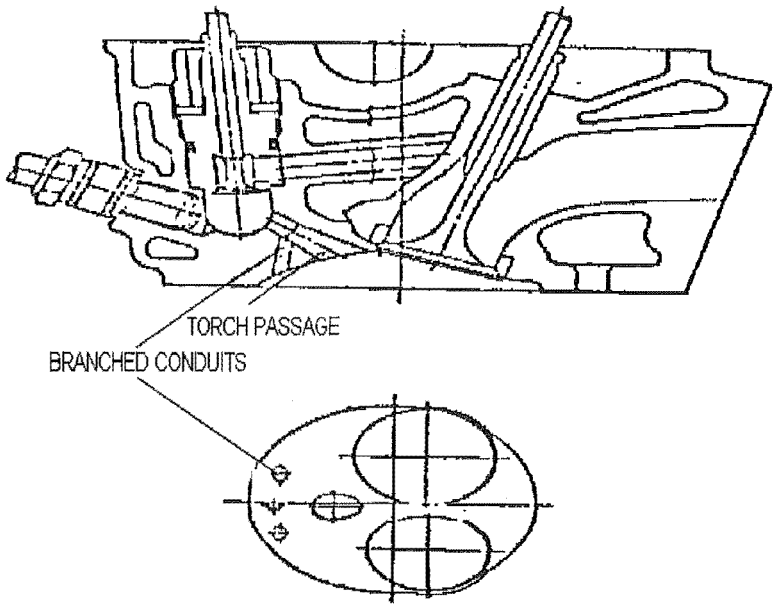

Figure 2,7 Honda Branched Conduit CVCC head.

2.3.7 LAG Process

Gussak[59,72,73,74] noticed that when a very rich mixture of a fuel was burned the presence of free radicals and other active species formed during the combustion was far in excess of the thermodynamic equilibrium concentrations. By utilising this effect he developed an ignition process that would ignite a lean mixture not by the presence of a conventional flame front, but by the action of high chemical activity of these active species.

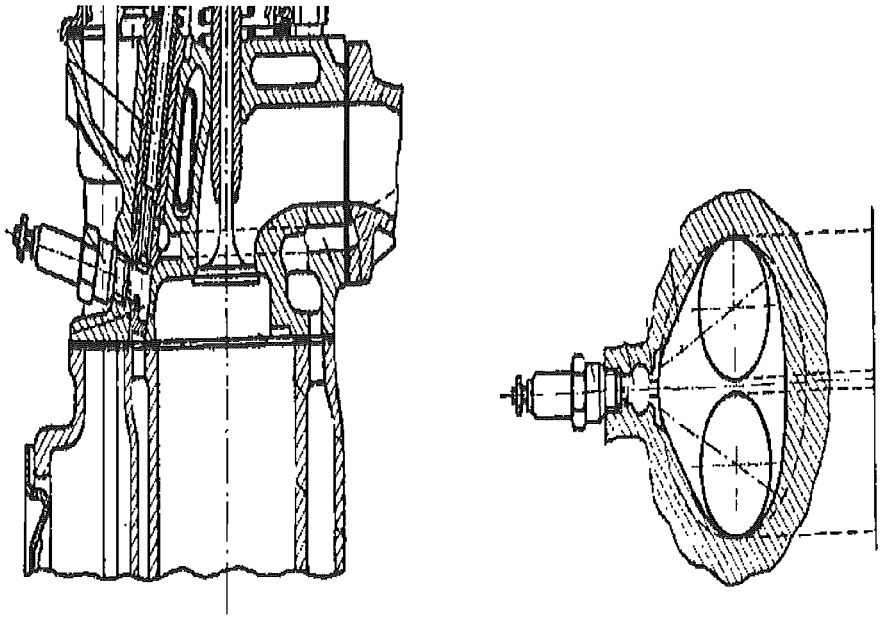

Figure 2,8 LAG-process engine.

He used a very small pre-chamber (2-3% of the total combustion chamber volume) with a total orifice area ratio of 0.03-0.04cm^2 per cm^3 of pre-chamber volume and sharp orifice exits to create a small non-critical pressure differential between the pre-chamber and the main chamber. This pressure differential would eject the highly active species into the main combustion chamber. The sharp edge of the orifice creates highly intense turbulence within the issuing jet, breaking up and extinguishing the flame. This turbulence also causes the active species to be widely distributed throughout the main combustion chamber. These act as the nuclei for many explosive ignition sources which begin to react within a very short period after they enter the main combustion chamber. The net result is the chemically active species lower the flammability temperature of the main mixture, hence reducing the

ignition delay for all the ignition sources and sharply increasing the combustion rate and improving the combustion stability.

The extinguishing of the flame is essential for the prevention of NO_x formation. Because the flame is extinguished in the torch passage the main chamber is not exposed to the associated high temperatures, but to the lower temperatures of the active species and burned and partially burned combustion products.

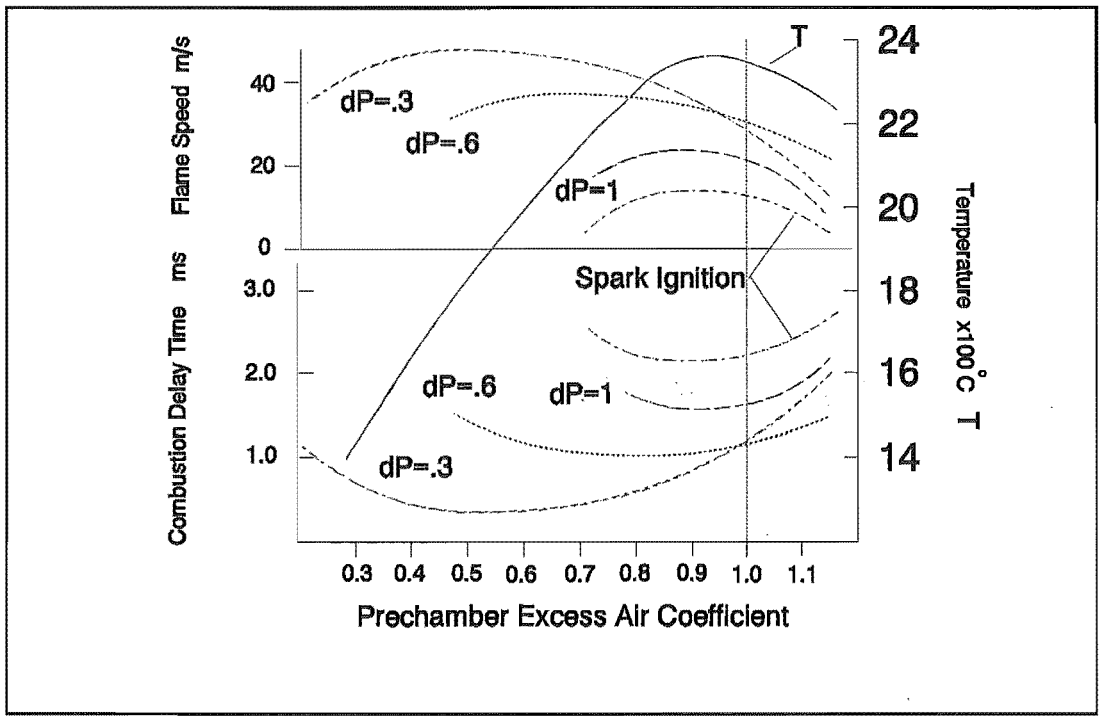

Figure 2,9 Pre-chamber excess air coefficient vs Temperature, Flame speed and Combustion delay time. (dP is the pressure differential across the torch passage)

Figure 2.9 shows the effect of pre-chamber excess air coefficient on overall

temperature, flame speed and combustion delay.

Comparison of emissions measured between two vehicles with identical engines, except one was ignited by a conventional spark and the other by the LAG process, showed that the LAG process reduced all three major pollutants substantially.[73] NO_x was reduced from 17 to 2.96 g/cycle, UHC from 8 to 2.29 g/cycle and CO from 50-70 down to 7.9 g/cycle. As can be seen the LAG process is very effective in the reduction of pollutants.

Summarising, the use of chemically active species as sources of ignition results in a lower temperature of ignition, a decrease in ignition delay and a higher rate of combustion. These factors result in a more stable combustion, a more efficient expansion stroke, improved fuel economy and a significant reduction in exhaust emissions.

2.3.8 Pre-chamber Variations

Various other factors about the pre-chamber engine (mainly the torch ignition system of the kind used by Honda In their CVCC engine) have been studied. These studies report increases in the combustion rate and increases in the combustion stability at lean air/fuel ratios.

Wyzczalek[75] et al used electronic fuel injection into a pre-chamber similar to that used by Gussak. His results supported Gussak's work with the exception of UHC. A substantial increase was noticed and was attributed to the formation of a film of fuel on the pre-chamber wall formed after the fuel was injected into the pre-chamber. A reduction in CO levels was attributed to improved mixture formation at the spark plug during the cold start period, reducing the necessity for extended carburettor choking. NOx reduction was attributed to lower combustion temperatures at the leaner air/fuel ratios.

Varde and Lubin[76] showed that the use of a nozzle connecting the pre-chamber to the main chamber promoted noise generation from the engine. They postulated that the presence of uneven mixture pockets caused periodical acceleration, deceleration of the flame front resulting in the generation of pressure waves in the process, which manifested themselves as audible noise.

Ryu et al[77] studied the effect of torch jet direction on the performance of a pre-chamber stratified charge engine. They found that the jet which was directed down onto the piston crown had the shortest combustion duration, best BMEP and BSFC and smallest spark advance. This was believed to be due to increased turbulence caused by the impingement of the jet on the piston crown.

Sakai et al[78,81] found that UHC emissions increased with increasing orifice diameter under part load. This was thought to occur because with the larger orifice more of the unburned fuel would escape from the pre-chamber during the expansion process. Under optimised conditions full load emissions were found to be lower than a standard engine. Optical studies showed that the flame did not spread through the main combustion chamber until it was deflected off the piston crown.

Purins[79] showed that the air/fuel ratio of the pre-chamber at ignition was a function of the of the angle of ignition, i.e as the ignition angle was retarded more of the lean mixture was forced into the pre-chamber due to the compression action of the piston, hence increasing the proportion of air in the pre-chamber. He found lower NOx levels for the pre-chamber engine, but higher hydrocarbon emissions and poorer fuel economy. The introduction of EGR into the pre-chamber resulted in a substantial drop in NOx emissions, without a significant increase in hydrocarbon emissions.

Pischinger and Adams[80] found that by increasing the cylinder charge motion the fuel consumption was improved under part load, as well as reducing the UHC emissions because more complete combustion was obtained. They also claimed that the thermal efficiency of the stratified charge engine is strongly dependent upon cooling losses due to increased heat transfer at the pre-chamber and throat. This was believed to be due to increased rates of heat

transfer from the combustion chamber due to the increased turbulence levels.

Davis et al[82] showed that the pre-chamber could act as a resonator between the pre-chamber connecting passage and the main combustion chamber. Pressure traces measured at the combustion chamber side showed rarefaction and pressure pulses associated with this behaviour.

Krieger[83] proposed a three phase physical model to describe the operation of the jet ignition combustion phenomenon. He concluded that the jet flame issuing from the pre-chamber was the major source of NOx.

AL-Mamar[84] et al showed that the combustion rate in a dual chamber engine increased as the volume ratio (pre-chamber volume/main chamber volume) increased and as the interconnecting orifice diameter decreased. This was due to an increase in the turbulence levels within the pre-chamber caused by an increase in the volume and velocity of the incoming mixture.

2.4 PREVIOUS WORK AT THIS DEPARTMENT

Zavier[122,123] developed a relatively simple stratified charge system in the Mechanical Engineering Department which is the predecessor to this research. The system involved injecting a small quantity of methane through a

hypodermic needle located in the body of the park plug. The hypothesis being that near TDC the methane puff would be injected and form an "ignition" mixture which would develop a flame which could propagate through the remaining lean charge, which was either methane or gasoline.

Results of engine test work showed that the injected methane produced a positive ignition puff which extended the equipment lean limit of combustion. BTE increased at the leaner air/fuel ratios due to the improvement in the ignition process with the methane puff.

However, UHC emissions were substantially increased for the stratified system over the baseline spark ignition system. The reasons for the difference were believed to be a culmination of:-

1, The injected puff was burning at or near the rich limit of flammability, leading to unburned and partially oxidised hydrocarbons,

2, The methane within the hypodermic tube was unable to be burned as the inner diameter was smaller than the quench diameter for methane/air flames.

Schlieren photography and hot wire anemometry work performed during combustion chamber simulation work showed that the flow field produced near

TDC would sweep the injected puff away from the electrodes of the spark plug and parallel to the combustion chamber wall. This region is synonymous with the flame quenching phenomenon and hence would help to produce the higher UHC emission levels.

It was these points that led to the initiation of this work in order to try and reduce the hydrocarbon levels by reducing the available quench volumes and by controlling the injected methane puff.

CHAPTER 3

TURBULENCE AND COMBUSTION.

3.1 INTRODUCTION

In order to reduce the in-cylinder combustion generated emissions we must first begin to understand the processes occurring within the combustion chamber. When a predetermined charge is ignited within the chamber the resulting flame propagation is highly influenced and dependent upon the turbulent and bulk flows which exist at that time. The following sections look at the air flows within the combustion chamber and their interactions with the combustion of the air/fuel mixture.

3.2 TURBULENCE, SWIRL AND SQUISH.

3.2.1 Turbulence.

Bradshaw[85] defines turbulence as;

> *"a three dimensional time dependent motion in which vortex stretching causes velocity fluctuations to spread to all wavelengths between a minimum determined by viscous forces and a maximum determined by the boundary conditions of the*

flow. It is the usual state of fluid motion except at low Reynolds numbers."

These velocity fluctuations to the turbulent characteristic of rapid mixing of the fluid. Turbulence is energy dissipative by nature. The energy cascades from large scale low frequency eddies to small scale high frequency eddies. Finally the energy is dissipated into heat due to the viscous nature of the fluid. Therefore to maintain a turbulent field energy must be supplied.

The major parameters of interest are the turbulent length scales and the intensity of the turbulence. Figure 3.1 shows a schematic of a coherent turbulent structure.[86]

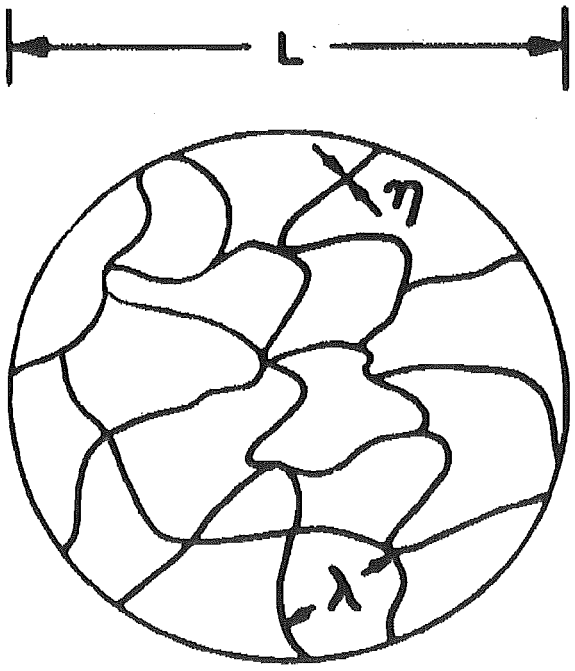

Figure 3,1 Turbulent structure visualisation.

Scale.

The largest eddies generally have a scale† in the order of magnitude of the container in which the turbulent fluid is present. These eddies are generally responsible for the majority of the transport of momentum and species. These large eddies have a characteristic length known as the *INTEGRAL LENGTH SCALE* (L). The smallest turbulent scale present are refereed to as the *KOLOMOGOROV MICROSCALE* (η). These are the dissipative eddies whose motion is dependent upon the kinematic viscosity (υ) and the energy dissipation rate per unit mass (ε). The eddies are characterised by the Kolomogorov length (η), velocity (v) and time (τ) scales given by[105];

$$\eta=\left(\frac{\nu^3}{\epsilon}\right)^{\frac{1}{4}} \qquad \tau=\left(\frac{\nu}{\epsilon}\right)^{\frac{1}{2}} \qquad v=(\nu\epsilon)^{\frac{1}{4}} \qquad (3.1\text{-}3.3)$$

whereas the integral length,velocity and time scales are given by;

$$\frac{\eta}{L}\propto RE^{-\frac{3}{4}} \qquad \frac{v}{u}\propto RE^{-\frac{1}{4}} \qquad \frac{\tau u}{L}\propto RE^{-\frac{1}{2}} \qquad (3.4\text{-}3.6)$$

where, L= integral length scale,

u= integral velocity,

---

†The term scale refers to the relative size of the eddies in the turbulent fluid.

RE= Reynolds number.

The integral scales are related to the Kolomogorov scales by the dissipative nature of the turbulence, i.e the rate of dissipation (ε) can be estimated as the product of the kinetic energy per unit mass of the large scale eddies (αu^2) and the rate of energy transfer (u/L). i.e $\varepsilon \propto (u^3/L)$.

The ***TAYLOR MICROSCALE*** (λ)is a representation of the characteristic length scale of the velocity gradients, or as stated by Tabaczynski[86]

> "*the spacing between the vortex tubes (dissipative eddies) which have a thickness of the Kolomogorov scale*".

The taylor microscale for isotropic turbulence is given as;

$$\frac{\lambda}{L} \propto RE^{-\frac{1}{2}} \qquad (3.7)$$

hence λ is always smaller than the integral length scale L.

Turbulence is said to be *HOMOGENEOUS* if all statistical properties are independent of the location in the field.

Turbulence is said to be *ISOTROPIC* if all statistical properties are independent of the orientation of the co-ordinate axes.

Intensity.

The velocity components of the turbulent flow can be revealed to a contain mean ($\bar{u}$) and fluctuating ($\acute{u}$) velocity components.

i.e $$u_i = \bar{u}_i + \acute{u}_i \qquad (3.8)$$

From this the intensity of the turbulent fluctuations can be given by;

$$\frac{(\acute{u}_i^2)^{\frac{1}{2}}}{\bar{u}_i} \qquad (3.9)$$

i.e a measure of the velocity deviation from the mean flow.

3.2.2 Swirl and tumble.

Swirl can be defined as the rotation of the charge in the cylinder about a vertical axis, not necessarily the cylinder axis. It is induced during the intake

$$C_s = \frac{EFFECTIVE\ TANGENTIAL\ VELOCITY}{RESULTANT\ PORT\ VELOCITY} = \frac{V_t}{V_r} \qquad (3.10)$$

process and the extent is determined by the geometry of the intake valve(s). The presence of a shroud around the valve can aid in the formation of swirl. Swirl is generally described by a swirl coefficient, such as that given by Ma[52],

whereas Kowalewicz[59] gives a swirl ratio as the ratio of rotary speed of the charge within the cylinder to the engine speed.

Fenton[87] states the main effect of swirl is to deviate the flame pattern from a symmetrical path about the spark plug and in doing so increases the flame frontal area hence increasing the burn rate. Fuller[89] concluded that the formation of swirl increased the turbulence intensity of the charge and hence increased the rate of flame propagation.

Quader[88] used a combination of swirl and fuel injection to induce axial stratification of the charge. An early injection, prior to the inlet valve opening, produced unfavourable stratification characteristics with a rich mixture forming just above the piston crown and a lean mixture adjacent to the spark plug and upper combustion chamber wall. A later injection timing had the reverse, and more favourable, effect of producing the richer mixture adjacent to the spark plug.

A characteristic of multi-valve cylinder heads is the ability to produce flow known as tumble or barrel swirl. This can be visualised as a cylindrical rotation of the charge down the horizontal axis of the cylinder as the piston is drawn down the length of its stroke. This flow aids the formation of a more homogenous mixture within the chamber by cyclically mixing the incoming charge with the charge already in the cylinder. The energy associated with the

large tumble eddies is dissipated as turbulence, aiding in the increased propagation rate of the turbulent flame.

3.2.3 Squish.

Squish is the radial inward motion of the cylinder charge due to the movement of the piston nearing top dead centre (TDC). Its presence is brought about by combustion chamber and piston geometry. Squish is used to generate turbulence about the spark plug and to direct the unburned gases into the flame area in order to increase the overall burn rate as the piston approaches TDC. The turbulence generated is generally an-isotropic.

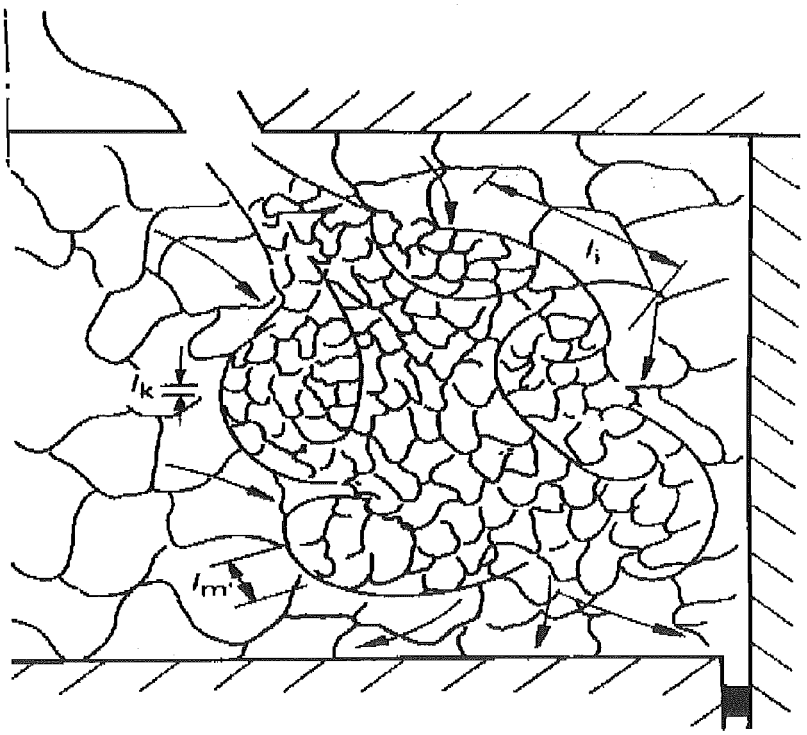

Figure 3,2 Intake flow visualisation.

3.3 FLOWS INSIDE THE CYLINDER.

The work discussed here relates to disc shaped combustion chambers unless otherwise stated. Extensive work has been undertaken on determining the fluid flows within the combustion chamber on both motored and firing engines. However limitations within the measuring processes have prohibited accurate measurement of turbulent length scales. Results obtained to date do show general trends of the gas flow within the chamber from which a great deal has been determined.[97]

The flow of fluid during the intake process is highly dependent upon the geometry of the intake valve(s). The intake process is the main source of the major bulk flows, such as swirl and tumble, as well as the source for turbulence generation. The flow into the cylinder takes the form of a jet characterised by large velocity differences between adjacent points beside the intake valve.[89,90,91] This character produces highly intense turbulence as well as the largest mean flow velocities throughout the induction and compression processes.[90] At low engine speeds there may be some reversal of flow after BDC due to the low inertia of the incoming flow and unfavourable valve timing. At higher engine speeds this phenomena is less likely to occur.[91] Turbulent frequency spectra during induction shows a high frequency bias, the characteristic of a highly turbulent fluid.[92]

As the inlet valve closes the mean flow reduces as well as the turbulence intensity.[90] The original an-isotropic turbulence field produced during induction tends towards isotropy during this time.[92]

Compression of the fluid reinstates the an-isotropic state of the turbulence, due to the energy input into the fluid by the motion of the piston, however as the piston nears TDC viscous dissipation of turbulence energy tends to produce an isotropic field unless a highly directed and strong squish action occurs. However investigations have revealed a certain level of an-isotropic flow at TDC, especially at higher engine speeds for disc shaped chambers with no squish.[94,93] At this stage the energy spectra shows lower frequencies of the flow, compared to the induction process.

Initial investigations of the length scales at TDC show that the integral scales are 3→4 times the microscale and are approximately 1/5th the clearance height between the piston crown and the cylinder head.[93,96]

Grasso[97] summarised the general flows for reciprocating internal combustion engines at TDC for chambers with and without bulk flows. The main points are listed below.

1, *Near TDC the turbulence does not resemble the turbulence produced during induction.*

2, *Near TDC turbulence is homogenous and generally isotropic. Intensity increases with engine speed, early results show a linear relationship, but more recent studies indicate a slightly higher than linear relationship.*[95] *Intensity also increases with increased volumetric efficiency,ie reduced throttling. The maximum attainable intensity is approximately half the mean piston speed.*

3, *In chambers with high initial bulk flows the angular momentum of the flow is dissipated due to viscous effects, but a large proportion generally persists to TDC and contributes to the TDC turbulence. The turbulence characteristics during induction and compression are similar to those mentioned above for flows without initial bulk flows.*

4, *Chambers with squish at TDC produce an-isotropic turbulence and the flow field is dependent upon the TDC chamber geometry.*

5, *Engines with both high initial bulk flows and squish are dependent upon the details of the initial flows and chamber geometry for the details of the TDC flow field.*

3.4 COMBUSTION.

If we were to able to look inside the combustion chamber of a spark ignition engine during the combustion phase of the cycle we would see that as the spark arcs across the electrodes of the spark plug a small, almost spherical, luminous "flame" would appear. It would slowly grow in size and propagate across the chamber at an increasing rate. This rate would continue to increase until the flame neared the edges of the combustion chamber where the flame would slow down and eventually be extinguished.[87] This phenomenon, as simple as it seems is a highly complex process which depends upon the interplay of the chemical and physical processes involved.

The next few sections will deal with the physical structure of the "flame" including the effects of turbulence, and several propagation theories followed by a look at the chemical processes involved with the flame.

NOTE:- Only premixed flames/combustion shall be dealt with, with particular reference to methane, as this is the general system which is involved in this project.

3.4.1 Flame Structure

When discussing the structure of a flame we are talking about the physical properties involved in the deflagration of a self propagating exothermic reaction.

To obtain an understanding of the complex structure of the turbulent flame within the engine combustion chamber we shall first look at the classical structure of a premixed laminar flame. Observing figure 3.3[98,99,100,102] it can be seen that the structure of the flame can be broken into three regions;

1, Preheat zone,

2, Reaction zone,

3, Post reaction zone.

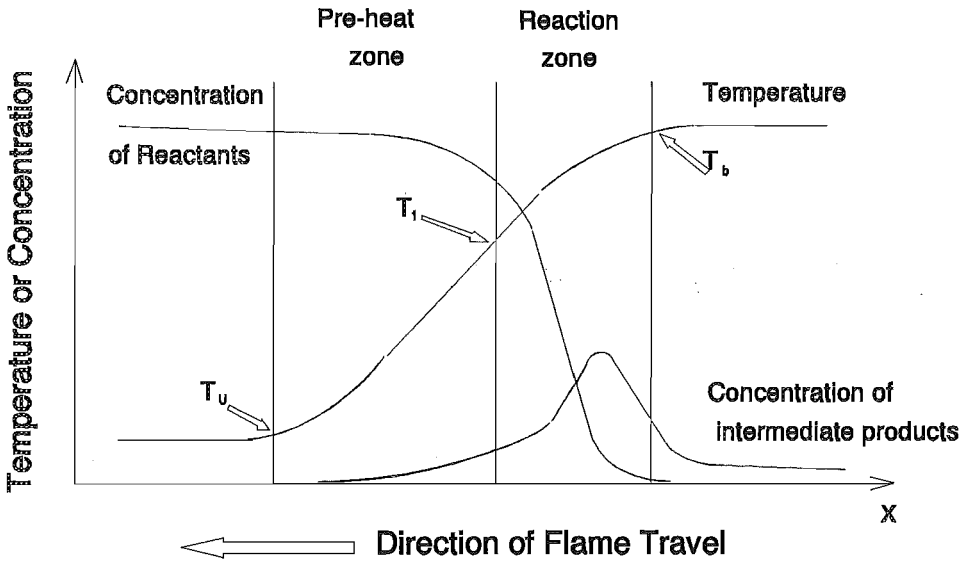

Figure 3,3 Scheme of a Plane Combustion Wave.

1, Preheat zone.

As a flame propagates through an air/fuel mixture heat is transferred from the reaction and post reaction zones ahead of the flame into the upstream gases by both conduction of heat and diffusion of high temperature species. This heat causes the temperature of these gases to rise towards the temperatures encountered within the flame. This temperature rise is generally exponential, although there is a slight deviation due to the variation of the conductivity of the gases with temperature.[100]

Gaydon and Wolfhard[100] have used a 99% temperature rise to define the thickness of the pre-heat zone ($T_u \rightarrow T_1$), however if a 99.9% temperature rise is used then the thickness increases by 50% due to the nature of the describing equations. Lewis and vonElbe[99] give the end of the preheat zone (beginning of the reaction zone) as a temperature T_1 at which time the gas loses more heat to the upstream gases than it receives from the burnt and burning gases downstream. The temperature continues to rise because the reaction rate has become sufficiently high to release a significant amount of heat.

Although called the preheat zone some reactions do occur. For higher order hydrocarbons considerable decomposition, dehydration and polymerization occurs leaving mainly olefins, hydrogen and lower hydrocarbons to react with the oxidiser in the reaction zone.[114] This also helps to explain the similar

flame speeds of most higher order hydrocarbons.[100]

Oxygen in this region acts as a catalyst aiding the decomposition and so little oxygen is consumed.[102]

2, Reaction zone.

The reaction zone is normally associated with the luminous region which is characteristic of most flames. Here the complex series of reactions which oxidise the hydrocarbon fuel occur.

Within the reaction zone the free radicals and other active species produced are dependent upon the fuel being burned. For hydrocarbon flames the OH radicals, O and H atoms are well above equilibrium concentrations within the primary regions of the reaction zone, although the OH level peaks well before either the O or H concentrations.[99,100,102] The high temperature and species concentration gradients found within this region are responsible for the diffusion of the species and heat into the preheat zone. Their role in the combustion process shall be discussed later.

As mentioned before the reaction zone is synonymous with a luminous region. Its presence is brought about by the active species returning to their ground states and emitting light of a certain characteristic wavelength. The light emitted from hydrocarbon flames generally contain the spectrum associated

with CH, C_2, CHO and OH radicals.[101] Behind these primary zones the CO concentration peaks, after which the CO_2 and H_20 concentrations rise to their maximum levels as discussed in chapter 1.

3, Post reaction zone.

This zone contains the products of combustion. Here also the slower reactions continue, such as those of the formation of the oxides of Nitrogen, and the oxidation of CO to CO_2. From here heat is also convected towards the upstream gases. Diffusion of active species from the post flame gases also occurs which aids in the propagation of the flame.

3.4.2 Flame Propagation.

1, Laminar flames.

One of the main properties of a laminar premixed flame is the flame speed (S_L). i.e the rate at which the flame propagates through the unburned region. In a laminar premixed flame the front is thin, continuous and uniform.

Exactly how a flame propagates through a premixed hydrocarbon/air mixture is still not fully understood. Several theories have emerged with sufficient evidence to warrant a closer inspection. These are;

1, Thermal propagation,

2, Radical diffusion,

3, A combination of the above.

The thermal theories of Mallard and LeChatilier claim that the heat liberated during combustion is responsible for sustaining the flame propagation. They developed equations relating the flame speed to the surrounding temperature, thermal diffusivity and reaction rate. The thermal theories also require the concept of the ignition temperature (T_i) which requires careful determination/approximation if the equations are to be used accurately.[102]

Diffusion theories rely on the presence of active species to sustain the flame propagation. Again equations are developed for the flame speed based on the concentration profiles of the active species. However diffusion theories cannot be accounted for in the oxygen-cyanogen (C_2N_2) flame where Hirschfelder[98] reasoned that dissociation did not occur in this system. From these consideration it can be seen that a purely active species diffusion theory cannot fully explain flame propagation.

Attempts to prove one theory or another by experimentation are of little help as both the thermal and diffusion theories are governed by similar differential equations.[98,99,100,102]

Combined theories have been investigated. Berchart[100] theorised that the

active species serve as to eliminate or significantly reduce the highly endothermic initial step. Hence only the chain branching energy is required to sustain the flame. This energy is easily supplied by the heat released by the exothermic chain reactions. Further strengthening of combined propagation theories is obtained by the use of computer modelling in which a series of partial differential equations relating both species concentration and heat release rates are solved simultaneously to obtain the burning velocity. A closer correlation is obtained to experimental values for the combined models than for either the thermal or diffusion models.[102]

An important point to keep in mind is that it is the diffusion of heat and mass which causes a flame to propagate, i.e it is a diffusional process. Also the reaction rates determine the temperature gradient within the flame and hence it also effects the thickness of the reaction zone. These two points are clearly stated in the Mallard LeChatilier solution for laminar flame speed (S_L).

$$S_L \propto (\alpha RR)^{\frac{1}{2}} \qquad (3.11)$$

where; α=diffusivity,

RR=reaction rate

2, Turbulent Flames.

It is well recognised that turbulence interacting with a laminar flame causes an increase in the propagation velocity (or flame speed), hence an increase in the overall burning rate. Glassman[98] suggests that the increased rate may be due to one or a combination of three factors.

"1, *The turbulent flow may distort the flame so that the surface area is markedly increased, while the normal part of the burning velocity remains that of the laminar flame velocity.*

2, *Turbulence may increase the rate of mass and heat transfer and thus increase the actual burning velocity normal to the flame surface.*

3, *Turbulence may rapidly mix the burned and unburned gases in such a way that the flame essentially becomes a homogeneous reaction whose rate depends upon the ratio of burned to unburned gases produced in the mixing process.*"

Damkohler demonstrated that by consideration of the turbulent characteristics of a fluid and the laminar flame characteristics of the mixture that the structure of the turbulent flame would vary accordingly to the appropriate parameters. The Damkohler number[103,104] is defined as the ratio of eddy turn over time to

laminar flame residence time and the turbulent Reynolds number is the ratio of turbulent diffusivity to laminar diffusivity.

$$Da_T = \frac{\tau_T}{\tau_L} = \frac{L}{\delta_L} \cdot \frac{S_L}{\acute{u}} \tag{3.12}$$

$$Re_T = \frac{\acute{u}L}{\nu} = \frac{L}{\delta_L} \frac{\acute{u}}{S_L} \tag{3.13}$$

where; δ_L=laminar flame thickness,

S_L=Laminar flame speed,

L=integral length scale.

u'=turbulent intensity

ν=kinematic viscosity (set equal to the molecular diffusivity, $=\delta^2/\tau_L$.)

Bracco[103,104] claimed that if the size of the eddies at which molecular viscosity is controlling (Komologorov scale η) is much larger than the laminar flame thickness ($\eta >> \delta_L$) the structure of the flame is unaffected by the dissipative turbulence and the large scale eddies will wrinkle the flame front. Here the residence time is much smaller than the eddy turn over time. At the other extreme he claimed that if the integral length scale is smaller than the laminar flame thickness ($L << \delta_L$) then a laminar flame could not exist in the turbulent field.

In relation to propagation rates, consideration of the wrinkled laminar flame model first suggested by Damkohler, shows that by increasing the turbulence the distortion and/or distortion rate will increase the flame frontal area and hence the flame propagation rate. Here the local turbulent flame speed is given by;

$$S_T=S_L+u' \qquad (3.14)$$

Consideration of the second point from Glassman shows that by increasing the turbulent intensity the rate of mass and heat transfer would increase and hence the propagation rate. However, for a given mixture there is an upper limit to the turbulent intensity which can sustain combustion. Beyond this limit bulk quenching occurs resulting in the extinguishing of the flame. This will be discussed further later.

One limitation to the wrinkled laminar flame model is that it is assumed to have a thin reaction zone given by the equation;

$$\delta_L=S_L.\tau_L \qquad (3.15)$$

Tabaczynski et al[86] developed a turbulent burning model based upon the entrainment of the unburned mixture into the flame at a rate governed by the

local turbulence intensity and the laminar flame speed given by:

$$\frac{dm_e}{dt} = \rho_u A_e (\acute{u} + S_L) \tag{3.16}$$

where: m_e=mass entrained,

ρ_u=density of unburned mixture

A_e=area of flame front.

The combustion of this mass takes place in eddies the size of λ_c at a rate of;

$$\frac{dm_b}{dt} = \frac{m_e - m_b}{\tau_b} \tag{3.17}$$

where: m_b=burned mass,

τ_b= time for eddy of size λ_c to be burned by a laminar flame, $(=\lambda_c/S_L)$

The reaction zone thickness is given by;

$$l_f \approx u'\tau_b \tag{3.18}$$

$$\approx u'\lambda_c/S_L$$

Hence the flame thickness is a function of both the turbulence characteristics (λ_c and u') as well as the laminar flame speed S_L. This later point relates any changes in A/F ratio, etc to the model. Note that at the limit of instantaneous burning of the entrained mass ($\tau \rightarrow 0$), the flame thickness tends to zero. This is synonymous with Damkohler's wrinkled flame model. Although good correlation has been found with this model it does not address the mechanisms by which the flame propagates through the turbulent fluid.

Chomiak[105] postulated that as the flame front reaches the dissipative eddies

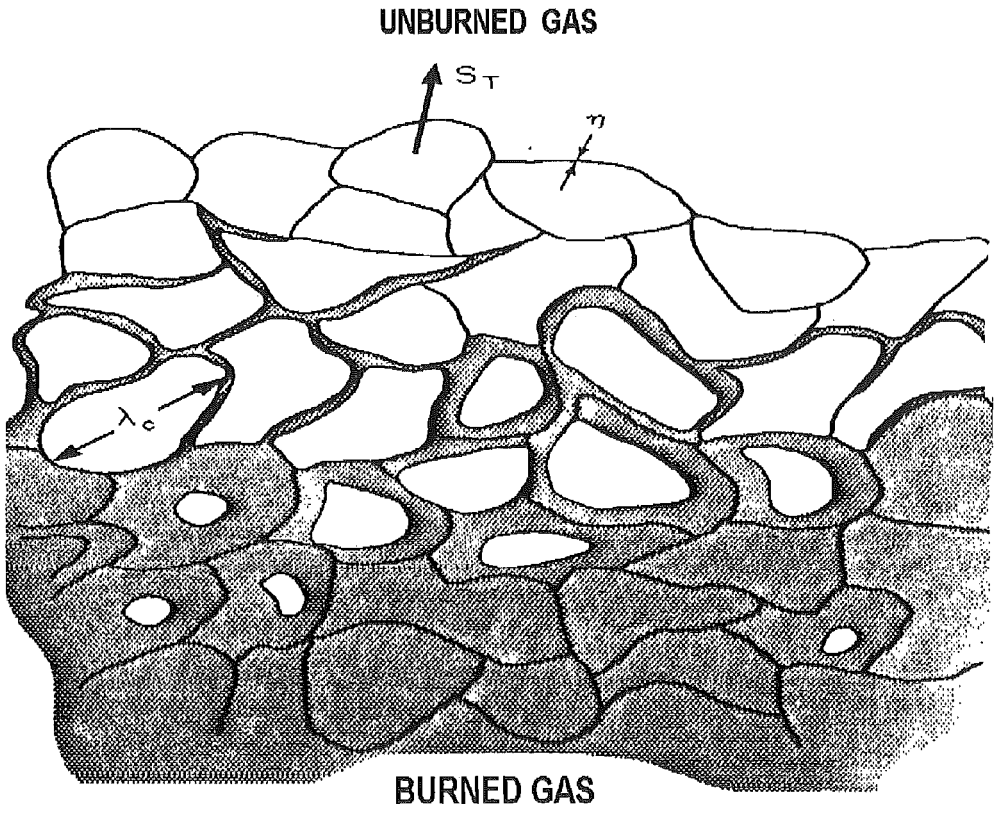

Figure 3,4 Chomiak's turbulent flame visualisation.

the high shear associated with these eddies quickly propagates the flame across the dissipative eddy. The burned gases expand and increase the pressure in the burned gas region of the dissipative eddy relative to the unburned region. This provides a driving force for the motion of the hot gases towards the cold gases. This s to increased propagation of the flame along the dissipative eddies with a velocity proportional to the intensity of the turbulence. The flame propagates across the fluid within the Taylor microscale eddies at a rate similar to the laminar flame speed.

3.4.3 Bulk Quenching of the Flame.

Exactly how a flame is extinguished by excessive turbulence is not yet fully understood, although there are several models which go some way to understand the phenomenon.

Using the wrinkled laminar flame front theory, Shelkin[113] predicted that the turbulence could distort the flame front so much that "islands" of flame could break away form the main flame, lagging behind the flame front . If the "island" consisted of a sufficiently large quantity of fresh gas then the "flamelet" would become extinguished due to insufficient heat available from the burnt gases in the "island" to initiate the combustion within the unburnt gases within the "island".

Lewis and vonElbe[99] proposed that the larger wrinkled area of flame increased the rate of which heat and active species are transferred to the unburned gases. Hence the amount of heat a mass element loses to the cooler unburned increases. From this there must be a critical level whereby the heat gained and produced by the reacting mass element must equal the heat lost to the unburned gases. If this point is exceeded then the flame will be quenched.

Chomiak[106] argued that if the intensity was excessively high then the shear in the Kolomogorov scale eddies could mix the burned and unburned gases in the eddies at such a rate that the heat liberated by the reacting gases could be insufficient to maintain the deflagration through the gases in between the eddies. Hence the flame would become extinguished.

Lockwood and Megahed[107] proposed a small turbulent scale quench model whereby if the inter-diffusion rate between hot and cold eddies is greater than the volumetric rate of chemical reaction then quenching would occur. Several other theories have evolved along these lines, generally claiming that for small scale turbulence the lifetime of the eddy must be greater than the time for the reaction to occur, else quenching would occur.

Daneshyer et al[108,109] looked at the effect of strain fields on the development of laminar flames, with special attention paid to the development of the flame

kernel at a spark plug in order to reduce cyclic variations in the internal combustion engines. They concluded that the strain fields induced by the velocity gradients reduced the burning velocity and could produce extinction of the flame. This effect was more pronounced when heat loss from the region also occurred.

3.4.4 Flame Structure inside the Engine.

Consideration of the turbulence characteristics, engine speed, compression ratio, stroke, bore, clearance height, residual gas mass fraction and volumetric efficiency of the engine the laminar and turbulent burning characteristics of an engine can be estimated by consideration of the Damkohler (Da_t) and turbulent Reynolds (Re_t) numbers.[103,104]

Consideration of the meaning of the Damkohler and turbulent Reynolds numbers infer that at low engine speeds the engine combustion would be dominated by wrinkled laminar flame theories.[103,104] This has been supported experimentally by the use of visual techniques such as schlieren photography. Bracco et al[103] showed mild wrinkling of the flame below 600rpm and extensive wrinkling and some fragmentation of the flame above 1200rpm. (See figure 8 in reference 103) The use of lasers by Baritaud and Green[110] in order to section the flame into a two dimensional field has enforced these observations. The technique was not able to obtain accurate data above

1500rpm. However it was noted that at these speeds that both burned and unburned pockets of gas were observed inside the flame, and their size varied from a few tenths of a millimetre to several millimetres. The presence of these pockets of unburned mixture could be construed as evidence for entrainment models of turbulent combustion.

Keck et al[111] studied the early flame development using high speed schlieren photography on a square piston engine operating at 1400rpm. Their experiments supported the wrinkled laminar flame and extrapolation of the flame growth rate revealed that at a burned gas radius of zero the flame velocity was in close approximation with the laminar burning speed for the mixture at the spark plug. They also claim that the most important parameters controlling the initial growth of the flame are the laminar flame speed and the size of the first burned eddy.

Grasso[97] et al have summarised the general combustion properties of homogeneous charge spark ignition engines as follows;

a, The ignition kernel is influenced by the engine turbulence as soon as it is formed.

b, The turbulent flame is made up of a wrinkled laminar flame which is altered by the engine turbulence. The degree of wrinkling, ratio of

turbulent burning speed to laminar burning speed and the thickness of the turbulent flame zone increases with engine speed.

c, Wrinkling and fragmentation of the flame increases with leaner charges and local extinction is likely at very lean conditions.

d, Turbulent intensity ahead of the flame is not significantly influenced by the propagation of the flame, but increases markedly across the flame front.

3.4.5 Combustion within the Engine.

The combustion of the charge within the combustion chamber can be separated into four principle stages;

1, Ignition/kernel development, θ_k
2, Ignition delay period, θ_i
3, Turbulent combustion, θ_c
4, Flame extinction.

When discussing the combustion of the charge within the combustion chamber it is more useful to discuss it in terms of mass fraction burned rather than the distance propagated across combustion chamber, as this allows a comparison of combustion chambers/engines to be made. See figure 3.5.

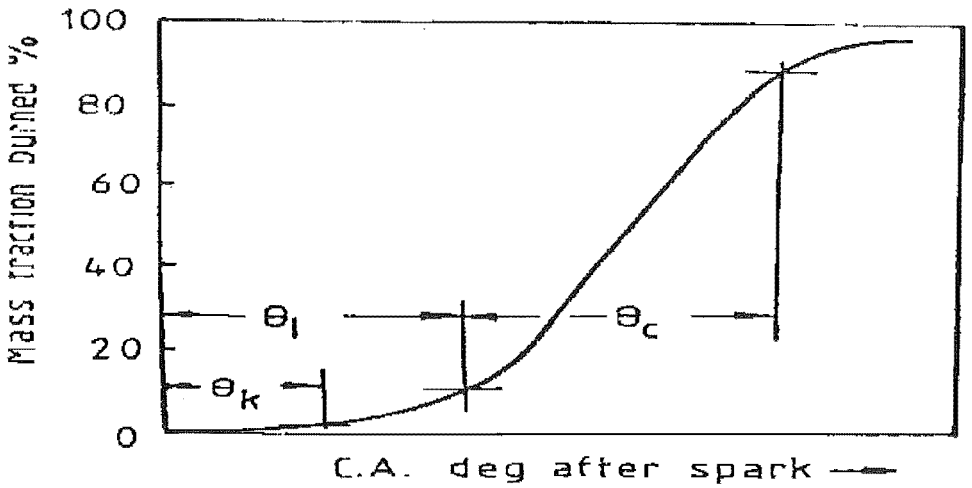

Figure 3,5 Mass fraction burned as a function of crank angle.

1. Ignition/kernel development. θ_k (0-1% of charge burned.)

The generation of a spark produces a high temperature, highly ionised and chemically active volume of air/fuel mixture around the spark plug electrodes.[114] Depending upon the charge motion around the electrodes at that time one or multiple turbulent eddies may be ignited. The combustion at this point is laminar and is occurring within the ignited eddies. These first eddies must be burned before the turbulent effects on the flame can begin to occur.[118]

2. Ignition delay. θ_i (1-10% of charge burned)

The ignition delay can be defined as the time, or crank angle duration, from the time of the spark until a measurable pressure rise in the cylinder, by combustion, is detected. Ignition delay is caused by the relatively slow initial combustion rate due to the large thermal mass of the unburned charge extracting energy from the small reacting region. The reduction of the ignition delay period is widely recognised as aiding in the reduction of the overall combustion period.[111,112,114] This can be achieved by the introduction of swirl into the main chamber, or the introduction of directional turbulence, ie squish, towards the spark plug. Excessive turbulence or bulk motion around the spark plug can have a detrimental effect on the development of the flame front as discussed in section 2.2.

The establishment of a reduced ignition delay is also dependent upon the chemical properties of the air/fuel mixture. A fuel with a high laminar flame speed will have a shorter ignition delay under identical operating conditions than a fuel with a slow flame speed. A homogeneous and easily ignitable (stoichiometric) mixture around the spark plug area will have a shorter ignition delay than a heterogeneous mixture. Consistent reproduction of the ignition delay has been shown to reduce the cyclic variability of the combustion duration.[118]

3, Combustion duration. θ_c (10-90% of charge burned)

This duration is primarily dependent upon the bulk and turbulent flows within the cylinder. For a given air/fuel ratio the combustion duration on a crank angle basis has been shown to be almost constant for any engine speed.[86,87,112] On a time basis, the duration decreases with increasing engine speed due to the increase in turbulent intensity associated with the increase in fluid flow velocities.

4, Extinction. (90%- of charge burned)

As the flame approaches the cylinder walls heat is transferred from the flame to the walls. This reduces the flame speed and hence the burn rate. At a certain point the heat removed from the flame to the walls will exceed that generated by the flame and hence the flame will be extinguished.

3.5 HYDROCARBON OXIDATION

3.5.1 Introduction

Chemical reactions involving the oxidation of hydrocarbons can be represented by an overall reaction detailing the exact amounts of fuel, oxidiser and products. Within this overall reaction there exists a series of sub-reactions, some exothermic, some endothermic, some promoting the overall reaction and others terminating the reaction. It is this overall system which will be discussed

in this section, ending with a look at the oxidation of methane.

3.5.2 Chemical pathways

In reacting a hydrocarbon fuel with an oxidiser a network of simultaneous, interdependent reactions, called branching chain reactions, will occur. The products of one reaction being the reacting constituents of another This continues until the final overall reaction has occurred. The intermediate species being formed will generally be free atoms or radicals.[101,102] The initial production of these species is highly endothermic, but once produced they react rapidly with stable molecules to form less stable species which will further react. This "chain" reaction process consists of four stages;

1, Initiation reactions,

2, Propagation reactions,

3, Chain branching reactions,

4, Chain terminating reactions.

1, Initiation reactions.

This is the process by which the initial active species are produced, generally by the dissociation of a reactant molecule. This is achieved by either thermal degradation, or by an external energy source such as a spark. Within internal combustion engines these reactions are normally associated with the relatively long ignition delay period after the spark.

These reactions can generally be represented by;

$$I \rightarrow A^{\circ} + B^{\circ} \qquad (3.19)$$

eg $$CH_4 \rightarrow CH_3 + H \qquad (3.20)$$

where; I = initial reactant,

A°, B° = resultant radical species.

2, Propagation reactions

Propagation is the result of radicals produced in the initiation reaction attacking more fuel molecules producing new propagating radicals and stable products, generally expressed by;

$$B^{\circ} + I \rightarrow C^{\circ} + P \qquad (3.21)$$

where; C° = new propagating radical,

P = stable product.

These are generally high temperature reactions and in hydrocarbon combustion reactions OH and H radicals are the major participants.[101]

3, Chain branching reactions.

In this process a single radical reacts with a stable molecule to form two or more radicals, ie

$$A^\circ + P \rightarrow 2B^\circ + \ldots\ldots \qquad (3.22)$$

The chain branching reactions generally have higher activation energies than the propagation reactions with which they compete. Because of this higher activation energy and hence lower reaction rate, a thermal explosion can be avoided.

4, Chain termination reactions.

This is the result of the recombination of two radicals to form a stable species which is unable to further self-propagate. This recombination is highly exothermic and generally requires an inert third body to absorb the energy released. ie

$$A^\circ + B^\circ + M \rightarrow AB + M \qquad (3.23)$$

where; M = inert body.

These reactions tend to predominate in the post flame regions just after the main reaction zone. The high exothermic nature of these reaction provides the energy to further propagate the flame. Barnard and Bradley[102] claim that as much of 75% of the available enthalpy is liberated by the reactions in this phase.

3.5.3 Reaction Regimes.

When looking at the combustion of hydrocarbons it must first be pointed out that two distinct regimes of combustion occur, namely low temperature and high temperature combustion. These two regimes are separated by a distinct boundary, across which the reaction goes from a slow reaction to a sometimes explosive fast reaction.

Low temperature.

Consider a gaseous hydrocarbon/ oxidiser mixture within a vessel which can be externally heated. At ambient temperatures generally no observable reactions take place.(Depending upon the hydrocarbon and oxidiser present) Increasing the temperature to about 200°C may to the formation of various other compounds, including some CO and H_2O, but the major products are generally hydrocarbon based, such as alkenes, aldehydes, ketones and alcohols. The reactions involved within this system generally have low reaction rates and hence proceed over a relatively long period of time. These reactions can be associated with the degradation of higher order hydrocarbons in the preheat zone of a propagating flame.

For high order hydrocarbons a further increase in temperature (@ 300→400°C) results in the appearance of one or more "cool" flames. These cool flames are associated with knocking combustion for the higher order hydrocarbon fuels.

However these do not occur for methane and will therefore not be discussed further.

High temperature.

The mechanisms and reactions involved in high temperature oxidation of hydrocarbons differ markedly from those involved in the low temperature regime. High temperature reactions can be associated with the self propagating flame discussed earlier.

Within the reaction phase the temperatures favour the chain propagation and branching reactions, ie the high temperatures promote the formation of radicals, particularly hydrogen atoms.[102] The reactions end in the recombination and post flame regions with chain termination reactions releasing large amounts of energy which aid in the propagation of the combustion reactions throughout the remaining fuel/oxidiser mixture.

3.5.4 Methane oxidation

The high temperature oxidation of methane can be summarised by the tree diagram in figure 3.6. The propagation reactions are primarily;

$$OH + CH_4 \rightarrow H_2O + CH_3 \quad (3.24)$$

$$H + CH_4 \rightarrow H_2 + CH_3 \quad (3.25)$$

$$O + CH_4 \rightarrow OH + CH_3 \quad (3.26)$$

The methyl radicals produced will react with either molecular O_2 or O atoms to give formaldehyde. The formaldehyde is quickly removed by radical attack to form formyl radicals which in turn form CO.

Chain branching of the above reactions is believed to be due to the hydrogen oxygen reaction;

$$H + O_2 \rightarrow OH + H \quad (3.27)$$

The hydrogen atoms being produced by the methyl oxygen reaction;

$$CH_3 + O \rightarrow HCHO + H \quad (3.28)$$

In fuel rich situations methyl radicals can be removed by other methyl radicals to form ethane;

$$CH_3 + CH_3 \rightarrow C_2H_6 \quad (3.29)$$

The high temperature oxidation reactions of methane are highly dependent

upon the presence of the H atom, which in turn is dependent upon the overall air fuel ratio.

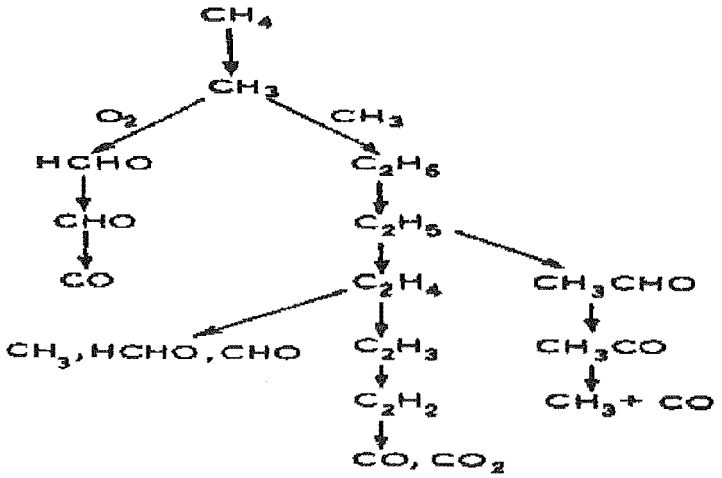

Figure 3,6 Methane reaction path schematic.

3.5.5 Methane as an automotive fuel.

Methane for industrial and automotive use is primarily sourced from natural gas which is typically composed of 80-95% methane, depending upon the site of the gas field.[119,120] Methane can also be produced by the scrubbing of bio-gas produced from the anaerobic decomposition of organic material from such places as sewages works and refuse dumps. This generally has a composition of 65% methane and 35% CO_2. The methane for this work was sourced from Christchurch city councils bio-gas works and contained 99.6% methane after scrubbing.

Thermodynamic properties of methane are given in the table below.[‡]

Table 3.1 Thermodynamic properties of Methane.

Formula	Density at 0°C & 101.3kPa	Boiling point at 101.3kPa	Heat of Combustion	Auto ignition temp.	Ideal Air Req.	RON
CH_4	0.72kg/m^3	-162°C	50.0MJ/kg	813 °C[¥¥]	17.2kg/kg	130[£££]

As an automotive fuel methane has distinct advantages and disadvantages. The high octane number allows its use in most automotive engines without fear of knock occurring. This high octane number also has the potential to increase the compression ratio of the engine to increase the power output and thermal efficiency. The heating value of a stoichiometric mixture is comparable to a stoichiometric gasoline-air mixture. The use of methane generally produces lower emission values of hydrocarbons than an identical gasoline operated engine,[115,116,117] the majority of these emissions comprising of methane with very little photochemically reactive hydrocarbons being produced.[115] These lower emissions can generally be attributed to enhanced combustion characteristics obtained by good mixture formation of the gaseous

---

‡ From Bosch automotive handbook.[124]

¥¥ From Bond ,"Sources of Ignition".[125]

£££ From Lenz "Mixture formation in spark ignition engines."[114]

fuel. It has also been noted that engine wear has been reduced when using methane.[116] This is believed to be due to the inability of the methane to dissolve the lubricating oil film on the cylinder walls as is the case with gasoline, aswell as reduced solid matter fromation on the combustion chamber surfaces.

A "not so useful" characteristic of methane is its slow laminar flame speed.(S_l) Figure 3.7[114] gives the flame speeds of methane and other fuels. This slow flame speed leads to long combustion duration periods and hence requires excessive ignition advance angles, especially if lean mixtures are to be used.

The good mixture formation of the gaseous fuel is offset somewhat by the displacement of air by the fuel due to its low density. This lowers the volumetric efficiency and hence the power output by as much as 15%.[115] This could be overcome by the use of direct injection during the compression stroke. However careful design of the system would be required in order to ensure satisfactory mixture formation occurs.

A major safety problem with methane is its storage. Heavy thick walled high pressure cylinders are required to store a sufficient quantities of the fuel at pressures up to 200 bar. The alternative is to liquify and store it under moderate pressures. However the cryogenic temperature of liquid methane also presents a problem, from a safety point of view if a leakage or vessel

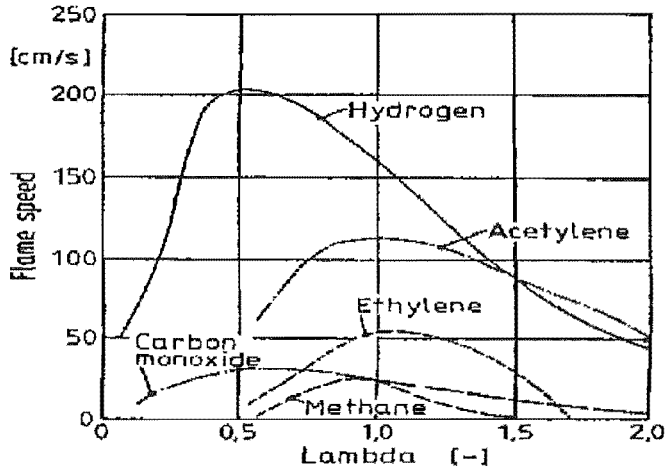

Figure 3,7 Flame speeds of methane and various fuels.

fracture should occur. Heat leakage into the cryogenic vessel would result in continual boil-off of the methane. This would have to be vented to prevent excessive pressure build up in the storage vessel. This boil-off can be reduced with the appropriate insulation materials for the storage vessel, but the increase in capital costs cannot be justified for the increase in fuel capacity and reduced boil off benefits.[115]

CHAPTER 4

EXPERIMENTAL APPARATUS

4.1 INTRODUCTION

In order to test the developed combustion system, a large amount of experimental equipment was necessary for engine operation as well as data observation, capture and analysis. The following chapter deals with the design, construction and use of this equipment.

The equipment utilised in this project can be divided into two main sections;-

1, equipment associated with the operation of the test engine,

2, equipment associated with the appropriation of experimental data.

4.2 DESIGN PHILOSOPHY

Zavier[122] concluded that the methane injected through the spark plug apparatus was burning at approximately the rich limit of flammability, hence high levels of unburned hydrocarbons were detected in the exhaust gases. Consideration of Schlieren photographs of the flow simulation work within a constsant volume combustion bomb, also by Zavier, showed that the injected puff was being swept tangentially away form the spark plug along the combustion chamber walls. This region, being associated with the flame

quench phenomenon, would also to increased levels of unburned hydrocarbons. Consideration of these factors pointed towards of the use of a pre-chamber to try and control the flow field around the spark plug in this research project. By utilising the existing spark plug hole in the cylinder head, the necessity for a new cylinder head casting could be eliminated, hence producing a more cost effective solution to the research.

In a further attempt to reduce the likelihood of extremely rich methane pockets being present within the combustion chamber, it was decided to attempt to "pre-mix" the ignition charge prior to ignition. Mixing of this charge in a separate mixing vessel, under the pressures required for injection was believed to be both highly complex and dangerous. Special mixing and monitoring systems would be required to carefully ensure that the injected

Plate 4,1 Pre-chamber location in cylinder head.

ignition mixture was both homogeneous and consistently mixed within tight limits. Damiano[119] found the mixing of methane and oxygen mixtures to be highly temperamental, in so much that they were easily ignited by a small static discharge from the operator to the mixing vessel. This resulted in several explosions within his mixing vessels. Although the ignition energy requirements for methane/air mixtures is higher, the possibility of lightback into a premixed mixture was seen as just a potential hazard. These factors were considered important enough to abandon the idea of external formation of the ignition mixture. Formation of the ignition mixture within the pre-chamber was decided upon and would be accomplished by the induction of a small quantity of air and the subsequent injection of methane into the pre-chamber to produce this mixture.

The primary difference between this work and other pre-chamber work undertaken by other researchers is that the "ignition" mixture is formed within the pre-chamber, with both air and fuel being introduced into the pre-chamber space separately to form this mixture. Other research has either used pure fuel injection and relied upon mixing between the fuel and the main lean air/fuel mixture to form an ignitable mixture around the spark plug, or used low pressure external mixture formation (generally carburation) to provide the ignition mixture.[69,70,71]

4.3 ENGINE APPARATUS.

4.3.1 Pre-chamber Design

The main pre-chamber design philosophy was based upon the Honda CVCC[††] (flame torch ignition) system developed by Date et al.[(69)] The design was selected as the basis for this work because of the large amount of previous work undertaken to determine the optimum dimensions of the pre-chamber, and the relative success that Honda had with the design with respect to the reduction of engine emissions.[‡‡] Date et al[(69,70,71)] have described the optimised pre-chamber volumes, connecting passage areas, etc in terms of the main chamber volumes. These equations for the pre-chamber dimensions are given below.

$$\frac{V_a}{V_c} = 0.073 \qquad \frac{F_t}{V_a} = 0.091 \qquad (4.1, 4.2)$$

where; F_t= pre-chamber throat area,

V_a= pre-chamber volume,

V_c= clearance volume = (V_a + V_m)

V_m= main chamber volume at TDC.

[††] Compound Vortex Controlled Combustion

[‡‡] See chapter 3 for a more detailed description of the system.

However certain parameters did exist which limited the application of these equations to the design of the pre-chamber for the engine used in this research project.

These factors were:

1, the use of the 14mm spark plug hole as the connection to the main chamber,

2, The maximum chamber dimensions were limited by the Ricardo cylinder head dimensions.

Zavier[122] and Damiano's[119] work utilised the spark plug to inject the methane into their respective combustion chambers. However with the pre-chamber present it was visualised that the methane and air could be directly supplied to the pre-chamber into the vicinity of the spark plug electrodes without modification of the spark plug.

4.3.2 Test Engine.

The engine used throughout this project was a **Ricardo E6/MK6 variable compression ratio research engine,** located in a test cell in the thermodynamics laboratory of the Mechanical Engineering Department. The power generated by the engine is absorbed through an **electric swinging field direct current type dynamometer**, which facilitates measurement of the torque and power generated, and is finally dissipated through a resistance bank. The

dynamometer also serves to motor the engine over the speed range when the motor is not firing, or is loosing power. **Control and measurement** of the engine speed is facilitated by the associated dynamometer controller. The controller also enables the engine/dynamometer set to be operated in one of three modes;-

1, **MOTORING** - the dynamometer acts as the power source to crank the engine, the engine does not fire in this mode.

2, **LOAD** - the dynamometer absorbs the power generated by the engine. The speed will also be held constant if the load applied is varied.

3, **FIXED SPEED** - the dynamometer is used both as a dynamometer and as a motor, automatically switching modes in order to hold the speed constant, even if the engine ceases to fire.

The control console also houses the controls for the oil, water and fuel temperatures, the temperature readout for the various thermocouples distributed around the engine, and the charge amplifier for the pressure transducer.

Lubrication and cooling of the engine are undertaken by separate pumping systems, ensuring that the measured power from the dynamometer is not effected by the power required to operate these pumps.

Ignition of the engine is undertaken by an electronic system whereby the timing may be varied between TDC and 60°BTDC by adjusting a lever located on the front of the engine. An infra red slotted optical switch supplies a signal to an amplifier which in turn supplies the primary voltage to the ignition coil thereby supplying the ignition energy. By varying the point at which the beam of the optical switch is uncovered the timing of the ignition is also varied. The coil fitted is a Lucas sports coil. The spark plug used throughout the project was a **NGK B6HS** plug with the gap set to 0.6mm. Accurate determination of the spark timing was obtained using a stroboscope flashing on the flywheel which was marked with 1° increments around the circumference. The stroboscope was triggered by a signal from the input to the ignition coil.

An **Alcock Viscous Flowmeter** was used to measure the flowrate of air through the main inlet system into the engine, by means of measuring the pressure drop across within the flowmeter with a variable slope manometer. By use of this data the volumetric air flowrate could be obtained with the equation;

$$\dot{V} = 7.7 * 10^{-5} * h * k \qquad (4.3)$$

where; V = Volumetric flowrate (m^3/s)

h = Manometer height (mm)

k = Temperature correction factor.

A table was supplied with the flowmeter to allow for variations in the ambient temperature. The mass flow rate could be further calculated if the local barometric pressure is known and applying these quantities to the ideal gas equation.

4.3.3 Auxiliary Equipment

In order to prevent reversal of flow into the pre-chamber air and methane supply systems from the pre-chamber during the compression stroke and combustion process, as well as to prevent the methane injector coming into contact with the combustion products, non return valves were fitted. However the requirements of the air system are different to that of the methane injection system.

AIR SYSTEM:- The air system is required to supply the pre-chamber with a volume of air so that the mixture formed in the pre-chamber during induction can vary between a mixture near the rich limit of flammability and a stoichiometric mixture. It is assumed at this stage that the volume of "ignition" mixture to be supplied will have maximum volume of twice the pre-chamber volume. This value was seen as a starting point at the design stage and was optimised during the engine testing. The flow would be regulated by the use of a metering valve upstream of the check valve. The NRV selected was a standard Swagelok SS-2C-1/3 check valve with the reseating spring removed to aid the flow at low manifold pressures and a spacer inserted to reduce the

amount of "dead" quench space where the production of UHC's could occur. The minimisation of downstream volume in the air NRV was not assumed to be as critical as that in the methane injector NRV, as the mixtures which could form in the air NRV are assumed to be extremely lean due to the excess air in the NRV after the induction stroke has been completed.

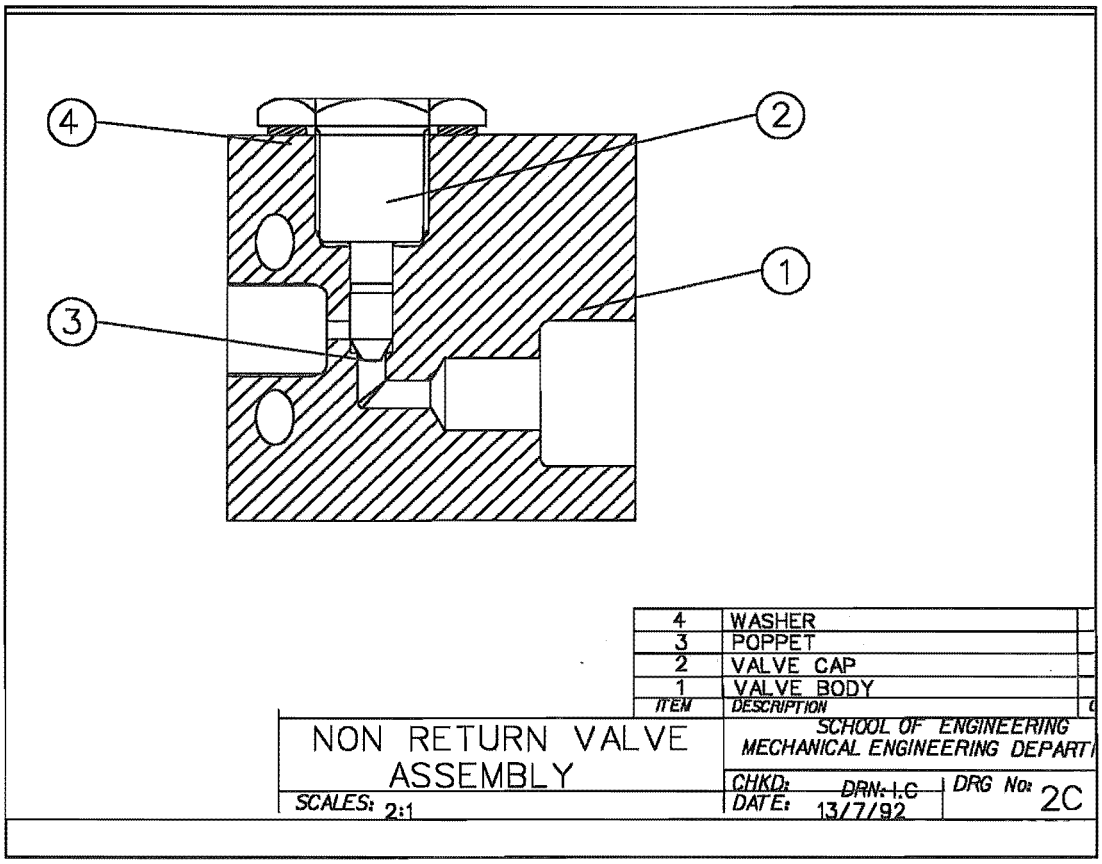

Figure 4,1 Methane Injector Non-Return Valve.

METHANE SYSTEM:- The methane injector would contain pure methane on the downstream side just after injection had ceased, so the minimisation of the downstream volume was critical. For this situation a special NRV was constructed to secure the injector on the upstream side and to connect directly

to the pre-chamber supply line on the downstream side. The internal valve mechanism and gas lines are shown in fig 4.1.

INJECTOR:- The injector that was used was a commercially available BOSCH petrol injector, part number 0 280 150 201. This injector is identical to the ones used by both Zavier and Damiano. Plate 4,2 (pp110) shows the injector and NRV assembly.

INJECTOR CONTROL:- To drive the injector the pulse generator in figure 4.2 developed by Zavier[122] and Glasson[121] was used. The start of the injection pulse was controlled by a slotted optical switch mounted on the rear of the camshaft. A slot in a disc attached to the camshaft exposed the switches sensor to an Infra-red light beam, triggering the circuit. The signal delay was provided by a mono-stable multivibrator (74121). The duration of the delay, and hence the injection duration, is controlled by a variable resistor/capacitor circuit within the injection control circuit. By varying the resistance of the R-C circuit the time constant would change, hence the duration of the pulse will vary accordingly. The variable resistor within the circuit would allow a pulse duration of between 1 and 20ms. The signal was finally inverted by the 7406 inverter to provide a 5volt square pulse applied to the gate of a BUK453 transistor. This signal would switch the transistor to the **ON** state, connecting

the drain terminal to the source terminal. This would have the effect of earthing one of the output terminals, producing a 12 volt square pulse which was used to activate the injector.

Incorporated within the circuit was a trigger output for the stroboscope. This was used to accurately define the start and end of the injection pulse as the strobe flashed on the flywheel which was marked at 1° increments around the circumference. The start or end of the injection was selected by a switch located on the injection control box.

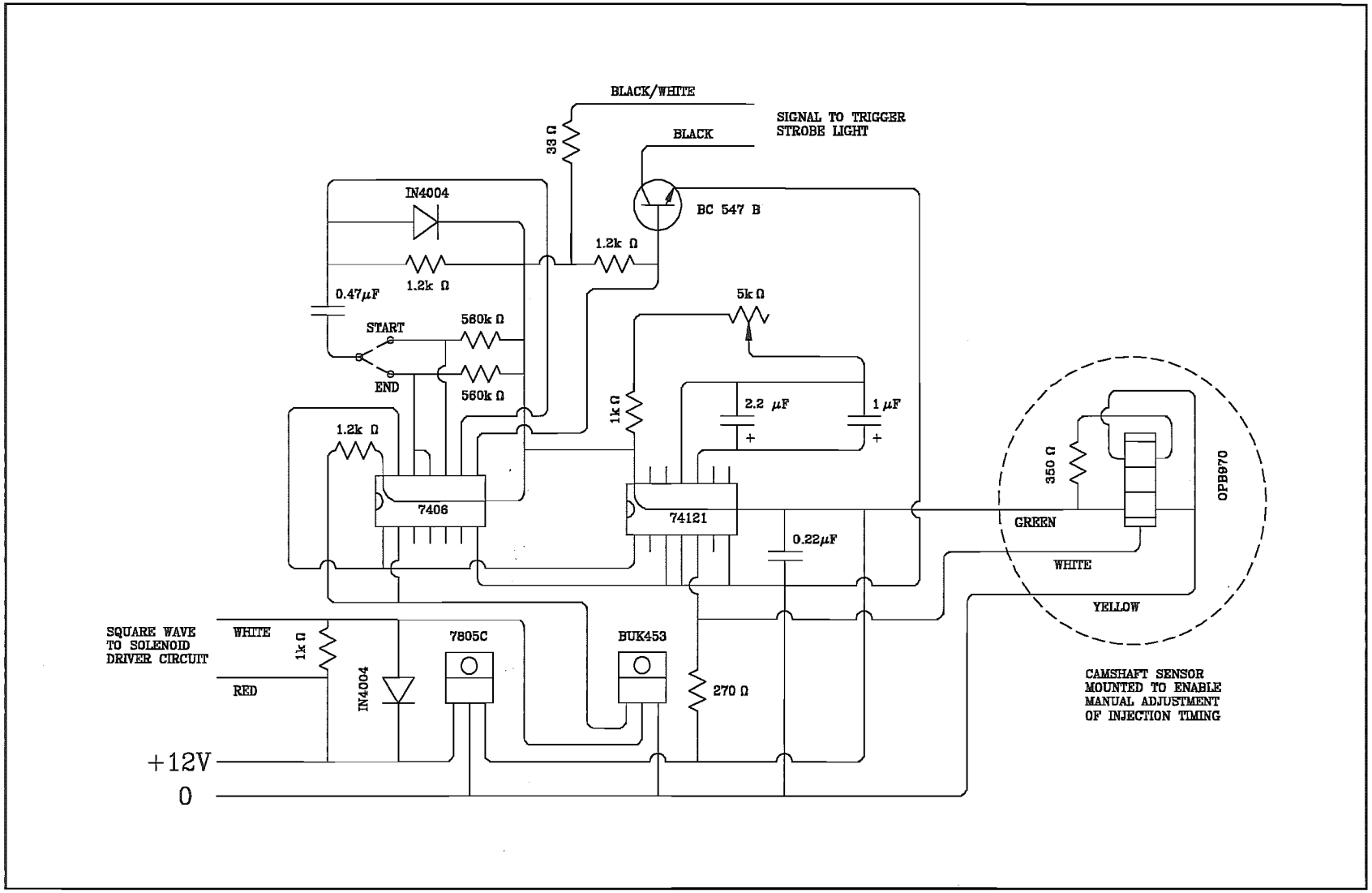

Figure 4,2 Injector driver circuit.

INJECTOR OVER-VOLTAGE PROTECTION:- When the voltage signal supplied to the injector is switched off, the magnetic field of the injector coil is required to decay before the injector can begin to close. This decay of energy can create extremely large back EMF's in the order of hundreds of volts, which if left unaccounted for can cause serious damage to both the control circuitry and the injector coil itself. A simple circuit was designed to prevent excessive voltages occurring across the injector terminals. Figure 4.3 shows the protection circuit.

When the control circuit is in the **OFF** state all three input terminals are maintained at a voltage of +12volts. This state is a characteristic of the injector control circuit described in the section above. When the control circuit becomes **ON** input terminal T2 is set to zero volts, producing a voltage drop across the gate and source terminals of the power MOSFET M1. This switches on the MOSFET and allows current to flow through the solenoid coil, actuating the injector. When the control circuit switches back to the **OFF** state, T2 returns to +12volts, removing the gate-source voltage and switching the injector solenoid off. As the magnetic field collapses within the injector coil a back EMF is generated. The maximum level of this EMF is limited by the Zener diode Z1 to 90 volts, protecting the power MOSFET from over-voltage exposure. The power MOSFET was rated at 150 volts maximum. The power diode D1 allows the residual current to circulate through the injector and the 6Watt power resistor R1, where the energy is dissipated as heat.

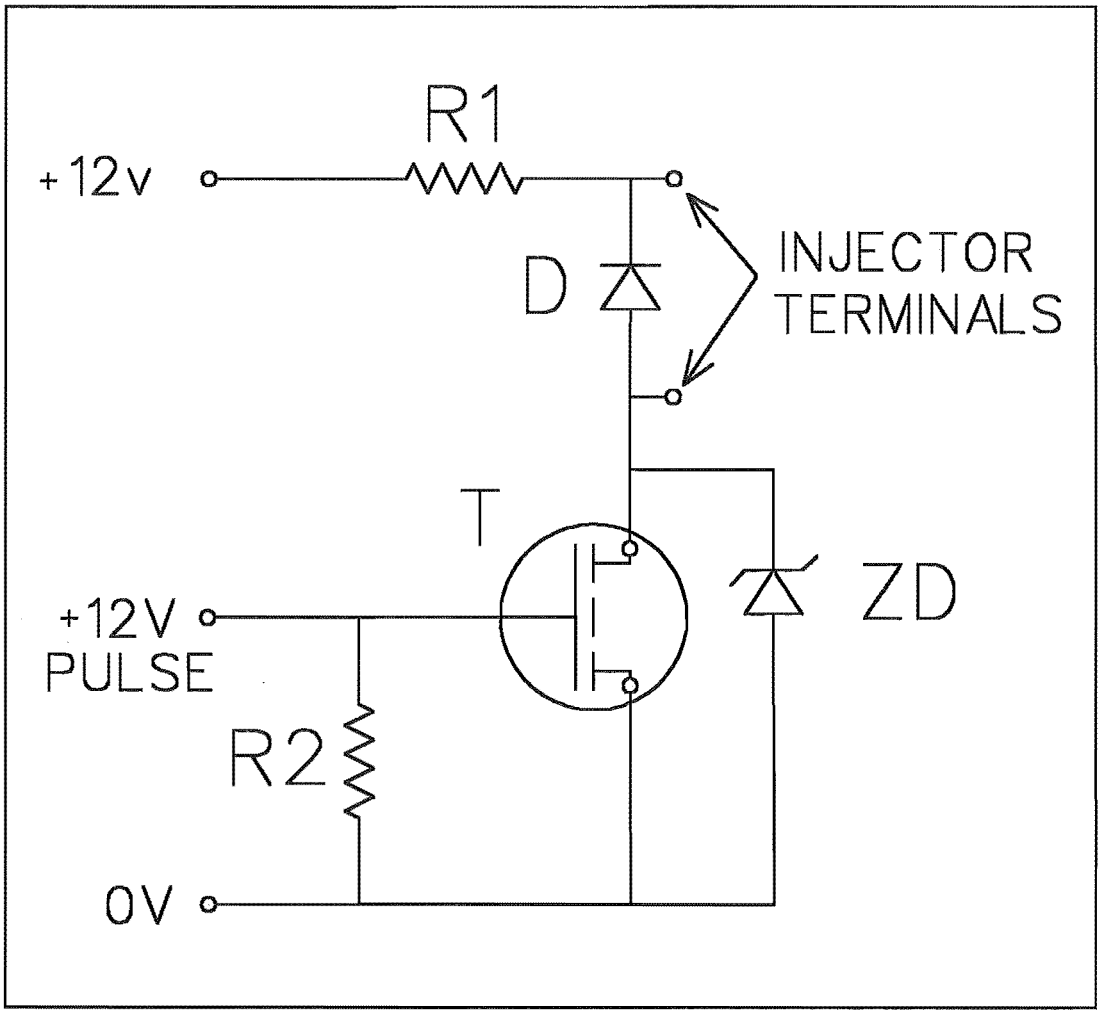

Figure 4,3 Injector over-voltage protection circuit.

FLOWMETERS:- Rotameters were employed to measure the flow rates of both the methane (through both the injector and gas carburettor) and the air induced into the pre-chamber.

The rotameters used to measure the methane flows through both the gas carburettor and the pre-chamber injector were Matherson FM1050 series rotameters, models 604 and 602 respectively. These rotameters were calibrated for a supply pressure of 12 barg.

The air rotameter used to measure the air flow into the pre-chamber was a Platon Gap Meter with an A6 tube with a hollow "Duralumin" float. As the air flowmeter was to be origionally used at atmospheric pressure the standard calibration chart supplied was used to determine the volumetric flow rates passed through. Variations in temperature and pressure were accounted for by the correction factor formulae supplied with the calibration chart. Tests later showed that the air system was required to be pressurised to supply the required amount of air. This was achieved by the use of the departments air supply system, regulated to a pressure of 0.5bar. This pressure was within the range specified by the correction factor formulae.

PLENUM CHAMBERS:- Pressure fluctuations caused by the rapid opening and closing of the methane injector, the cyclic nature of the induction/gas carburation process and that of the air NRV were potential sources of error for the rotameters. To attempt to remove these fluctuations, plenum chambers were to be placed between the sources of the fluctuations and the rotameters. The dimensions of the chambers used were based upon the chambers used by Zavier. The chambers were manufactured from mild steel pipe and were painted with an anti-rust paint to prevent rust formation inside the chambers. Once manufactured the vessels were pressure tested for leaks up to a pressure of 30 bar.

4.3.4 Fuel Supply System.

The fuel used throughout this project was methane supplied by the Christchurch Drainage Board.[126] The fuel supplied was 99.6-99.9% pure with CO_2 and Nitrogen making up the majority of the impurities. A schematic diagram of the fuel supply system is given in figure 4,4. The fuel was stored under high pressure (≈180 bar) in automotive CNG cylinders located within the engine test cell. This was regulated down to the required pressure of 12 barg by the use of a **Victor SR4F** regulator.

Whitey 1/4" stainless steel ball valves were placed on either side of the plenum chamber system so that either the supply to the plenums, pre-chamber injector, or to the gas carburettor could be isolated and detached without first having to depressurise the fuel system and venting the methane to

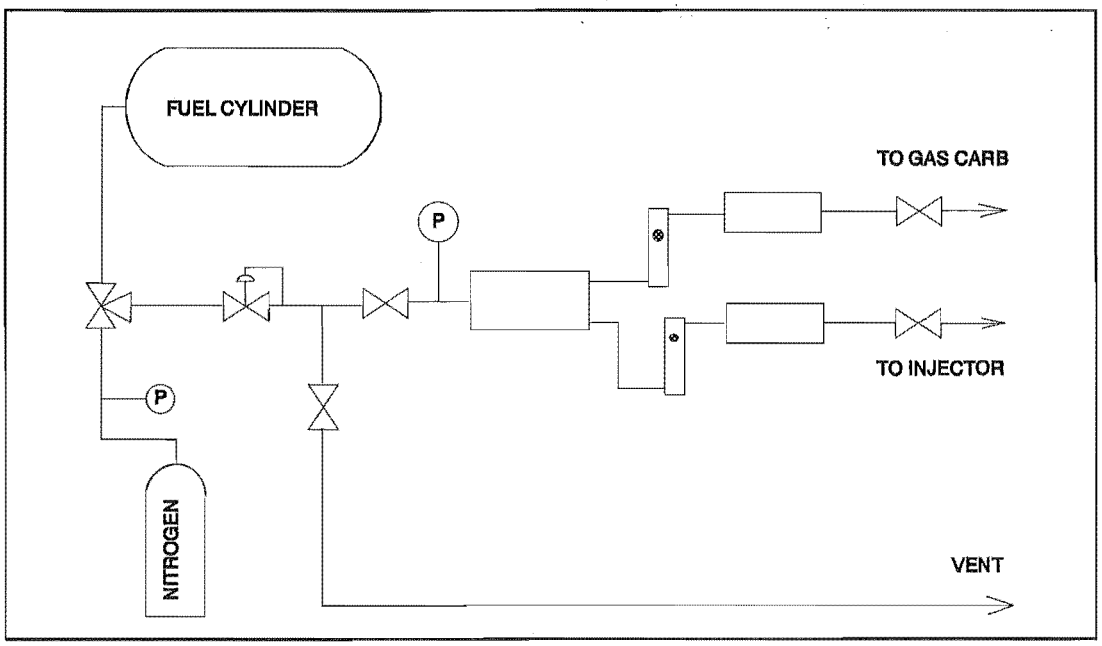

Figure 4,4 Fuel supply system.

atmosphere.

The majority of the gas supply pipe work was manufactured from 1/4" stainless steel tubing and swagelok fittings. The connections to the primary plenum chamber from the pressure regulator and to the gas carburettor from the plenum system were implemented with flexible stainless steel braided hoses. These were used for ease of access and their flexibility.

A vent valve was located in between the regulator and the plenum chambers so that any part of the fuel system could be depressurised to enable work to be performed on the pipework when necessary.

Removal of all air from the plenum chambers was perceived as essential to prevent the formation of an ignitable mixture within the chambers. This was achieved by the connection of a nitrogen cylinder into the fuel system, via a three-way valve located between the pressure regulator and the methane cylinder. The valve was orientated in such a way so that the contents of the methane cylinder could not transfer into the nitrogen cylinder, or vice versa. Prior to filling the surge chambers with methane they were purged by pressurising up to 12 barg with the nitrogen and then venting to atmosphere through the vent system. This was repeated twice more to ensure a negligible amount of air was present.

It was at this point that the entire fuel system was leak tested with a commercially available leak testing soap solution. By applying to all fitting connections leaks were detected if bubbles formed.

After purging with nitrogen the chambers were then purged with methane so as to remove any nitrogen from the fuel system.

To prevent any foreign matter from entering the injector from the fuel system and causing possible blockages and/or damage to the injector pintle a 20 micron sintered element filter was placed immediately up stream of the injector assembly.

Pressure gauges were fitted throughout the supply system so that the supply pressure could be monitored from any location within the engine test cell. Calibration of these gauges was undertaken prior to installation using a Barnet Instruments Industrial Deadweight tester. By varying the load applied to the tester the pressure applied to the gauge could be varied and checked against the gauge reading.

4.4 EXHAUST GAS ANALYSIS

4.4.1 Exhaust Gas Analysers.

One of the primary objectives of this project was to analyse the exhaust gases emitted from the engine during testing. To achieve this, whilst the engine was operating on a hydrocarbon based fuel, two analysers were necessary; one to detect the carbon/hydrocarbon based emissions and another to detect the oxides of nitrogen. The exhaust gases were sampled from sampling points located approximately three meters down stream of the engine exhaust valve. This was done to ensure that any reactions still occurring within the exhaust system had ceased prior to the removal of the gases to be analysed.

The **Horiba MEXA-534GE** exhaust gas analyser was used to detect and measure hydrocarbons, carbon monoxide, carbon dioxide and any residual oxygen within the exhaust gases. The hydrocarbon emission data was given as a ppm n-Hexane equivalent. This was corrected to ppm methane for analysis. The exact composition of the hydrocarbon species could not be obtained with this analyser. Carbon monoxide (CO), carbon dioxide (CO_2) and oxygen (O_2) are all given in percentage volume. (%Vol). The analyser operates on the principle of Non-Dispersive Infra Red Light Absorbtion (NDIR).[127]

To analyse the exhaust gases for oxides of nitrogen a **Beckman 951A NO/NOx** analyser was used. As this analyser was primarily located within the

rolling road test bay, a means for using the analyser within the Ricardo test cell was necessary. A portable system was designed to allow the analyser to be moved to any engine test cell within the thermodynamics laboratory.

The analyser operates on the principle of chemiluminescence[128]. Briefly, within the analyser nitric oxide (NO) molecules are reacted with ozone (O_3) to form nitrogen dioxide (NO_2) in an excited state.

$$NO + O_3 \rightarrow NO_2^* + O_2 \qquad (4.3)$$

$$NO_2^* \rightarrow NO_2 + h\upsilon \qquad (4.4)$$

On returning from this excited state to the ground state a photon of a characteristic form (given by $h\upsilon$) is emitted by the NO_2 molecule. The intensity of this light emission is directly proportional to the concentration of the NO_2 (and hence the NO concentration) present within the gas being analysed. The light emission is measured by a photomultiplier and compared to a set value obtained when calibration of the analyser occurs.

The system requirements to utilise the analyser were:

1, supply of an oxygen source to produce ozone

2, supply of the engine exhaust gas to be analysed,

3, removal of the analysed exhaust gas to a safe area, as it

considered toxic.

4, supply of a suitable SPAN gas mixture to calibrate the analyser.

Figure 4,5 shows the system used to meet all these requirements.

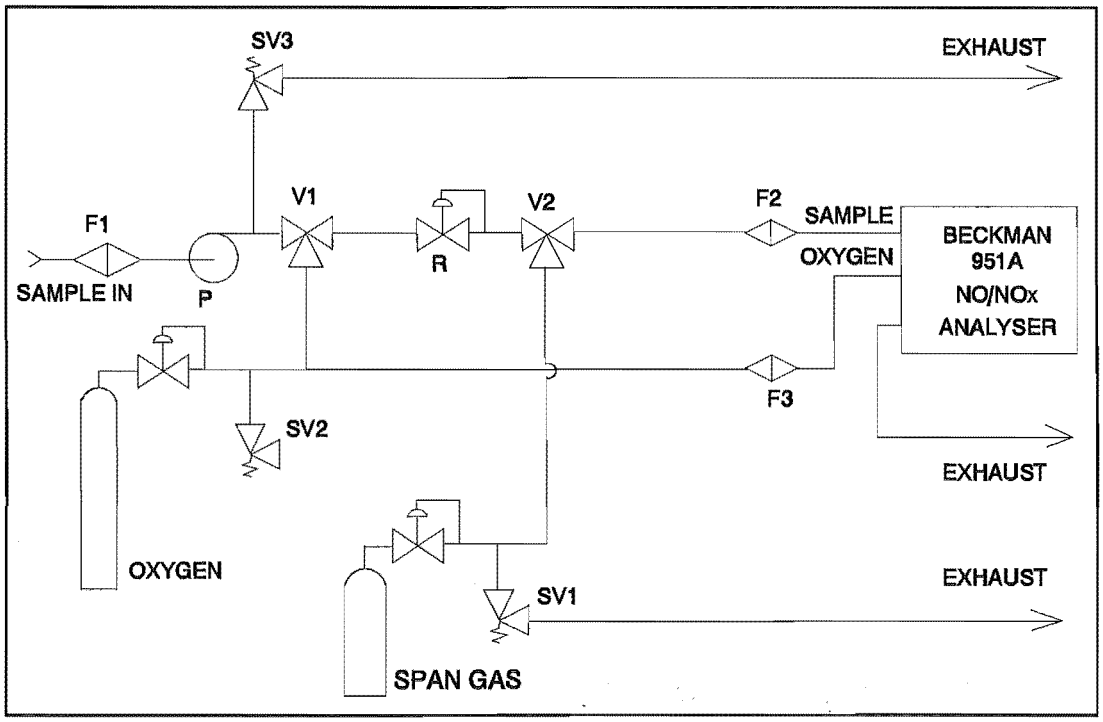

Figure 4,5 NOx Meter gas supply system.

Due to the corrosive nature of the exhaust gases being analysed and the gases produced by the NOx analyser, all components and piping used were constructed of either 316 stainless steel or PTFE[¶¶].

To supply the analyser with a continuous exhaust sample at the required

[¶¶] Polytetrafluoroethylene.

pressure and flowrate a Gast DOA P101-BN piston air compressor was used. Prior to the compressor the sample was passed through a moisture trap to reduce the moisture content to an acceptable level. This trap was located outside the engine test cell in order to take advantage of the lower temperatures to aid condensation of the moisture. After leaving the compressor the sample pressure was regulated to the required inlet supply pressure of 15psig by a Matherson 3141 pressure regulator. A second moisture trap was placed in-between the regulator and the compressor as a safe-guard in case the unit was used at a future date on another engine without the externally mounted trap. Before finally entering the analyser the exhaust sample was filtered through 2 micron filter.

Oxygen was supplied to the analyser as the ozone generator supply source. This was supplied from industrial oxygen cylinders and regulated to a supply pressure of 40psig before entering the analysers ozone generator. Prior to entering the analyser the oxygen was passed through a 2 micron sintered element filter to remove any foreign matter. The oxygen was also used to zero the analyser during the calibration procedure. A three way ball valve was connected between the oxygen and sample gas systems so that the oxygen could be supplied at the sample inlet to zero the analyser as well as to purge out any unwanted gases from within the analyser prior to switching the analyser off.

Calibration of the analyser was accomplished by the use of a span gas of a known nitric oxide concentration. This was supplied from a pressurised cylinder to a second three way ball valve connected to the sample line at a regulated supply pressure of 15psig. By selecting the appropriate valve position the span gas would be supplied to the analyser sample inlet, allowing calibration of the analyser to be undertaken.

Throughout the supply systems pressure relief valves were fitted to prevent any over-pressurisation of the analyser.

Plate 4.4 shows the complete NOx analysis system. (pp111)

4.4.2 Span Gas Mixtures

Due to the unavailability of a standard span gas, the nitric oxide span gas mixtures used to calibrate the Beckman NOx analyser were produced within the thermodynamics laboratory in a purpose built mixing apparatus. The system schematic is shown in figure 4,6. The mixtures were produced based upon the method of partial pressures.

99% Nitric oxide was supplied to the span gas cylinder to be filled, from a separate cylinder. The flow was controlled with a precision metering valve so that the correct amount of NO could be delivered to the span gas cylinder. The

nitric oxide was diluted in a background of nitrogen supplied from an oxygen free grade[§§] nitrogen cylinder. This was used to prevent any possible further formation of nitric oxide within the span gas cylinder from any oxygen

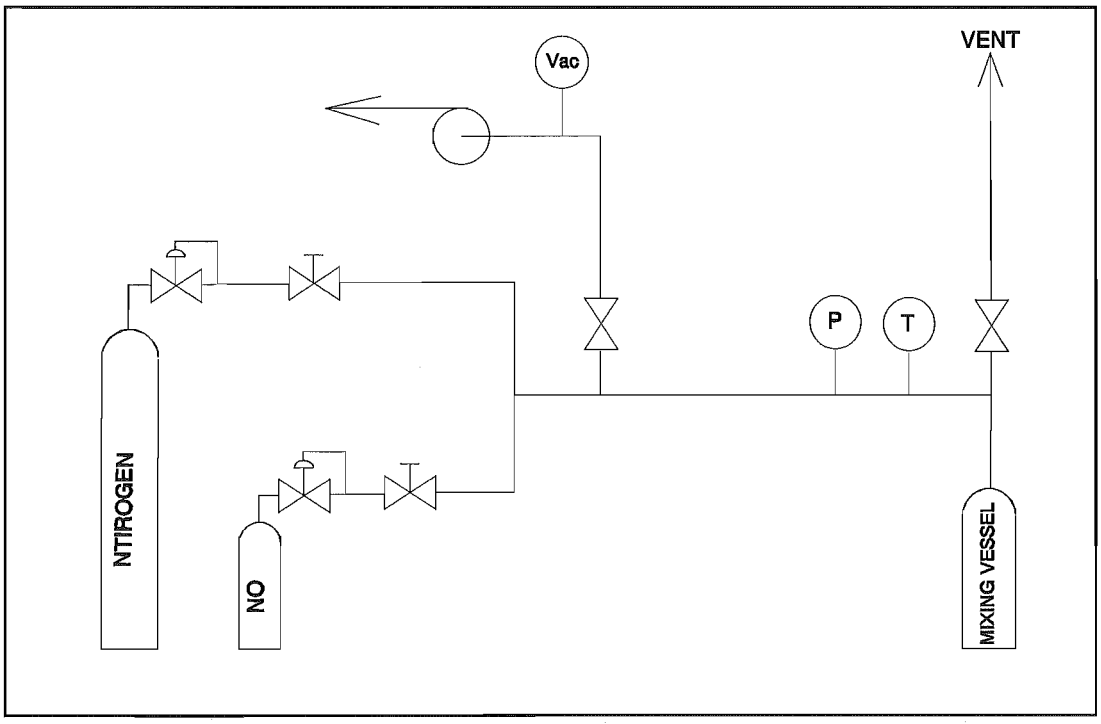

Figure 4,6 Span Gas Mixing system.

impurities found in normal industrial grade dry nitrogen.

Prior to filling of the mixture the span gas cylinder was evacuated by the use of a rotary vacuum pump so as to minimise any errors due to any residual gases within the cylinder. The vacuum obtained within the cylinder was measured by the use of a bourdon tube type vacuum/pressure gauge.

[§§] Manufacture by New Zealand Industrial Gases ltd.

Accurate measurement of the pressure within the span gas cylinder was obtained by the use of a SenSym SSX 300 G piezo resistive differential pressure transducer. This gave a linear 60mV output at 20 bar for a 12volt input. The analogue output from the transducer was read by a computer using Metrabyte Dash-8 A/D Data Acquisition system after first being passed through the EXP-16 Multiplexer/Amplifier. This system was configured by Damiano[119]. The voltage input was converted to an absolute pressure by a BASIC program. The temperature of the mixing vessel contents was detected by a K-type thermocouple connected to a digital thermometer. By knowing these two parameters the determination of the mass of each component could be calculated by use of the appropriate equations of state[¥¥¥]. The procedure for the production of these mixtures is given in appendix 4. (pp112)

4.5 ENGINE DATA ACQUISITION

4.5.1 System inputs

Previous to this work a data acquisition system had been installed into the engine test cell by Glasson[121]. This system interfaced many of the thermocouples, sensors and transducers through a DAS-20 12 bit A/D board and EXP-20 multiplexer with a 386 personal computer. A program enabling the display and storage of this data was written by Glasson and utilised throughout

---

¥¥¥ See appendix 3.

this work. Details of the specifications of the system can by obtained from the above reference.

Of importance to this work were the pressure transducer input, the lambda sensor input and the engine temperature thermocouple inputs. The temperature data was used to verify the engine was up to operating temperature before a set of tests were performed, as well as providing the ambient temperature so that the air mass flowrate into the engine could be calculated. The lambda sensor data was used to accurately determine the stoichiometric operating point.

4.5.2 Pressure Data

A useful feature of the acquisition system was the ability to perform DMA (Direct Memory Access) transfers of data directly to the memory of the computer at a maximum rate of 100 kHz and a maximum usable array size of 10 000 data points. This feature was used to acquire the engine pressure data from the pressure transducer installed in an auxiliary spark plug hole in the cylinder head. After the DMA transfer was complete the data was automatically saved to a data file on the computers hard disk drive for later analysis. It should be noted that the pressure data obtained was a series of voltage data, which could be converted to pressure data when a calibration constant was applied in later analysis.

Pressure data alone can generally only be used to qualitatively investigate the engine performance. A more useful set of data is Pressure-Volume data. By knowing the engine speed and having an identifiable reference position, the conversion of pressure data, stored at a known fixed rate, can be converted to pressure volume data with minimal error. This can be used in a quantitive manner to determine such properties as indicated power and indicated mean effective pressure. Glasson used a second input channel to determine the displacement of an injector needle. Imposed upon this trace was a voltage spike correlating to the ignition point. He used this as a reference point to analyse the pressure data. By using this system the amount of memory available to accommodate pressure data was halved. This reduction in available memory and the absence of the injector developed by Glasson to the development of a signal interrupt generator.

4.5.3 Pressure Trace Reference Point

The idea involved a system which when triggered by the ignition system would ground the pressure signal to the A/D system for a short time, effectively introducing a reference spike to each pressure trace. Figure 4,7 shows the voltage characteristics throughout the circuit. Figure A shows the voltage signal from the transducer amplifier. A comparator compares the ignition input voltage with a known voltage source. When the optical switch senor is uncovered (B) this ignition voltage increases and triggers the comparator. The output from the comparator is modified by a Schmit trigger integrated circuit

so that response of the system is increased by "squaring off" the rising edge of the trigger signal. This signal sets a "one shot flip-flop" circuit (74121) into a high state. The time that the circuit remains in the high state is determined by an R-C circuit attached to the flip-flop. By varying the resistance of the R-C circuit the time constant could be increased or decreased accordingly to meet the requirements of the engine test. The output signal from the flip-flop was used to activate an open collector, (C). When the signal was applied to the gate terminal, the collector would be switched on, effectively earthing the pressure signal.(D) When the signal was removed from the collector the pressure signal was restored to its original form.

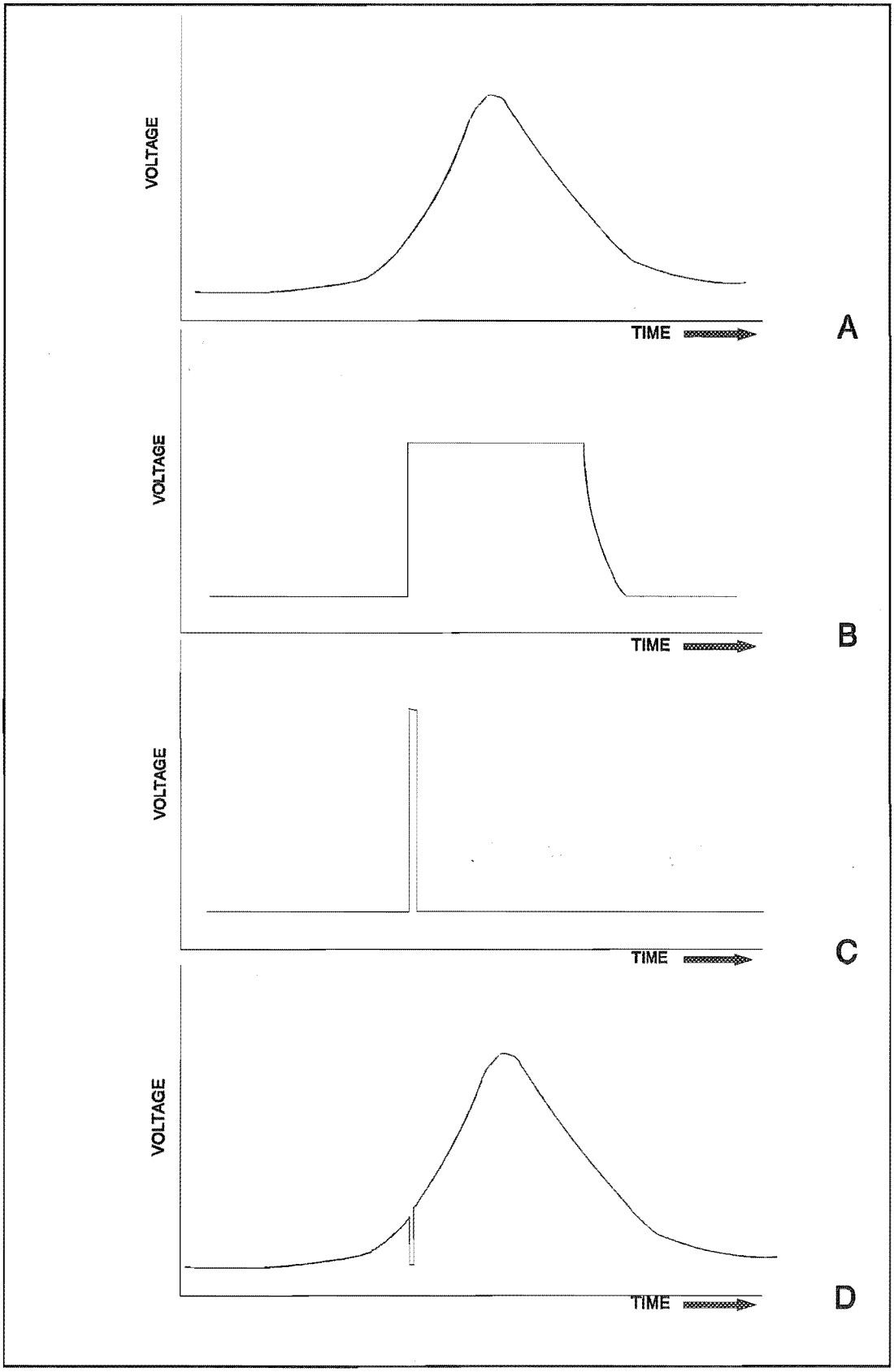

Figure 4,7 Pressure signal and spike generator signals.

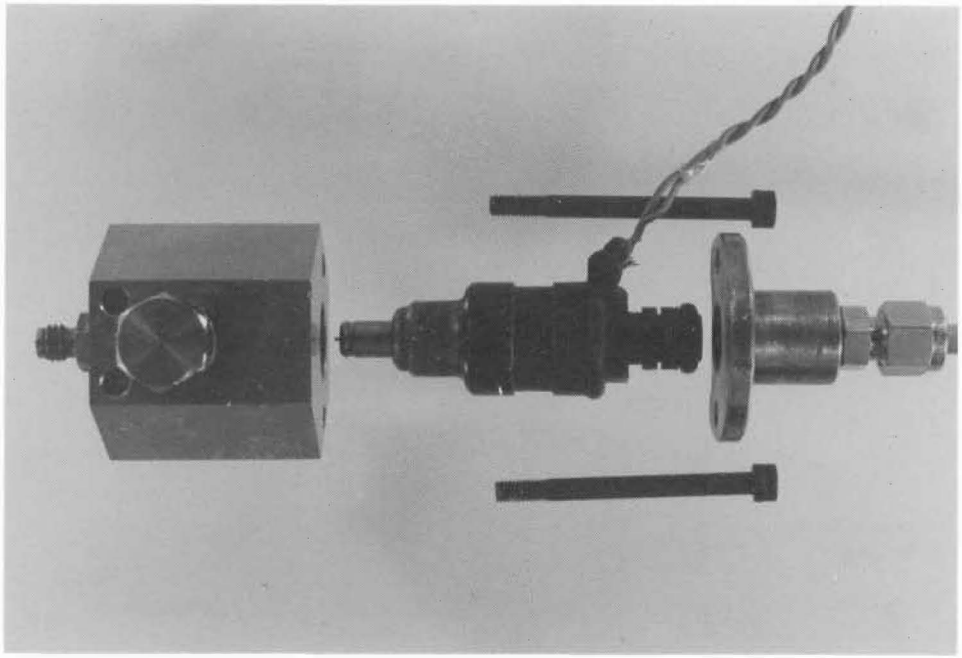

Plate 4,2 Methane Injector assembly.

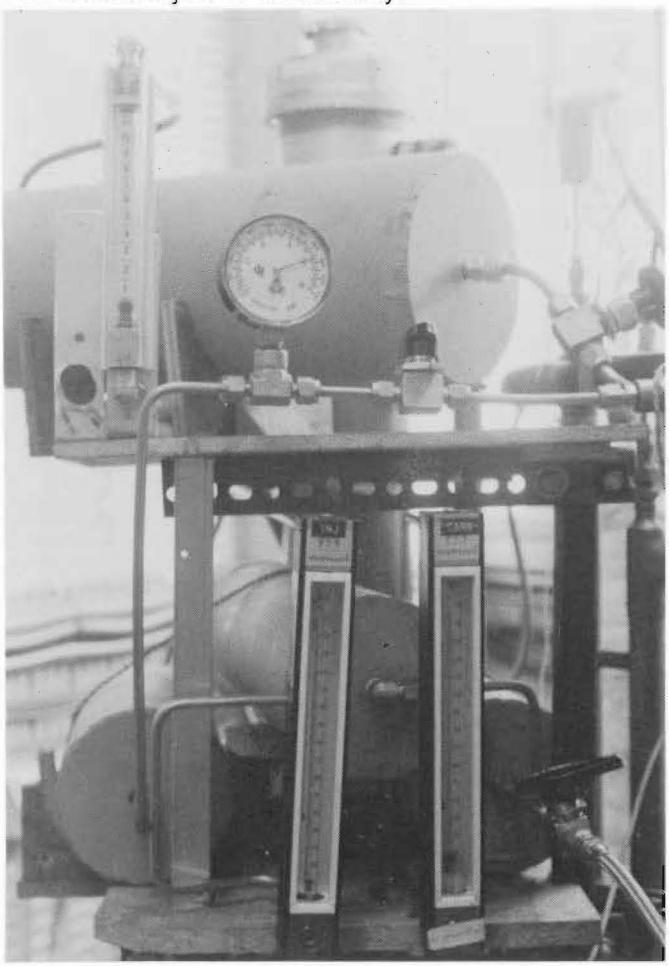

Plate 4,3 Rotameters and plenum chambers.

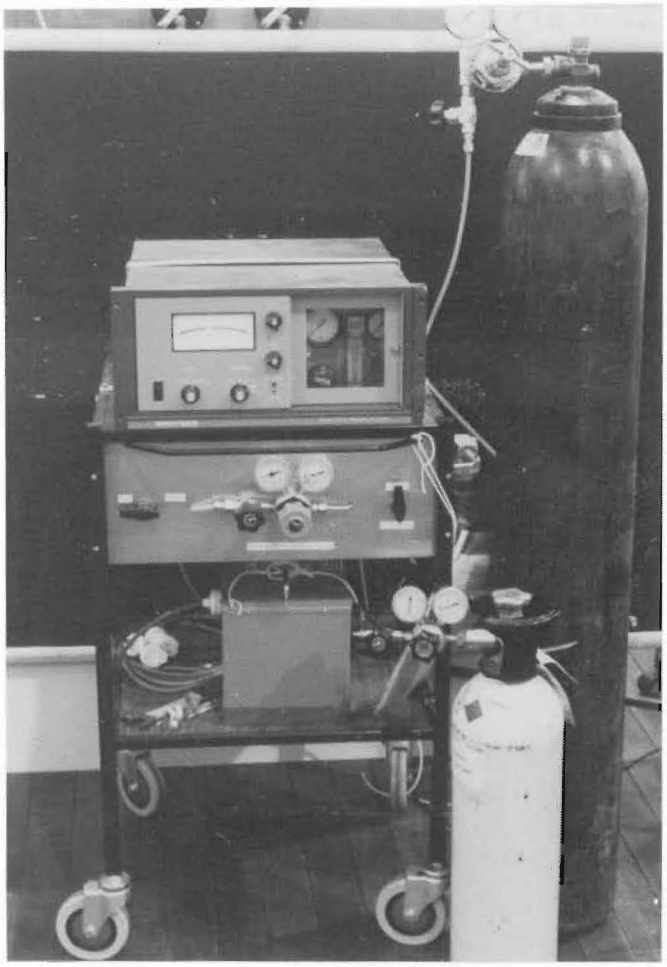

Plate 4,4 Beckman 951A NO/NOx analyser and associated equipment.

Plate 4,5 NO/N_2 span gas mixing system.

CHAPTER 5

EXPERIMENTAL PROCEDURES

5.1 INTRODUCTION

As discussed in Chapter 4, a large amount of experimental equipment was required in order to test the hypothesis of this project. In order to undertake accurate and repeatable measurements, procedures were necessary for the calibration and operation of this equipment. This chapter deals with these procedures and the reasons why they were conducted.

5.2 CALIBRATION OF ROTAMETERS

Accurate knowledge of the air/fuel ratios required an accurate knowledge of the mass of air and fuel introduced into the engine, through both the main inlet valve, as well as the air induced, and the methane injected into the pre-chamber.

Both the gas carburettor and injector rotameters were calibrated for methane

under a supply pressure of 12 bar.[†††] A schematic of the rotameter calibration test set up is given in Figure 5,1.

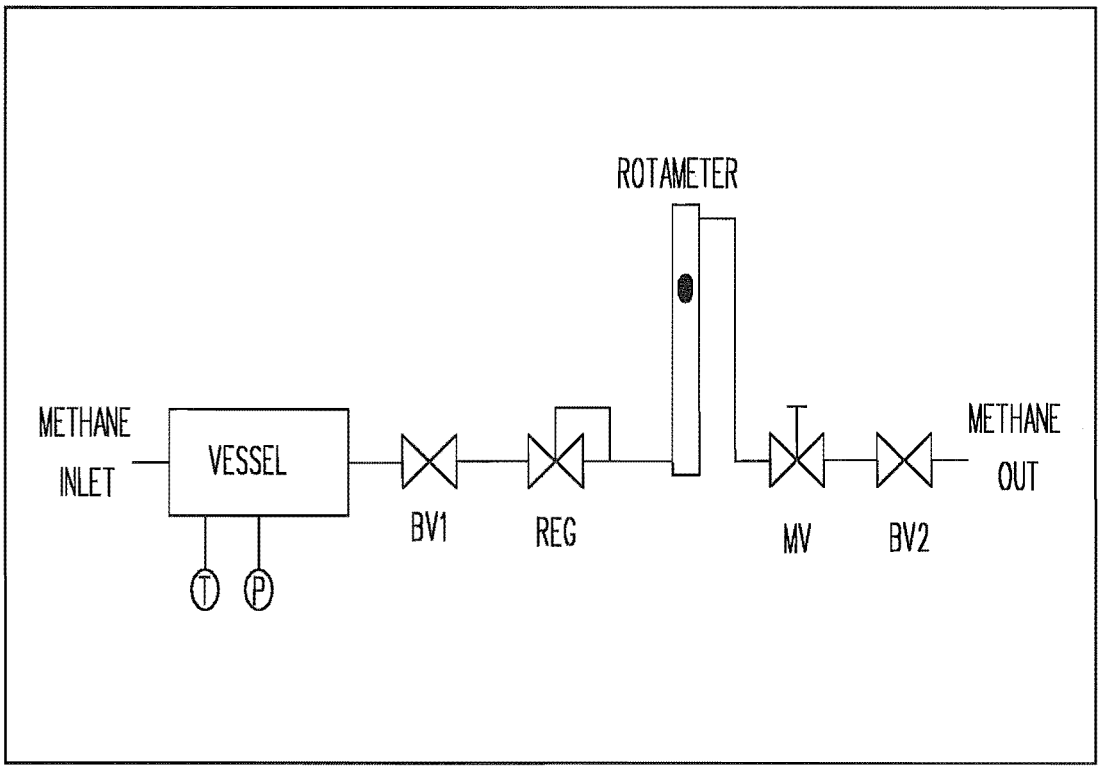

Figure 5,1 Rotameter Calibration Rig

A vessel of known volume was pressurised with methane up to a maximum pressure of 20 bar. This was allowed to stabilize before initial pressure and temperature readings were taken. The vessel was connected to a regulator which would keep the rotameter supply pressure at a constant 12 bar. The methane would then pass through the rotameter and then through a metering valve which was used to vary the flow rate. A ball valve was connected

[†††]All pressures and gauge pressures

downstream of the metering valve so that the flow could be started and stopped quickly.

At the start of the calibration run the position of the metering valve was set and then the ball valve was opened for a set period of time, (usually 30 seconds - 2 minutes depending upon the rotameter and flowrate). The height of the float was recorded once it had stabilized.

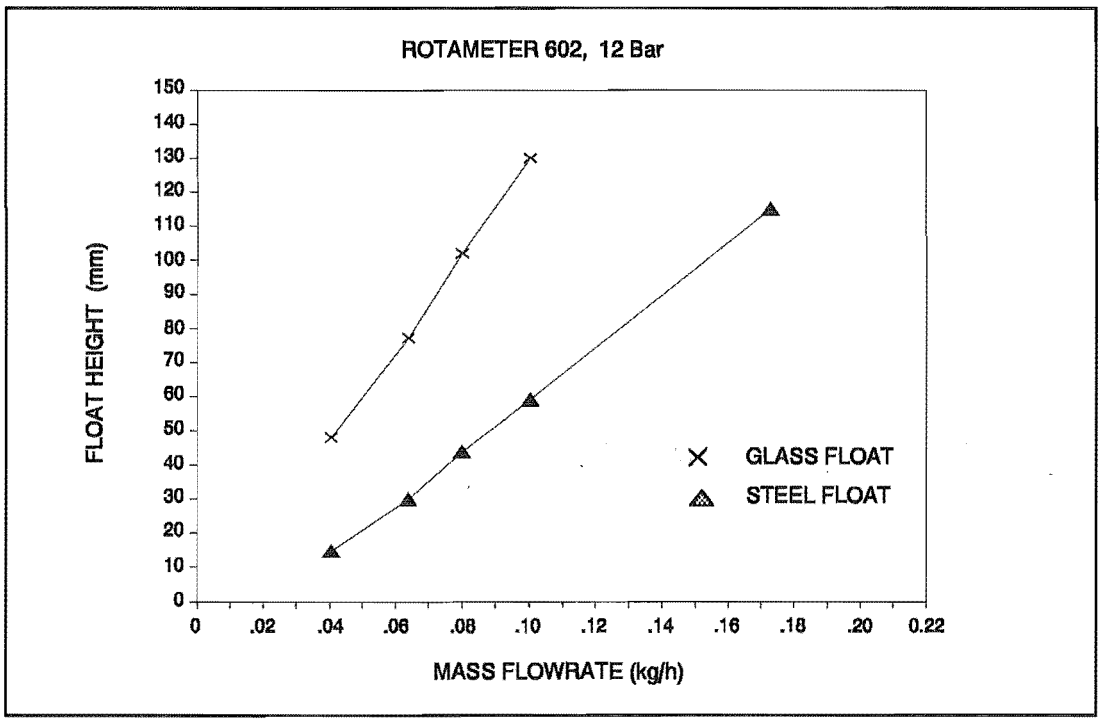

Figure 5,2 Gas Injector calibration curve.

At the end of the test the ball valve was closed and the pressure and temperature within the pressure vessel allowed to stabilize before their final values were recorded. The position of the metering valve was varied and the process repeated until a representative calibration of the rotameter over its full

scale was achieved. The data was then applied to the relevant equations of state to yield the mass flowrate at the relevant float heights. This data was plotted graphically and the gradient and y-intercept determined by a line of best fit for use in the engine test data analysis program RICPC.BAS (see Appendix 1). The calibration curves used are given in Figures 5,2 and 5,3.

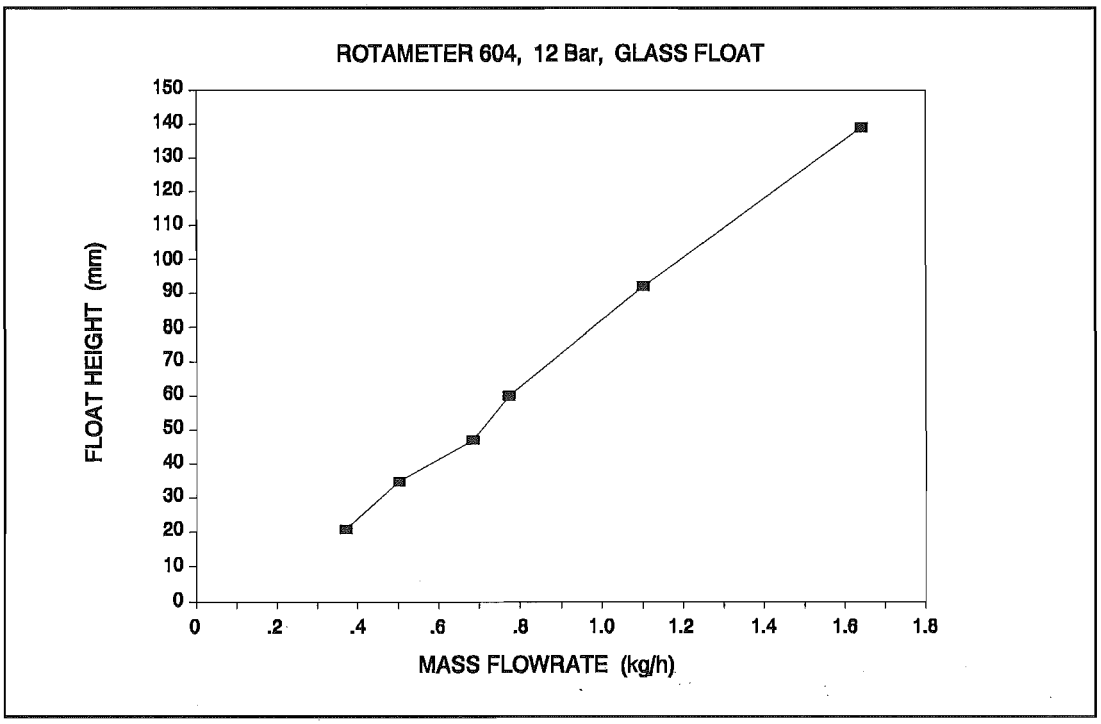

Figure 5,3 Gas Carburettor calibration curve.

The flow of air into the pre-chamber was also measured by the use of a rotameter. Further calibration of the selected rotameter was not necessary as a calibration chart was supplied. Variations in temperature and pressure could be accounted for by the relevant correction factors outlined on the calibration chart.

5.3 CALIBRATION OF PRESSURE TRANSDUCER

Piezo-electric pressure transducers rely upon a changing pressure to produce a signal. Therefore, in order to calibrate the piezo-electric pressure transducer used to monitor the engine cylinder pressure, a known change in pressure was necessary. This was achieved with the use of a modified Barnet dead weight tester which could rapidly release a known pressure.

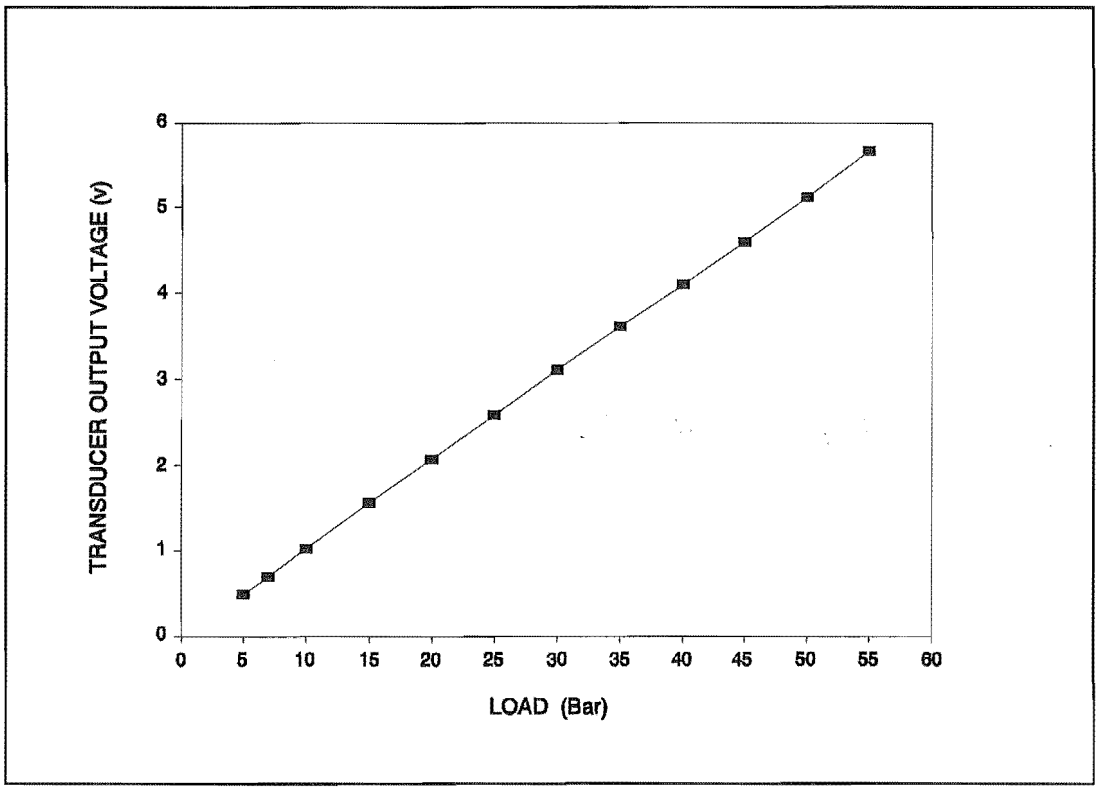

Figure 5,4 Piezo-electric Pressure Transducer Calibration Curve.

The transducer was connected to the dead weight tester. The output from the transducers charge amplifier was connected to a Hewlett Packard 54602A

4 channel oscilloscope which was set to a single-shot mode to capture the output trace from the transducer. The transducer was then loaded with an appropriate pressure by the dead weight tester, and then the signal grounded momentarily before the applied pressure was released.

Each test load was conducted three times in order to ensure repeatability and to minimize errors. Pressures from 0 to 60 bar in 5 bar increments were tested. The change in pressure was correlated to the change in voltage obtained from the trace on the oscilloscope and the results graphed. A typical calibration curve is given in Figure 5,4. From this graph the calibration constant was determined which was used in the QuickBasic program **PRESANAL.BAS** to analyse the combustion chamber pressure. The calibration of the transducer was checked at regular intervals to minimized any errors.

5.4 CALIBRATION AND USE OF EXHAUST GAS ANALYSERS

A calibration check of both exhaust gas analysers was conducted at the beginning of every engine test day. This was done in accordance with the instructions found in each analysers respective manual.[127,128] However a brief description shall be given.

5.4.1 HORIBA MEXA-534 GE :- CO, CO_2, UHC,O_2

Prior to switching on the analyser all filters were checked and replaced if necessary. The sample line was disconnected and air blown through to remove any condensed moisture. The analyser was then switched on and set into PURGE mode and allowed to induce air through the sample line for 15 minutes whilst the analyser reached its operating mode. Once ready, the analyser was set into STANDBY mode and the sample line disconnected before returning to the PURGE mode. The display was then zeroed by pressing the AUTO-ZERO key. The analyser was then returned to the STANDBY mode and the span calibration checked. The span gas container was connected to the span gas inlet for about 7-10 seconds. The displays were allowed to settle before any necessary adjustments were made by turning the appropriate span pot screw to restore calibration. The trimmer adjustments were then checked by returning to the PURGE mode, and once the displays were reading zero, the SPAN CHECK key continuously pressed and the appropriate trimmer pot adjusted to the required specification.

Finally the oxygen sensor calibration was checked by pressing the PURGE key and checking the oxygen reading was between 19.4 and 22.4%. If outside this range the oxygen span pot was adjusted.

Prior to sampling the engine exhaust gases the analyser was set into STANDBY mode and the sample line connected to the sample point and the

analyser. The MEASURE key was then pressed and the readings allowed to stabilise before being recorded.

The analyser SPAN CHECK was checked at regular intervals during a tests day to ensure the analyser was not drifting.

After use the analyser was left in PURGE mode for 30 minutes with the sample hose disconnected to purge any exhaust gases from the analyser.

Plate 5,1 HORIBA MEXA 534GE Exhaust gas analyser.

5.4.2 BECKMAN 951A NO/NOx Analyser.

One hour before engine testing began the NOx analyser was switched on and allowed to reach operating temperature. At this time the moisture traps were emptied of any water. Once warm the oxygen supply to the analyser was established by opening the cylinder valve and setting the regulator output to 40psi.‡‡‡ The engine test cell extraction fan was turned on to remove the gases from the analysers exhaust line, which was secured in close proximity to the extraction fan. This was necessary as the exhaust gases from the analyser contained ozone.

The analyser ozone pressure was set at 30psi by adjusting the ozone pressure regulator. Oxygen was also supplied to the sample inlet of the analyser by setting the right hand valve on the gas supply panel to ZERO and the left hand valve to SAMPLE. The sample regulator outlet pressure was set at 10psi. As only the total NOx concentration was of interest the mode switch was permanently set to NOx. The ppm switch was set to 2500ppm. The sample back pressure regulator was set at 4psi and the bypass needle adjusted to give a flow of approximately 2 litres per minute.

---

‡‡‡ Pressure units displayed may be psi or bar so that they are consistant with the equipment scales.

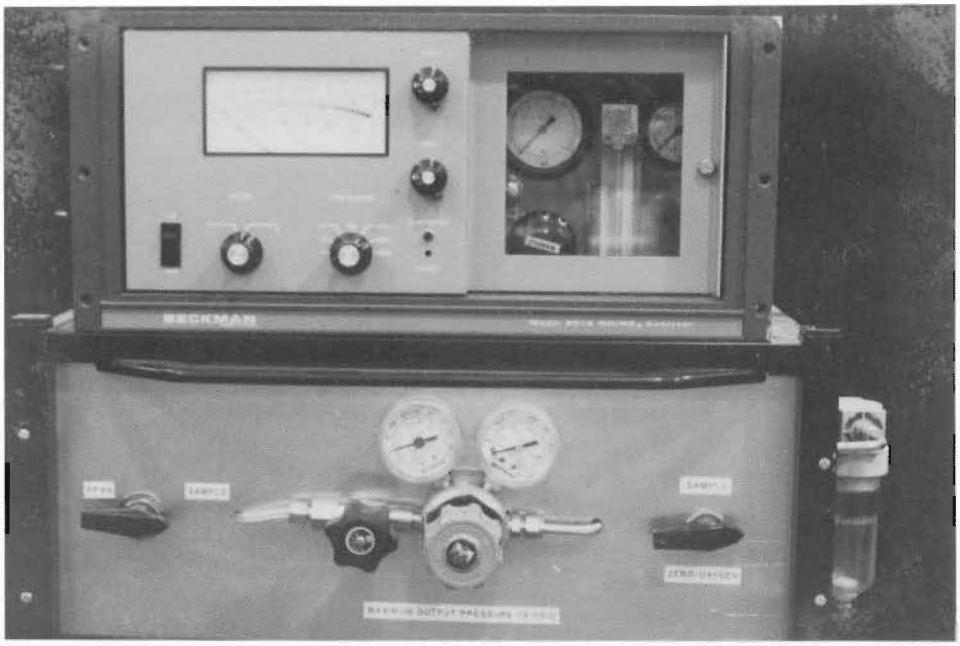

Plate 5,2 BECKMAN 951A NO/NOx Exhaust gas analyser front panel.

At this point, the reading of the meter was checked for zero and adjusted if necessary. The upscale reading of the meter was checked by supplying a span gas of known NO concentration to the sample inlet. This was achieved by setting the left hand valve on the gas panel to SPAN, opening the span gas cylinder and setting the regulator to 10psi. The sample back pressure and flowmeter readings were checked to ensure that the correct flow was established. The meter reading was allowed to stabilise before any adjustments were made to correlate the reading to the span gas concentration. Once calibration was complete the left hand valve was set back to SAMPLE to allow oxygen to purge the analyser, and the span gas cylinder valve closed.

When analysing exhaust gases from the test engine both valves on the gas

supply valves were set at SAMPLE and the sample pump was plugged in. The sample pressure to the analyser, sample flow rate and back pressure were all checked and adjusted if necessary, before the reading on the meter was recorded. The analyser was left in this state throughout testing.

At 1/2 hourly periods the sample moisture traps were cleared to prevent water from being induced into the analyser. Once testing was complete the sample pump was switched off and the right hand valve set to zero to allow oxygen to purge any sample gases from within the analyser for 10 minutes. The analyser was then switched off and the oxygen cylinder valve closed.

5.5 PREPARATION OF NO/N_2 MIXTURES.

Accurate calibration of the NOx meter requires the use of an accurately known mixture of nitric oxide (NO) in a background of nitrogen. For this research a mixture with a composition of either 2500ppm or 10000ppm NO in N_2 was required. A dedicated rig for the accurate mixing of these mixtures was constructed as outlined in section 4.4.2.

Production of these mixtures was a relatively simple, but time consuming task. The procedure is based upon the method of partial pressures, ie,

$$P_{total} = P_{NO} + P_{Nitrogen} \qquad (5.1)$$

For increased accuracy of the mixtures Van der-Waals equation of state was used to define the partial pressures of the NO and nitrogen for a given required concentration at the particular ambient temperature. The calculations for these mixtures are given in appendix A4.

The mixing cylinder was initially relieved of pressure in an open space and then evacuated, purged and then re-evacuated to remove the majority of any impurities. Oxygen-free nitrogen (OFN) was then introduced into the vessel to a pressure of approximately 2 bar, to bring the mixture cylinder pressure to within the linear range of the pressure transducer. The required quantity of nitric oxide was then added to the cylinder, after which the remaining OFN was added to give the required final pressure, and hence the required concentration of the mixture.

Before any constituent was added to the cylinder, the pressure and temperature within the cylinder were allowed to stabilise so as to reduce any possible error. Although a long process, it was felt that accurate mixtures were more important than the time required to produce the mixtures. Variations in atmospheric temperature and pressure were accomodated for in the initial calculations of the partial pressures.

5.6 TEST ENGINE PREPARATION.

Preparation of the test engine began one hour prior to the start of testing on each day. After switching on the main power supply to the engine, the engine coolant and oil heaters and pump were switched on. The coolant for the pressure transducer was also turned on at this stage to prevent the transducer from over heating. The NOx meter and the test cell extraction fan were also turned on.

The 386 PC monitoring the engine was switched on and the computer program RICARDO.BAS was operated so that the engine temperatures could be monitored to indicate when to start testing.

The compression ratio was set at the very beginning of engine testing (8:1) and not changed throughout the testing period, however, a check was made at the beginning of each test day to check it had not varied.

Fifteen minutes after the starting of the engine, the Horiba exhaust analyser was switched on and calibrated as per section 5.4.1. The Beckman NOx meter was also calibrated at this point as per section 5.4.2. The power supply to the lambda sensor was switched on and the sensor allowed to warm up. The oscilloscope, pressure trace spike generator and the injector drive circuits were all turned on as well. Finally the air conditioner was switched on and the

air manometer was set to zero.

5.7 ENGINE TEST PROCEDURE

Once the engine was ready to perform a series of tests, the methane fuel cylinder valve was opened and the three-way supply valve set to methane. The regulator outlet pressure was set at 12 bar and the isolating ball valve opened to the plenum chambers. For charge stratification tests, the pre-chamber air supply regulator was set at 0.5 bar and the pre-chamber cooling fan was switched on.

The engine was brought up to speed in the motoring mode and then switched to fixed speed. The throttle setting was set and then the methane supply valve to the gas carburetter was opened, followed shortly by the injector supply valve (for charge stratification tests). The ignition and gas carburetter flow rate were then adjusted until stable engine operation was achieved. The exhaust gas analysers were then set to sampling mode to analyse the exhaust gases. No further adjustment were made to the analysers during testing.

The air/fuel ratio was adjusted until a stoichiometric mixture was obtained. This point was determined by the rapid change in the lambda sensor output. Once obtained, the ignition timing was set for minimum advance for Best

Torque (MBT). From this point the testing procedure varied depending upon the test to be undertaken.

5.7.1 Baseline tests

Prior to any charge stratification work being undertaken, a series of baseline tests were performed. These involved running the test engine without the pre-chamber present. The engine was operated at a constant speed and throttle setting. The ignition timing was continuously reset to MBT and the air/fuel charge was gradually leaned off until the engine misfired. This was established by monitoring the exhaust hydrocarbon level, which displays a sharp rise during the onset of misfire, and observation of the pressure-crank angle traces on the oscilloscope.

5.7.2 Charge Stratification tests.

Optimisation of the charge stratification system was undertaken in a 3 part study, namely;

1, Optimisation of the pre-chamber air requirements,

2, Optimisation of the pre-chamber methane injection rate,

3, Optimisation of the pre-chamber methane injection timing.

Part 1 was undertaken by holding the injection rate and timing constant and varying the pre-chamber air flowrate.

Part 2 was performed by supplying the optimised pre-chamber air flowrate and varying the injection rate for a fixed injection timing. The injection timing used in part 2 was the same as for part 1.

Part 3 was performed by supplying the optimised pre-chamber air flowrate and methane injection rate and varying the injection timing. This section required the largest amount of work, as the possible injection window was from the point of inlet valve opening to the ignition point, (approximately 360° CA).

Throughout all phases of optimisation the main chamber air/fuel ratio was leaned in a stepwise manner. The ignition timing was adjusted for MBT before proceeding to the next air/fuel ratio setting, until the onset of misfire occurred as characterised by a sharp increase in hydrocarbon emissions, rapidly fluctuating power output, and observation of the combustion chamber pressure trace. The parameter under optimisation was then varied and the process repeated until a clear optimum point was located. This was determined by consideration of;

-brake thermal efficiency.

-exhaust hydrocarbon emissions,

-lean limit of combustion,

-stable engine operation.

5.8 TEST DATA RECORDED

For all engine combustion testing the following experimental data was recorded on a standardised data sheet.

- atmospheric pressure (mmHg)
- engine speed (RPS)
- compression ratio
- throttle position
- air manometer reading (mm)
- air temperature and correction factor
- gas carburetter float height (mm)
- gas injector float height (mm)
- air pre-chamber float height (1-10)
- number of dynamometer weights
- spring balance reading
- ignition timing (°BTDC)
- exhaust temperature (°C)
- exhaust NOx level (ppm)
- exhaust CO level (% vol)

- exhaust CO_2 level (% vol)
- exhaust Hydrocarbon level (ppm n-Hexane)
- exhaust O_2 (% vol)
- injection start angle (°ATDC)
- injection end angle (°ATDC)
- injection duration setting read.

Once this data had been obtained the pressure transducer output was captured by using menu option 5 in RICARDO.BAS. The number of cycles recorded and the number of data points per cycle could be varied under the options within the program. Once this data was recorded the required test variable was changed and the process repeated.

At the end of testing the engine was shut down by closing the isolation valves to the gas carburetter and injector and allowing the engine to run until it ceased firing. The engine was then switched to motoring mode and the engine speed reduced to zero. Once the engine had stopped the oil and water heaters and pumps were switched off, but the piezo electric pressure transducer coolant was left on while the engine cooled.

The methane cylinder and the plenum isolation valves were closed, and the three way valve set to the off position before the vent valve was opened to de-pressurise the regulator. The pre-chamber air system valve was also closed.

The exhaust gas analysers were switched off as indicated in sections 5.4.1 and 5.4.2. All remaining electrical equipment was switched off except for the ventilation fan which was left on for one hour to aid cooling the engine, and to remove any fumes given off by the exhaust of the NOx meter.

CHAPTER 6

DISCUSSION OF EXPERIMENTAL RESULTS

6.1 INTRODUCTION

This chapter deals with the results obtained from the experimental tests, as well as some of the changes in the apparatus brought about by knowledge gained during the initial testing. Primary investigations into the operation of the system were undertaken to give an insight into which direction the combustion system investigation should follow. These tests comprised a great bulk of the experimental work, but represent little in the way of presentable data. The results discussed in this section are representative of the data collected during the final testing period when the optimum combustion system was investigated. Not all results are shown, only those which provide useful information into the combustion phenomenon, or where they are required to illustrate a particular point.

6.2 INITIAL TRIALS

6.2.1 Air system trials.

Prior to any combustion work being undertaken, the pre-chamber air supply system was tested. The air supply was initially un-pressurised. The engine was motored at a fixed speed (either 1000,1500 or 2000rpm) and the throttle position varied from fully open to fully closed. The pre-chamber air induction ratio (IR[¶¶¶]) was calculated and plotted against throttle position as shown in figure 6,1.

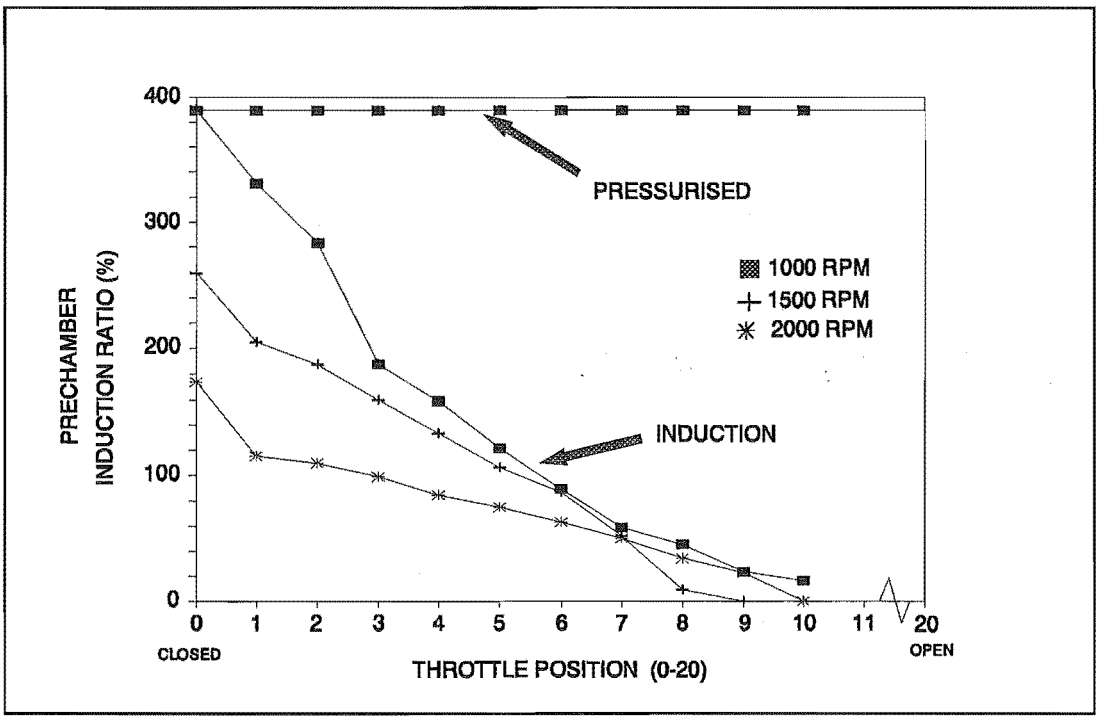

Figure 6,1 Pre-chamber air induction ratio vs throttle position.

[¶¶¶]Defined as the induced volume of air into the pre-chamber per cycle divided by the volume of the pre-chamber.

As can be seen, for low inlet manifold vacuums, (ie open throttle) the flow through the check valve was insignificant under induction conditions. This was believed to be due to the slow response of the air system check valve poppet caused by the low pressure differential across the poppet. This was overcome by pressurising the pre-chamber air system to 0.5 bar. The flow of air into the pre-chamber could then be totally controlled by the metering valve.

6.2.2 System durability.

As the combustion system was under-going the initial trials and tests, certain design factors became evident which required attention. The primary problem experienced was with the connection between the injector hypodermic tube and the pre-chamber. Initially after approximately 10-15 minutes running the brazing material used would be blown out of the connection by the combustion chamber pressure. Inspection of the hypodermic and pre-chamber connection surfaces showed good penetration of the brazing material. The initial brazing material used was "EASYFLO-34"[§§§]. This was found to have a relatively low melting temperature range of 612-668°C. This was initially used so to minimise the heating required of the hypodermic tube during the brazing process. This was replaced with a general brazing rod with a higher melting point (ENZIG Bronze, 890°C). A cooling fan was also located adjacent to the pre-chamber

---

§§§ EASYFLO-34 is a trade name used for this particular brazing rod.

to aid in dissipating the heat transferred from the pre-chamber. Satisfactory operation life was accomplished with these design changes.

Problems also occurred with the injector pintle becoming partially blocked, and so leaking a significant amount of methane into the pre-chamber. Extensive testing and cleaning of the injector was undertaken, but no improvement was noticed. It was noted that this injector was also the injector used by Zavier.[122] He stated that leakage would quickly occur with this injector, but put it down to combustion particles bypassing the check valve and coming into contact with the injector pintle. Replacing the damaged injector with a new injector of the same model and specifications alleviated this problem immediately with no further leakage occurring from the injector. It was therefore concluded that damage had occurred to the injector prior to being used in this work.

Testing of the combustion system occurred in a step wise manner with all tests at 1000rpm occurring first, 1500rpm next and finally 2000rpm. All tests at 1000 and 1500rpm proceeded with minimal delays. However when running at 2000rpm the pre-chamber air check valve performed in an unusual manner. The check valve system initially would seem to operate correctly, but within 15 minutes of starting a test run at 2000rpm the poppet of the check valve would fail catastrophically. The Initial failure was believed to be due to metallurgical changes occurring over a relatively long period of time at the elevated temperatures encountered within the engine, but upon replacement of the

valve, failure occurred again within 15 minutes. A third test was undertaken with the same result.

It is now believed that the failure was caused by a dynamic interaction between the check valve poppet and the speed at which the engine was being operated. i.e the engine was operated at or near the natural frequency of the check valve poppet. This caused a resonant oscillating response of the poppet which initiated the failure, but at the same time allowing the air to enter the pre-chamber. Hence "normal" operation was seen to be occurring. The failure would have also been aided by the sharp change in section of the poppet. This would have acted as a large stress concentration aiding in the failure mechanisms of the material. Plate 6,1 shows the failed check valve poppet.

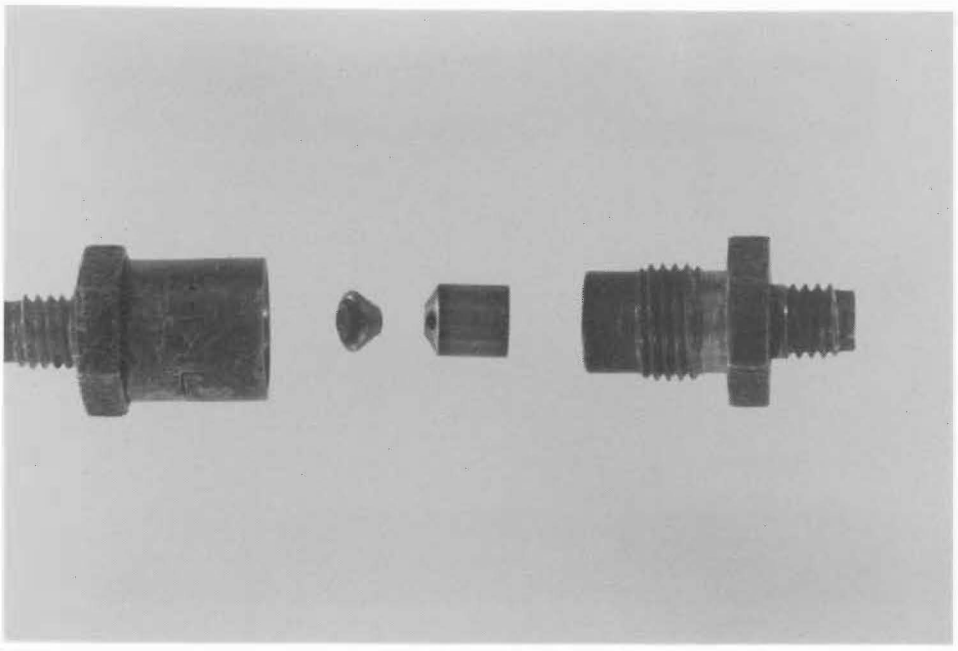

Plate 6,1 Failed check valve.

6.2.3 Errors associated with the system.

Glasson[121] outlined that the zero pressure output from the pressure transducer and the associated charge amplifier was prone to drift over a long period of time. Leaving this uncorrected would have no effect on the IMEP calculations but would effect the peak pressure readings. As the induction/exhaust mean pressures have relatively little effect on the overall pressure trace their adjustment to re-establish the zero voltage was seen as having little effect on the calculation of the IMEP for each cycle. The correction was accomplished in the pressure trace analysis program initially developed by Glasson, but modified for this work to analyse larger numbers of consecutive cycles than collected by Glasson.

A major limitation of the pressure data capture equipment was the limit on memory space available for Direct Memory Access transfer. For the system used, this was limited to 10,000 data points collected at regular time intervals. This limitation had major implications for the data collected, in that a trade off between cycle resolution and the number of cycles captured was necessary. As detailed investigations into knock and other combustion chamber vibrations were not envisaged, it was felt that 10 cycles, each containing 1000 data points, would give sufficient resolution for relatively accurate analysis of each cycle and allow larger cycle numbers to be captured to give a clearer indication as to the cyclic variations of the combustion system. Due to the large inertia of the flywheel, little variation in the rotational speed over one

cycle was expected.

As discussed in section 4.5.3 the reference marker for the analysis of the pressure data was generated by the ignition optical switch. This was done primarily because the addition of a second optical switch on the crank-shaft or cam-shaft would have been unnecessarily complicated. Using this system meant that any adjustment to the ignition point would accordingly vary the pressure reference point. A problem arose with the system when large ignition advances were necessary (over 40 °BTDC), in that the associated voltage output for the cylinder pressure at this point was approximately 0 volts. This was because of the voltage drift mentioned earlier. The result was that when the spike generator was activated, ie the pressure signal earthed, there was no voltage difference to generate the spike, and hence no reference point installed into the data. This resulted in all pressure traces with ignition angles greater than 40 °BTDC being rendered impossible to analyse.

6.3 COMBUSTION SYSTEM OPTIMISATION.

Initial optimisation of the system indicated that early injection of the methane (in the induction stroke), rather than late injection (in the compression stroke) as used by Zavier[122], into the pre-chamber was the research path to be followed. The early injection tests showed significantly lower amounts of

unburned hydrocarbons with minimal difference in the power output or fuel consumption compared to the late injection tests.

As the investigation was to be focused around the combustion system operating under overall lean conditions, all engine performance data are plotted against main chamber relative air/fuel ratio (MCAFR). The main chamber relative air/fuel ratio is defined as the ratio of air to methane (on a mass basis) introduced into the main chamber divided by the stoichiometric constant of 17.2 for air/methane reactions. From this it can be deduced that a value greater than unity represents an overall lean mixture and a value less than unity represents an overall rich mixture.

The injection timings given in the figures refer to the pre-chamber methane injection timing and are quoted as the start of injection after TDC during the induction period. Due to daily variations in atmospheric pressure and temperature, all power data were corrected[124] for these variations so that they may be directly compared.

Throughout all tests the basis for optimisation was consideration of:-

Unburned Hydrocarbons,

Brake Thermal Efficiency,

Lean Limit of Combustion,

Stable Engine Operation.

6.3.1 Air System Optimisation.

As mentioned in section 5.7.2 optimisation of the combustion system began with the pre-chamber air system. Here the injected methane timing and duration were kept constant whilst the amount of air entering the pre-chamber was varied. Figures 6,2, 6,3 and 6,4 show the brake thermal efficiency, hydrocarbon emissions and NOx emissions for the tests performed.

The tests show minimal difference in brake thermal efficiency (BTE) between main chamber air/fuel ratio's (MCAFR) $\lambda \approx 1.0$ and 1.6, with the 100% induction ratio (IR) having slightly higher efficiencies throughout. As the MCAFR is further increased the 200% induction ratio misfires first at $\lambda \approx 1.85$, followed by the 50% induction at $\lambda \approx 1.95$ and finally the 100% induction ratio at $\lambda \approx 2.05$. This can be explained in terms of the dilution of the methane injected into the pre-chamber. With the 50% filling ratio only half of the pre-chambers volume of air has been introduced. Therefore the remaining volume must be composed of residual exhaust gases. These gases could further dilute the methane/air ignition mixture sufficiently during the compression stroke to prevent positive ignition at leaner MCAFR's. The same effect would be experienced by the addition of too much air into the pre-chamber as in the case of the 200% induction ratio, except that air would be the dillutant, not the residual exhaust gases.

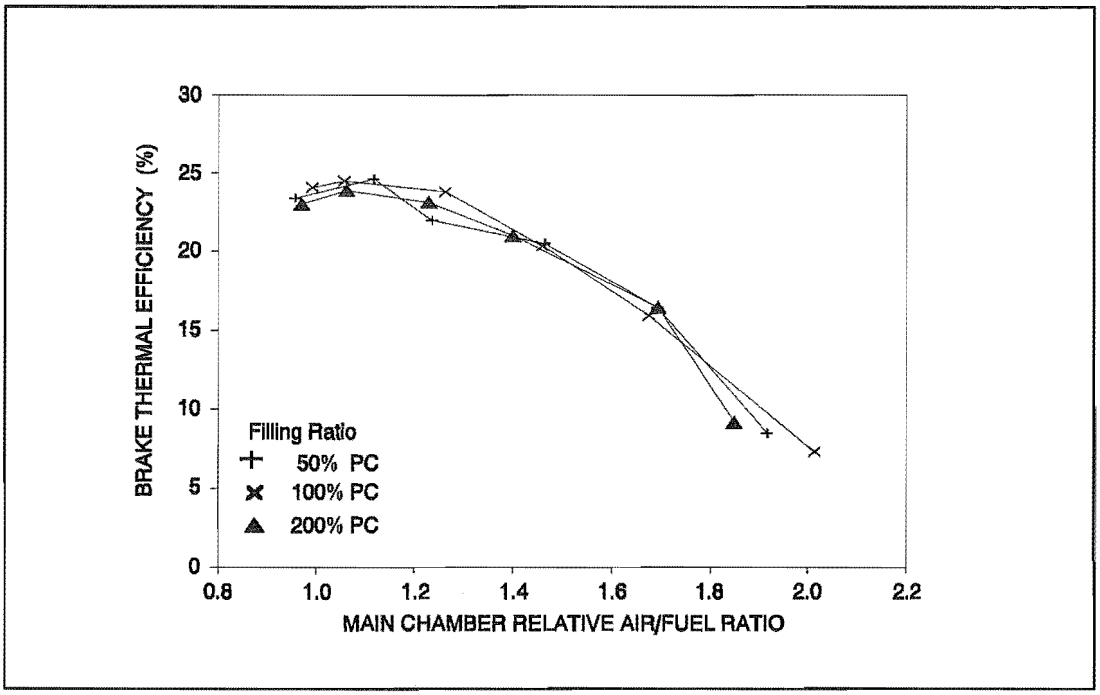

Figure 6,2 Brake Thermal Efficiency vs Main Chamber Relative Air/fuel Ratio for pre-chamber air optimisation tests. 1000 RPM, WOT, MBT.

The variation in hydrocarbon emissions (figure 6,3) shows little variation for all induction ratios at MCAFR $\lambda \approx 1.0 \rightarrow \lambda \approx 1.4$. After this the 200% ratio is slightly higher than both the 50% and 100% ratio's. As the respective lean limits are approached the 100% ratio hydrocarbon emissions remain lower than both the 50% and 200% ratio's.

This variation can be explained by the same argument used earlier. As the 100% ratio shows the most stable combustion for the same injection rate and timing, it should therefore follow that the hydrocarbon emissions associated should be the lowest for a given MCAFR.

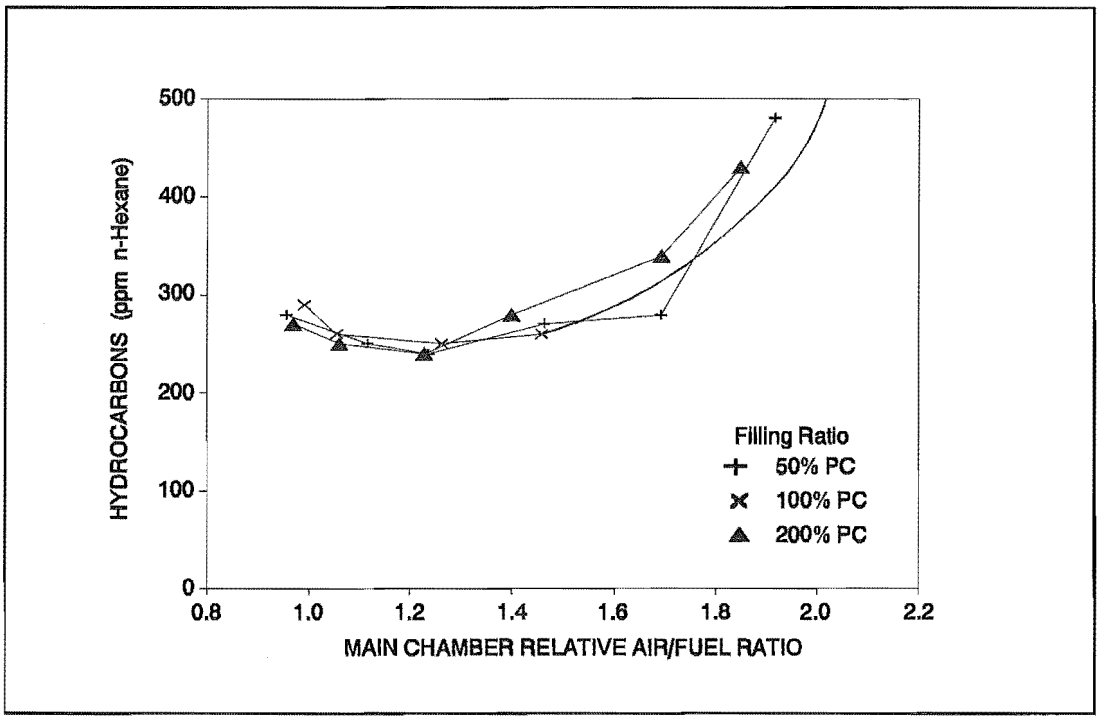

Figure 6,3 Hydrocarbon emissions vs Main Chamber Relative Air/fuel Ratio for pre-chamber air optimisation tests. 1000 RPM, WOT, MBT.

Figure 6.4 shows the variation in NOx emissions for the air optimisation tests. As can be seen the 50% ratio data shows higher NOx values, followed by the 100% ratio and finally the 200% ratio. The formation of NOx is synonymous with high temperatures. With an induction ratio of 50% the remaining gas in the pre-chamber must be exhaust gas (as mentioned earlier). The exhaust gases will have a higher temperature than the incoming air. Therefore the temperatures occurring under this situation must be higher than those occurring if the pre-chamber was pure air. Hence higher NOx emissions are present for the 50% induction ratio. At the other extreme, the addition of excess air would reduce the temperatures experienced within the pre-chamber, and hence further reduce the NOx emissions.

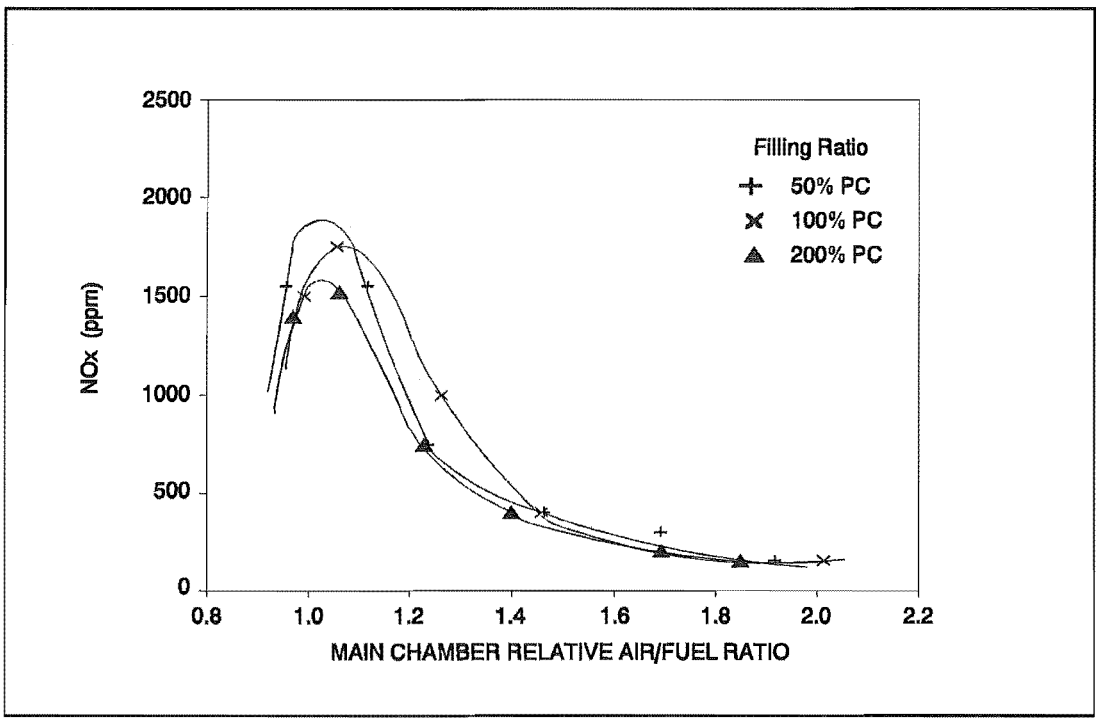

Figure 6,4 NOx Emissions vs Main Chamber Relative Air/fuel Ratio for the pre-chamber air optimisation tests. 1000 RPM, WOT, MBT.

Consideration of all these factors identified the optimum pre-chamber induction ratio (OPIR) to be 100%. This value was used throughout the remaining optimisation and testing work as the optimum amount of air to be introduced into the pre-chamber.

6.3.2 Methane Injection Duration Optimisation.

Optimisation of the methane injection rate was the next parameter to be optimised. Figures 6,5-6,8 show the relevant data to be discussed. Figure 6.5 shows the variation in BTE for the various methane injection rates. Little variation is experienced for all injection rates up to $\lambda \approx 1.6$. Beyond this some variation was experienced. For the smaller injection rates (0.0162, 0.0299kg/h) this would be due to the ignition mixture being made excessively lean by the incoming mixture from the main chamber, hence reducing the brake power produced due to slower burning of the ignition charge and hence of the overall charge. The high injection rate of 0.04069kg/h also has a lower BTE than that of the 0.0367kg/h injection rate.

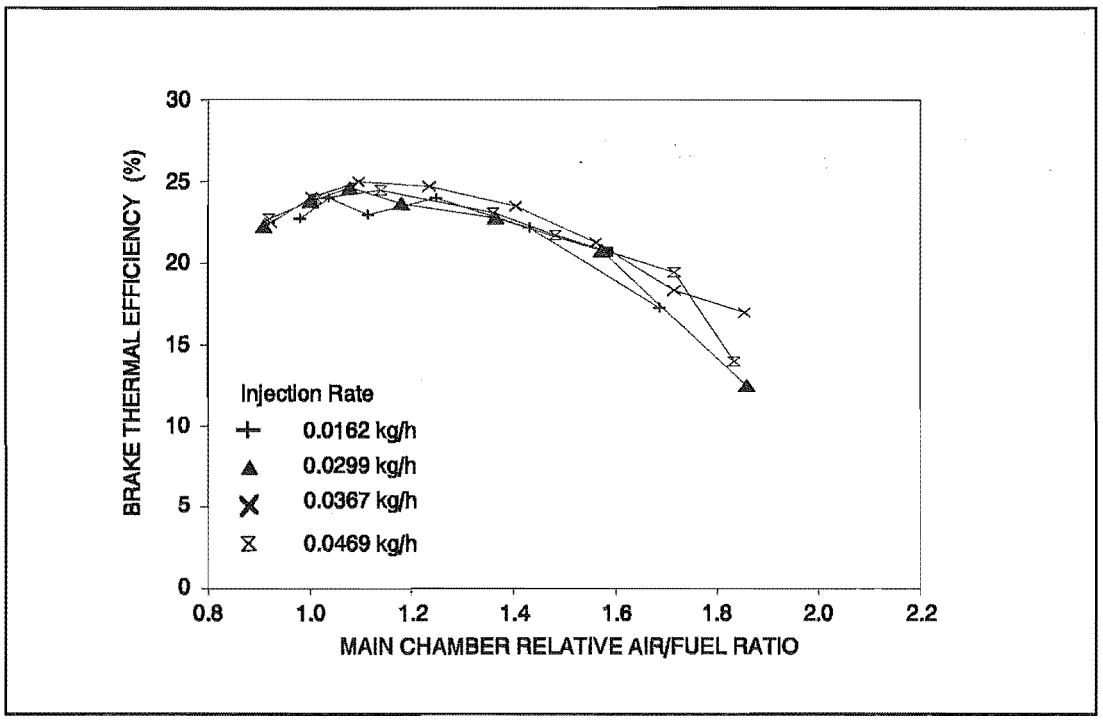

Figure 6,5 Brake Thermal Efficiency vs Main Chamber Relative Air/fuel Ratio for the methane injection rate optimisation tests. 1000 RPM, WOT, MBT 100%IR.

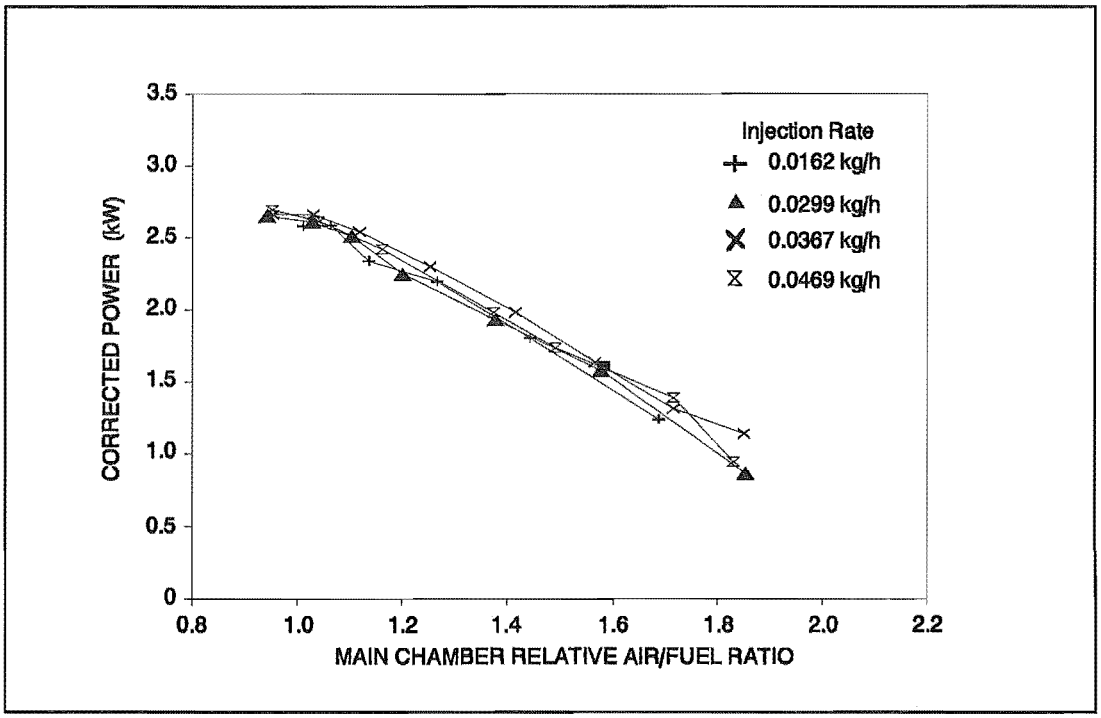

Figure 6,6 Corrected Power vs Main Chamber Relative Air/fuel Ratio for methane injection rate optimisation tests. 1000RPM, WOT, MBT, 100%IR.

Consideration of figure 6,6 shows that the observed reduction in BTE is also reflected in a reduction in brake power for the lower injection rates. As the flame speed of a rich mixture is also less than that of a stoichiometric mixture, it could be suggested that the reduction in power is due again to a lower overall flame speed. The injection rate of 0.0367kg/h gave the highest BTE at $\lambda \approx 1.9$.

Figure 6,7 shows the hydrocarbon emissions for the injection duration tests. Little variation occurs between injection rates until $\lambda \approx 1.5$. Here the hydrocarbon emissions begin to increase dramatically for the lower injection

rates of 0.0162 and 0.0299kg/h, indicating the effects of slow burning and misfire. At $\lambda \approx 1.75$ the emissions for the higher injection rate also begins to increase dramatically, again showing the instability associated with the richer than stoichiometric mixture as mentioned earlier. In comparison the 0.0367kg/h injection rate has fairly low hydrocarbon emissions at the lean limit shown of $\lambda \approx 1.9$.

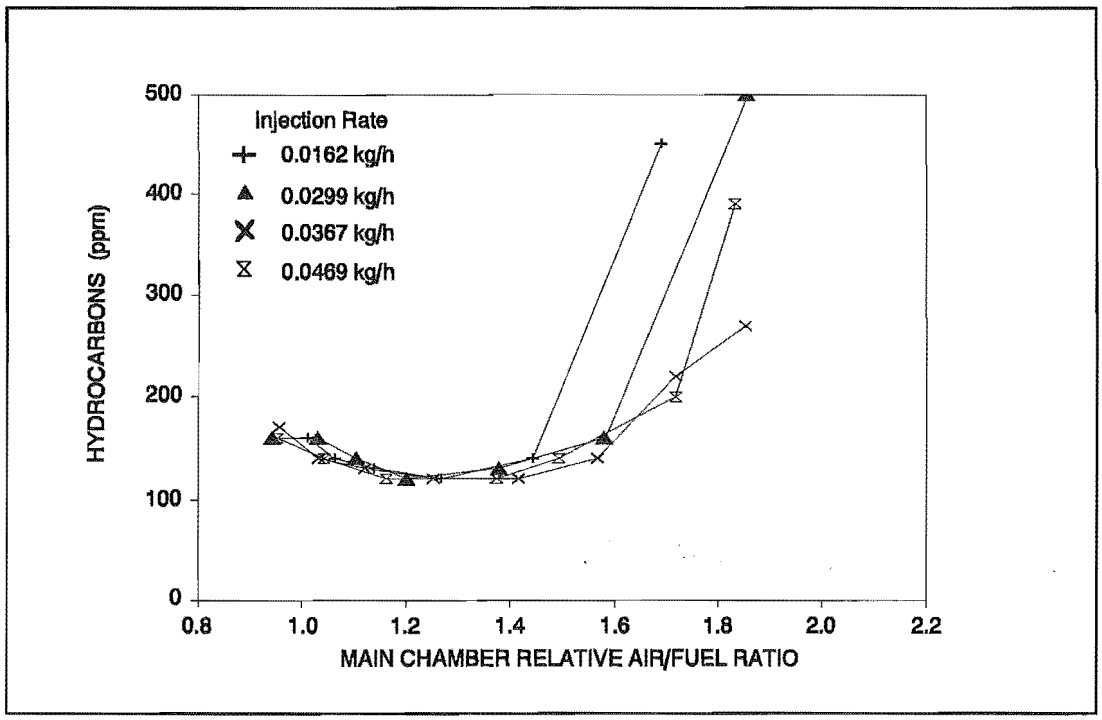

Figure 6,7 Hydrocarbon emissions vs Main Chamber Relative Air/fuel Ratio for methane injection rate optimisation tests.1000RPM, WOT, MBT, 100%IR

Figure 6,8 shows the NOx emissions for the methane injection tests. Little variation exists between the values for all the injection rates at all main chamber air/fuel ratios.

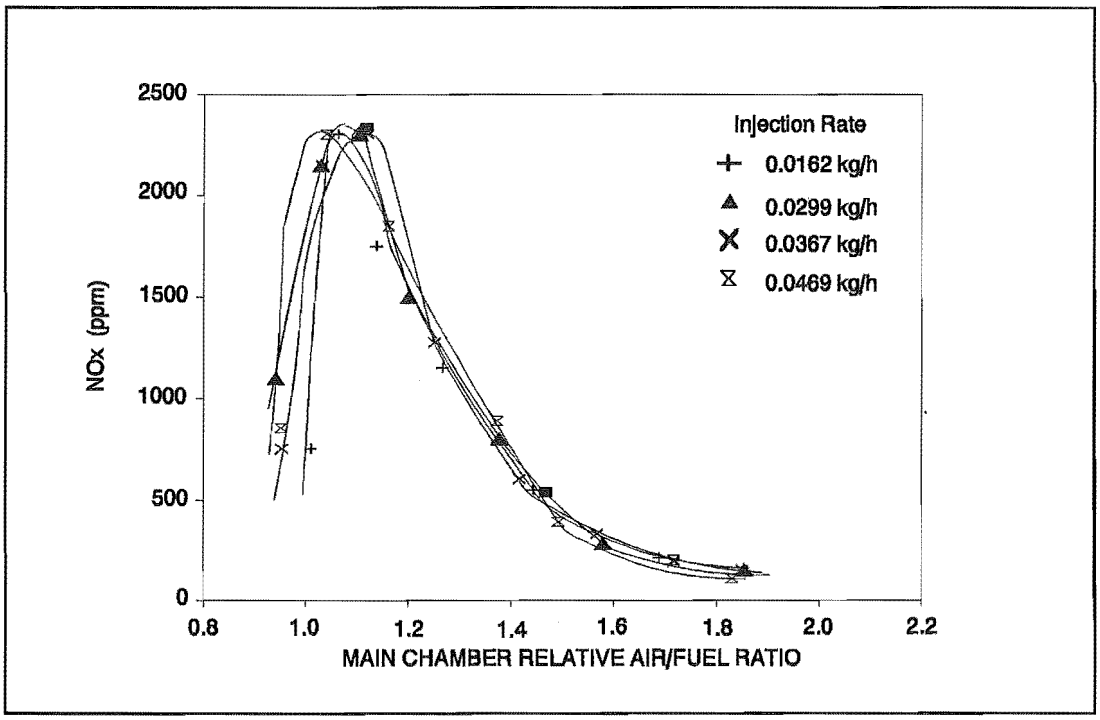

Figure 6,8 NOx emissions vs Main Chamber Relative Air/fuel Ratio for methane injection timing optimisation tests. 1000RPM, WOT, MBT, 100%IR.

From consideration of the above, the optimum injection rate (at 1000RPM) as 0.0367kg/h. This over all flowrate would be adjusted accordingly for different engine speeds so that the amount injected into the pre-chamber per cycle remained constant.

6.3.3 Methane Injection Timing Optimisation.

Optimisation of the methane injection timing was the last parameter to be optimised. Figures 6,9-6,10 give relevant information to the optimisation of the injection timing.[¥¥¥¥]

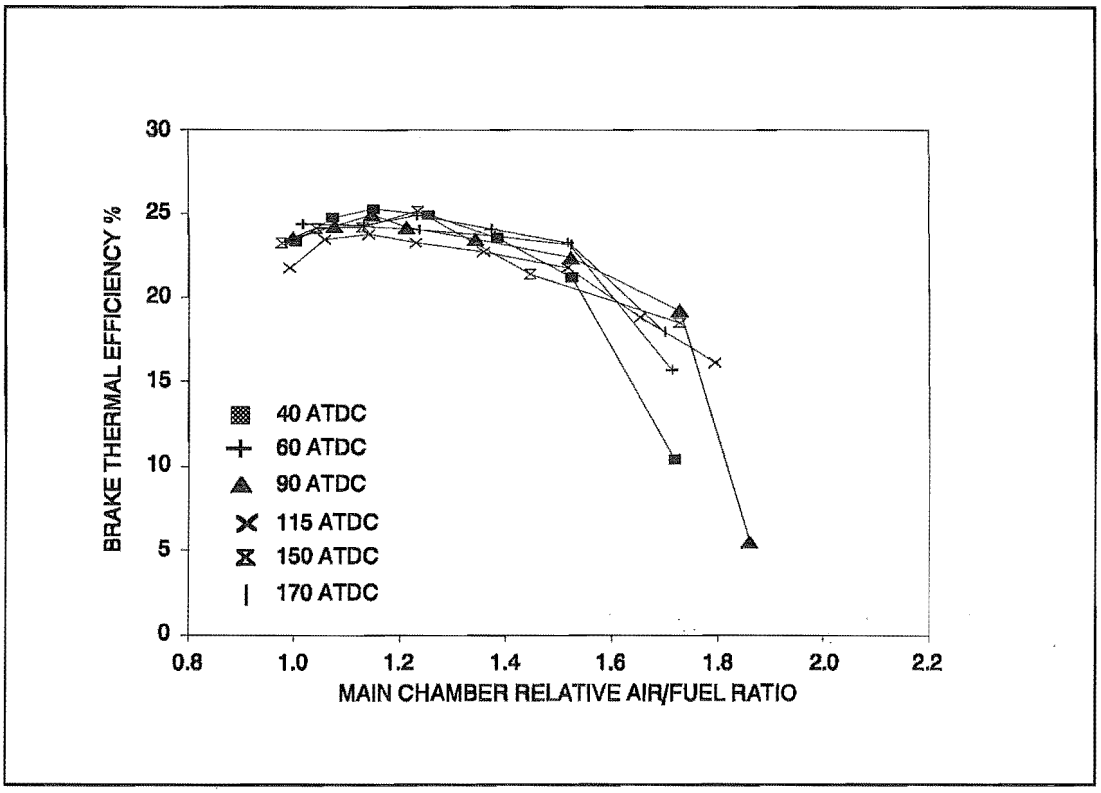

Figure 6,9 Brake Thermal Efficiency vs Main Chamber Relative Air/fuel Ratio for methane injection timing optimisation tests. 1000RPM,WOT, MBT 100%IR.

Figure 6,9 shows the BTE for various injection timings. Between $\lambda \approx 1.0$-1.6 there is not much deviation in the BTE traces. Consideration of the BTE at the

¥¥¥¥ All timings given are ATDC during the induction stroke.

leaner MCAFR's shows that the earlier injection timings (40,60°ATDC) show reduced efficiency at lower MCAFR than the later injection timings (150-170°ATDC), with the middle injection angle timings being the most stable (90-115°ATDC). Consideration of the relationship between injection timing and the induction of the pre-chamber air could explain this.

If the assumption is made that the air induced into the pre-chamber occurs over the period 0°ATDC and 180°ATDC then it would be possible to produce ignition mixtures in the pre-chamber with a "negative" stratification. That is, if the methane is injected relatively early in the induction stroke, the air which continues to flow into the pre-chamber after the end of injection could force the methane down the pre-chamber away from the spark plug, producing a layered effect with lean methane/air mixture adjacent to the spark plug, a richer mixture further down the pre-chamber, followed by the main charge. Quader[88] experienced these same problems with the development of the axially stratified charge engine if injection early in the induction stroke was used. A similar problem could occur with the late injection timings. The result would be a very rich mixture adjacent to the spark plug, followed by an extremely lean mixture further down the pre-chamber and finally the main chamber charge. Clearly an optimum would have to occur in between these two extremes, where a homogeneous mixture would be formed in the pre-chamber.

Figure 6,10 shows the hydrocarbon emissions for the various injection timings. The later injection timings (115-170°ATDC) show higher hydrocarbon levels throughout the MCAFR spectrum, indicating the presence of richer pockets of fuel within the pre-chamber. These pockets could be associated with the process discussed above. Early injection timing show lower hydrocarbon levels between $\lambda \approx 1.0$ and $\lambda \approx 1.6$. Beyond this the levels increase dramatically. This could also be a consequence of the negative stratification mentioned. The lean mixture adjacent to the spark plug would be harder to ignite, and would burn slower than the adjacent richer mixture. Hence higher hydrocarbon levels would occur due to the occurance of slow burning and misfire.

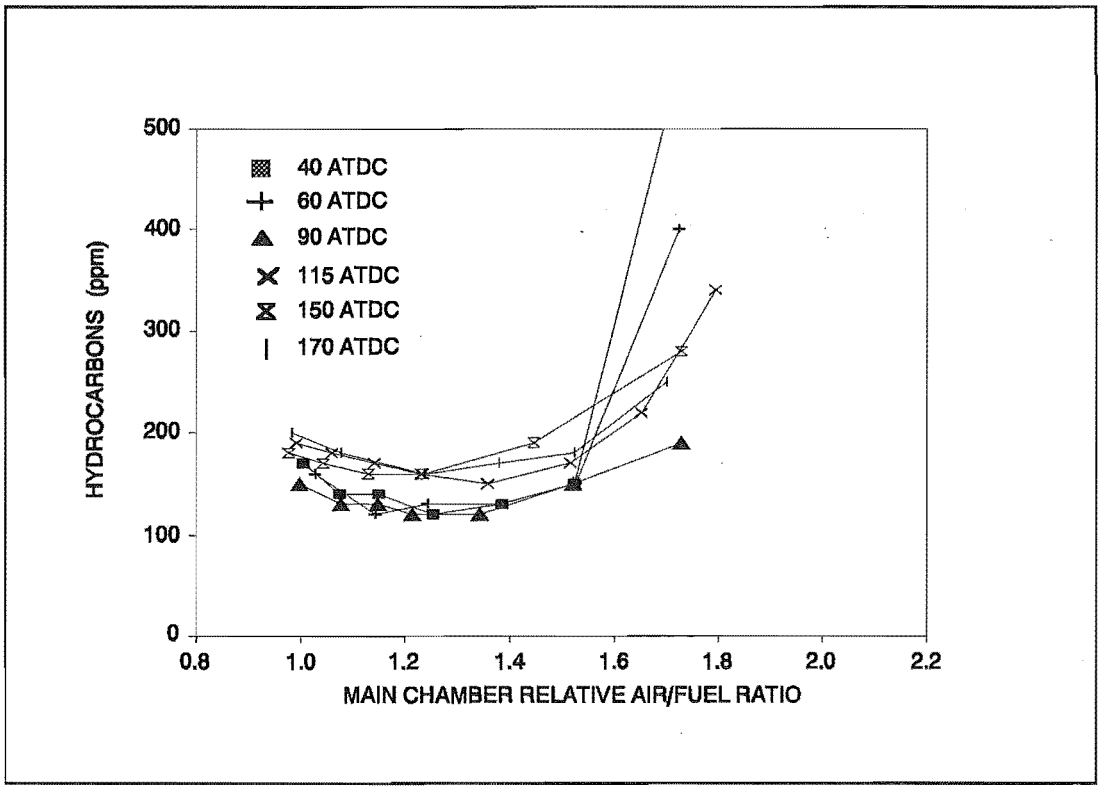

Figure 6,10 Hydrocarbon Emissions vs Main Chamber Relative Air/fuel Ratio for methane injection timing optimisation tests. 1000RPM, WOT, MBT, 100%IR.

For 1000RPM the optimum injection timing was 90°ATDC. For other engine speeds this parameter would have to be re-evaluated, as the time for the injection of the methane would be fixed, but the injection time window would decrease with increasing engine speed.

6.4 ENGINE PERFORMANCE.

This section deals with the comparison of the pre-chamber charge stratification combustion system, with the baseline spark ignition system and the charge stratification system developed by Zavier. Again it should be noted that not all experimental data is given, it is only given when a relevant theme is to be identified and discussed.

6.4.1 Extension of the equipment lean limit.

The lean limit of combustion for methane in air is approximately 5% (Vol). However, this limit cannot be obtained in internal combustion engines due to a number of factors, including heat transfer, turbulence and the available ignition energy.[25,27,31,38,46,49,52,] The lean limit achievable within the engine is known as the equipment lean limit of combustion (ELLC).[119] It is the extension of this equipment lean limit of combustion which is one of the main objectives of this work.

Figures 6,11-6,13 give the BTE vs MCAFR for various methane injection angles at engine speeds of 2000,1500 and 1000RPM respectively.

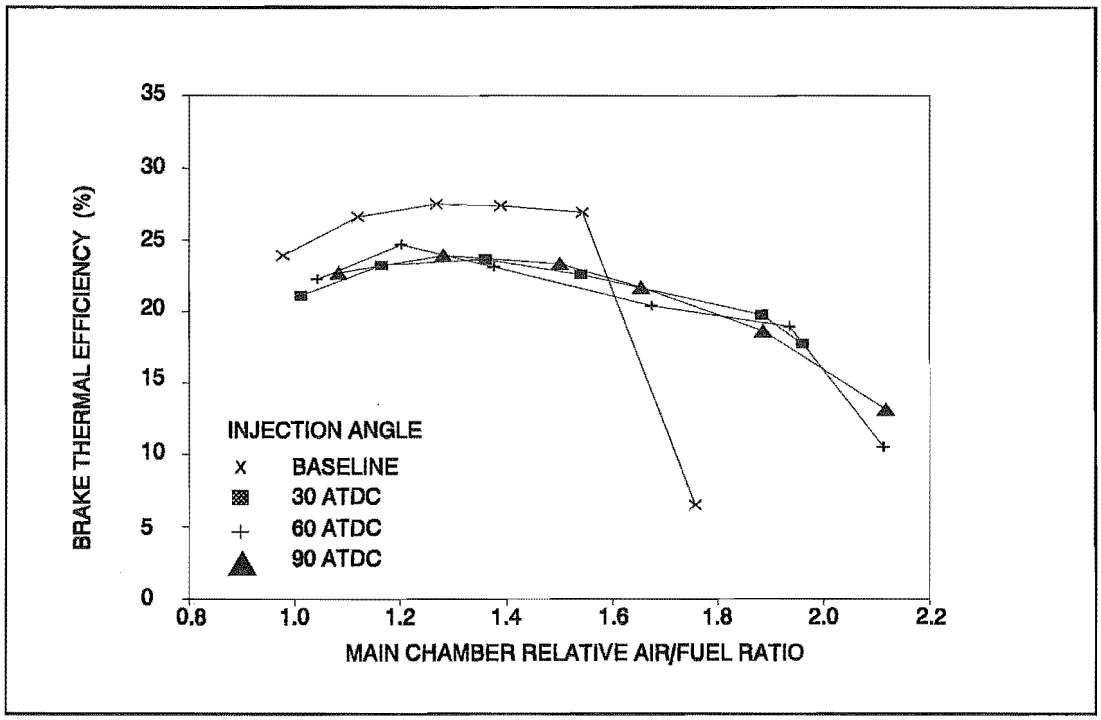

Figure 6,11 Brake Thermal Efficiency vs Main Chamber Relative Air/Fuel Ratio for various methane injection angles and baseline tests. 2000RPM, WOT, MBT, 100%IR, 0.07076kg/h.

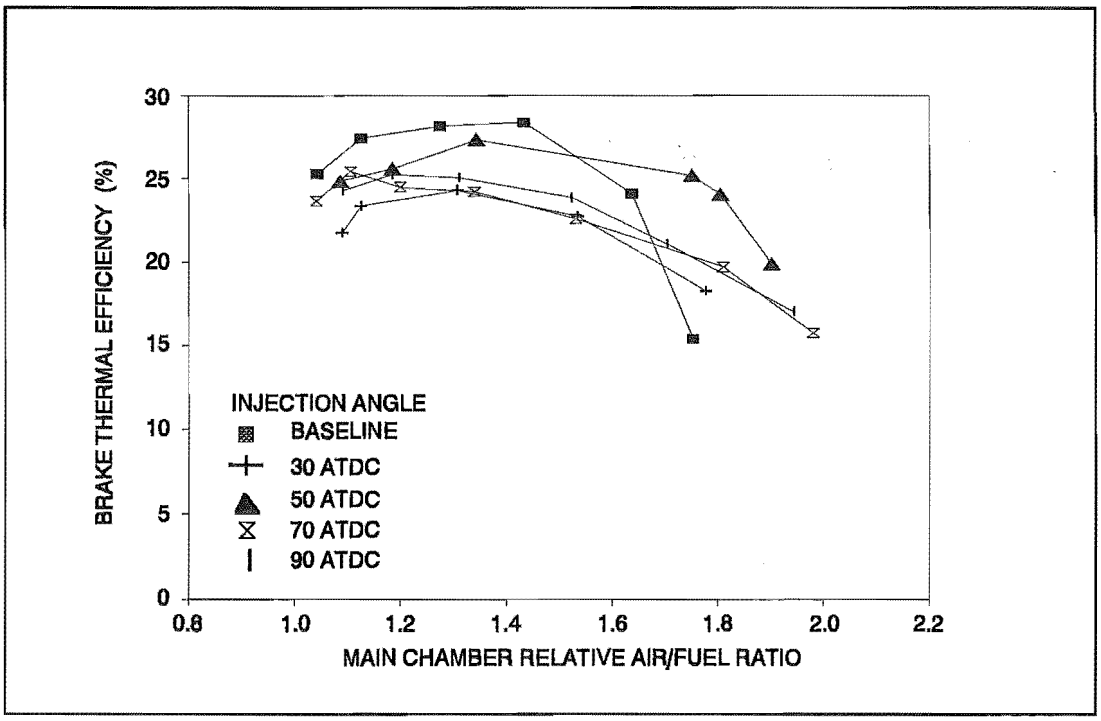

Figure 6,12 Brake Thermal Efficiency vs Main Chamber Relative Air/Fuel Ratio for various methane injection angles and baseline tests. 1500RPM, WOT, MBT 100%IR, 0.0537kg/h.

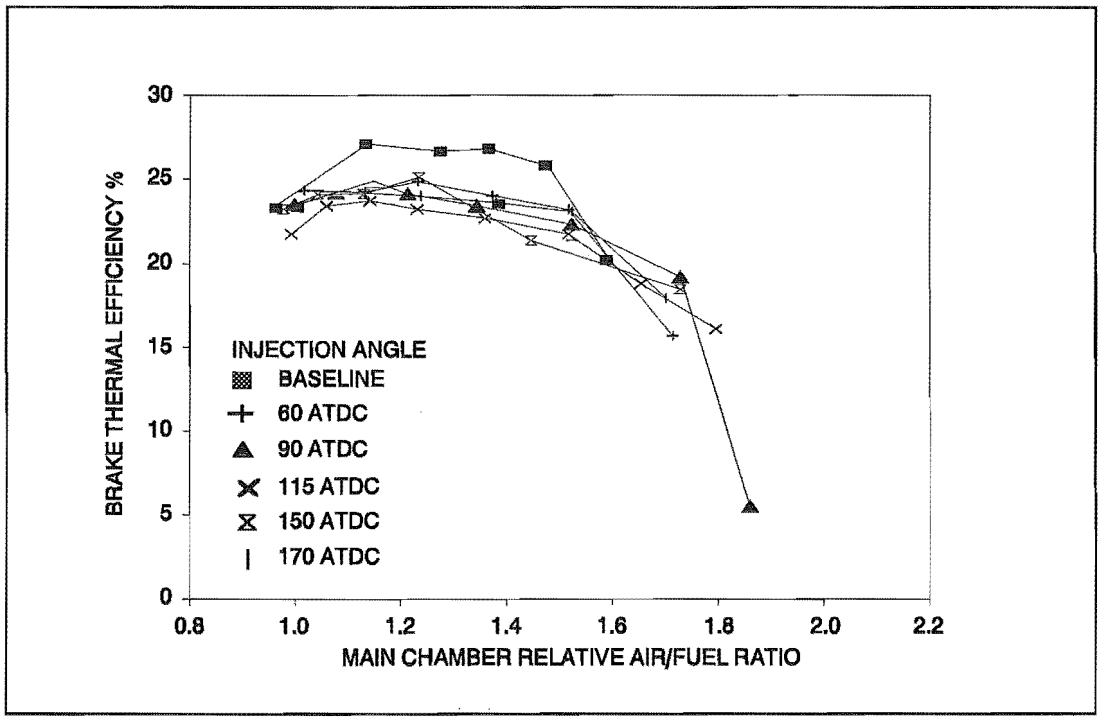

Figure 6,13 Brake Thermal Efficiency vs Main Chamber Relative Air/Fuel Ratio for various injection angles and baseline tests. 1000RPM, WOT, MBT, 0.0367kg/h, 100%IR.

There are three main points that can be deduced from these graphs;

BTE values for the baseline tests are higher than those of the charge stratification tests around $\lambda \approx 1.0 \rightarrow \lambda \approx 1.6$,

The equipment lean limit of combustion is extended for the charge stratification tests,

The degree of extension to the equipment lean limit of combustion increases with an increase in engine speed ($\lambda \approx 1.8$ at 1000RPM, $\lambda \approx 2.1$ at 2000RPM.) whereas the baseline equipment lean limit of combustion

remains relatively constant for an increase in engine speed.

The first point will be discussed in section 6.4.3 as it is relevant to that section. The second and third points can be summarised in the following argument.

Within the baseline tests a homogeneous charge was introduced into the combustion chamber and ignited with a conventional spark plug ignition system. As the air/fuel ratio was increased (ie leaned) the energy required to ignite the charge in the vicinity of the spark plug would increase.[27,28,30,33,34,35,36,37,99] A critical point would be reached whereby the energy supplied from the spark would be insufficient to ignite the eddies adjacent to the plug electrodes, and/or the slow rate of energy release due to the low flame speed from these lean eddies would be insufficient to propagate the flame in the turbulent environment. With the charge stratification system a small relatively rich mixture was introduced into the pre-chamber, with the majority of the charge located in the main chamber at a leaner air/fuel ratio. As the mixture around the spark plug (ie within the pre-chamber) was of an easily ignitable composition a flame front would be established which could propagate into the main lean charge and complete the burn cycle. This explains why the pre-chamber stratified charge combustion system operates at leaner air/fuel ratios, ie it is an improvement in the ignition processes which allow extension of the equipment lean limit.

It has been shown that an increase in the turbulent intensity of the charge will increase the flame propagation rate.[86,98,99,100,102,103,104,105,112]

$$\text{ie} \quad S_t = S_l + u' \qquad (6.1)$$

The turbulent intensity within an internal combustion engine has been shown to increase approximately linearly with an increase in engine speed. Hence as the engine speed increases so should the turbulent flame speed. However, as the air/fuel ratio is increased from stoichiometric (leaned) the laminar flame speed will decrease accordingly. (see figure 3,7) Within the engine a combination of these two effects will result in the extension of the equipment lean limit of flammability with an increase in engine speed. That is, at low engine speeds the slow laminar flame speed will have a dominating effect over the turbulence intensity, but this will be compensated for as the engine speed is increased for that air/fuel ratio, hence allowing even leaner air/fuel ratios to be burned.

With these points in mind the flame propagation failure mechanism must also be linked to the engine speed. For a given engine speed there is only a finite time for which the TDC volume remains constant, (within say a 10% change in volume). Within this time the combustion process must be undertaken, and generally completed. If the laminar flame speed reduces with an increase in air/fuel ratio then the time for the combustion process to occur will increase. A point will be reached where the increase in cylinder volume will become predominant, and begin to "stretch" the flame front. The stretching process

increases the flame frontal area for the same amount of reactants. This will reduce the heat available to be transferred per unit area of the flame. Heat transfer is a fundamental requirement for the flame to propagate, reducing this will reduce the propagation processes of the flame. The cooling effect associated with the expansion process is also significant. A critical point may be reached where the flame will become unsustainable, and become extinguished. An increase in turbulent intensity, say by an increase in engine speed, would reduce the burn time and ensure the flame does not become extinguished by flame stretch for that air/fuel ratio.

Summarising, the equipment lean limit of combustion for the pre-chamber stratified charge engine is related to the propagation of the turbulent flame, whereas the equipment lean limit for the baseline spark ignition engine is related to the ignition and development of the flame.

6.4.2 Emissions.

Figures 6,14 $\rightarrow$ 6,17 show a general set of emission results for the engine tests. They are for the 1500RPM tests and show the trends which were common to all tests at the various speeds.

One of the main objectives of this work was to try and reduce the hydrocarbon emission levels experienced by Green and Zavier.[122,123] From figure 6,14 it

can be clearly seen that for similar methane injection rates the hydrocarbon emissions have been substantially reduced over all equivalence ratios compared to Zavier's[122] levels. However the hydrocarbon levels are still higher than the baseline tests.

Green and Zavier concluded that the methane injected around the spark plug prior to ignition was burning at, or close to the rich limit of flammability, and that quenching of unburnt or partially hydrocarbons was occurring within the hypodermic injection tube. Furthermore the overall lean burning lowered the exhaust gas temperatures and this to reduced oxidation reactions occurring in the exhaust and hence an increase in UHC's.

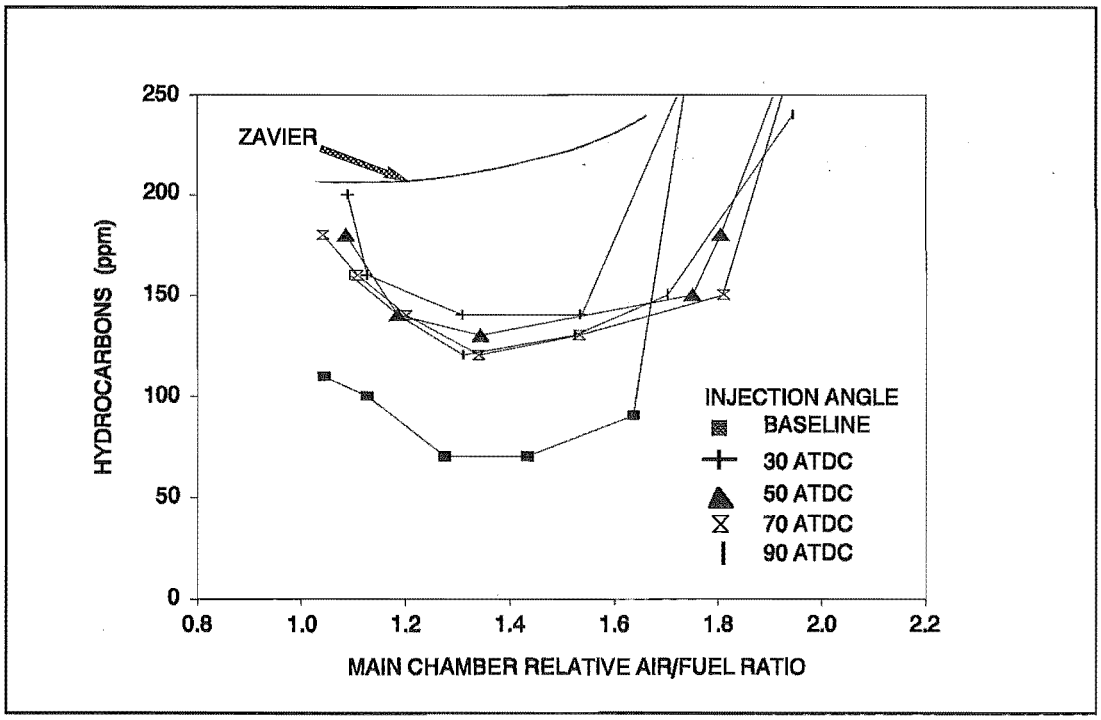

Figure 6,14 Hydrocarbon Emissions vs Main Chamber Relative Air/Fuel Ratio for various methane injection angles and baseline tests. 1500RPM, WOT, MBT, 100%IR, 0.0537kg/h.

In this work minimisation of quench volumes within the apparatus is believed to have helped in the initial reduction of these emissions. Another factor was believed to be improved control of the ignition mixture motion brought about by the pre-chamber. Early injection of the methane ensured a homogeneous ignition mixture was formed at the spark plug electrodes. The exact composition of this mixture at the point of ignition is a function of the injection rate, injection timing and the ignition timing.

The higher hydrocarbon levels relative to the baseline tests are believed to be the culmination of a number of factors, namely;

1: The continuing problem of lower exhaust temperatures ing to reduced hydrocarbon oxidation reactions occurring within the exhaust system.

2: An increase in the surface/volume ratio of the combustion chambers, hence an increase in the associated quench area.

3: Turbulent vortices created by the issuing flame front out of the connecting passage could stretch the flame, causing the flame to extinguish locally and hence increase the hydrocarbon emissions.

Figure 6,20 shows a comparison between the exhaust temperatures for the pre-chamber charge stratification combustion system and the baseline system. As can clearly be seen the baseline system has higher exhaust temperatures

than the charge stratification system. This could have the effect of reducing further hydrocarbon reactions which would occur in the exhaust system, hence increasing the hydrocarbons emitted from the exhaust relative to the baseline system.

Although careful design of the pre-chamber and its ancillary equipment was undertaken to minimise the quench volumes, a slight increase in the surface/volume ratio was unavoidable. Careful attention was paid to the design of the injector check valve and connection, but this would still contribute a relatively large amount of unburned hydrocarbons to the overall increase. Only a 3% increase in the surface/volume ration for the stratified charge system

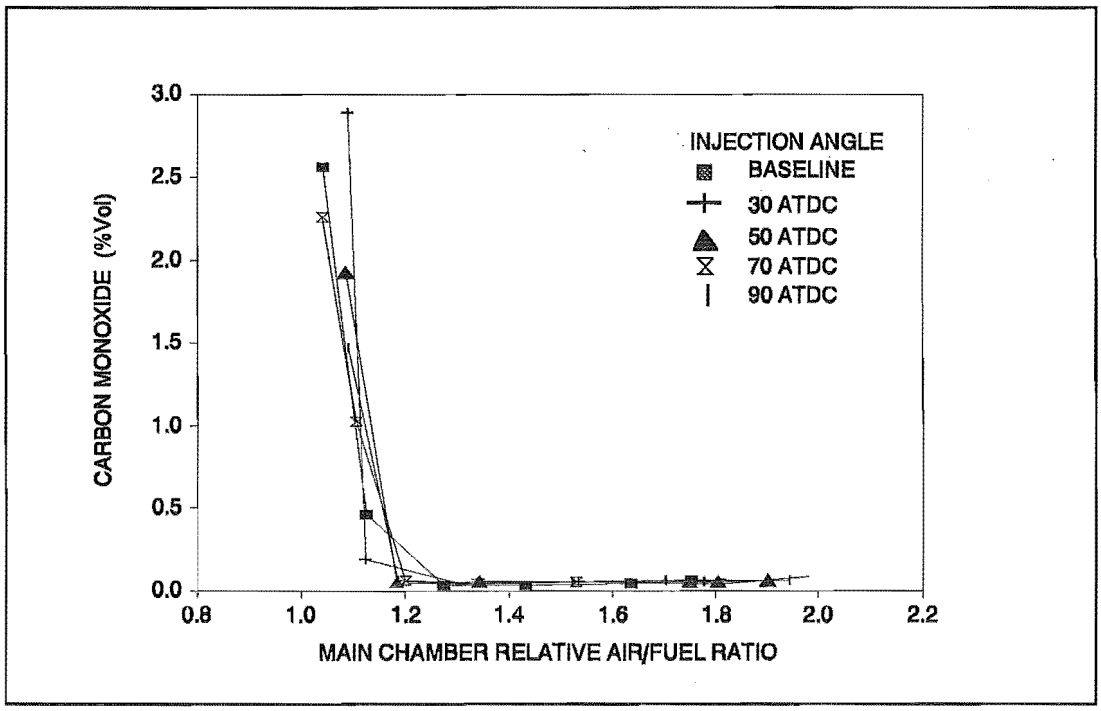

Figure 6,15 Carbon Monoxide emissions vs Main Chamber Relative Air/Fuel Ratio for various methane injection rates and baseline tests. 1500RPM. WOT, MBT, 100%IR, 0.0537kg/h.

was calculated for the main chamber and pre-chamber. Although this would increase the UHC's, it should only account for an increase of the same order.

As the ignition mixture within the pre-chamber is burned a pressure differential is developed between the pre-chamber and the main chamber. This causes the hot combustion gases to be forced out of the pre-chamber an into the main chamber. At the exit of the connection passage the velocity gradient between the issuing gases and the main chamber gases would be at a maximum. The shear stress developed would cause the formation of a toroidal vortex around the connection passage perimeter. This could stretch the propagating flame locally at these points and cause localised extinction of the flame. This would result in some fuel remaining unburned, hence higher hydrocarbon emissions would exists in the exhaust. Yagi et al[70] showed that recirculation of the gases near the connecting passage entry could further reduce the hydrocarbon emissions.

Figure 6,15 shows that carbon monoxide emissions for the charge stratification tests do not vary considerably relative to the baseline tests. Figure 6,16 shows a reduction in the NOx emissions for the optimum injection timing on a ppm basis, however consideration of the specific NOx emissions (figure 6,17) shows higher values compared to the baseline tests. This is primarily due to a reduction in brake power for the stratification tests when compared to the baseline tests.(figure 6.18)

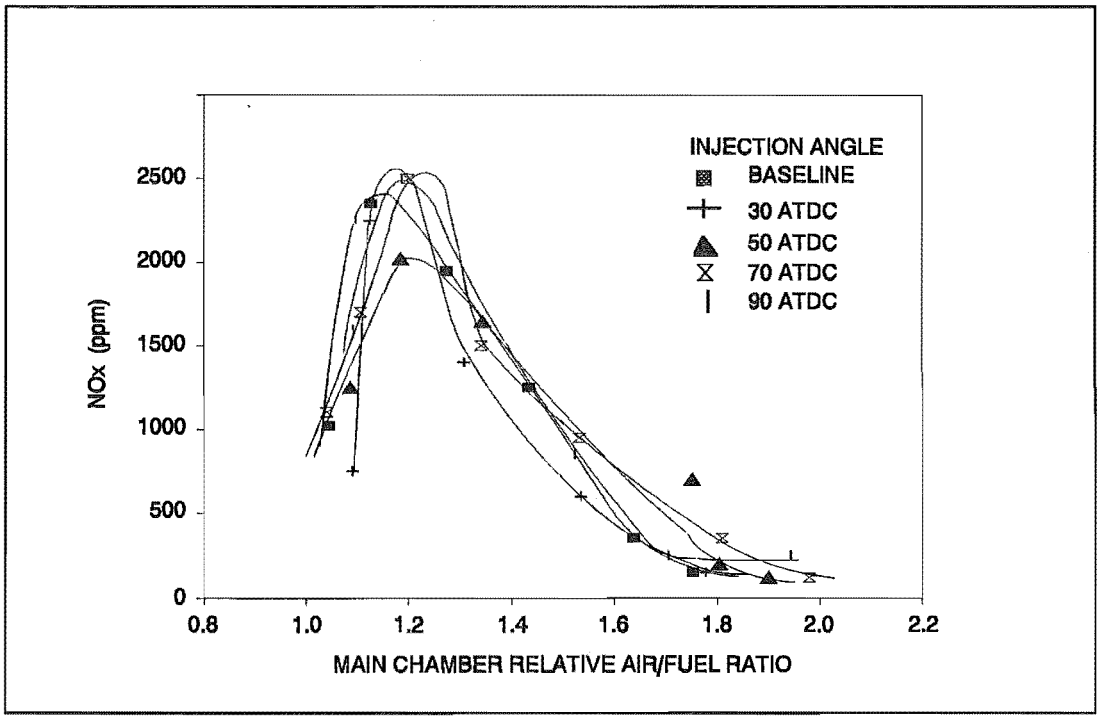

Figure 6,16 NOx Emissions vs Main Chamber Relative Air/Fuel Ratio for various methane injection angles and baseline tests. 1500RPM, WOT, MBT, 100%IR, 0.0537kg/h.

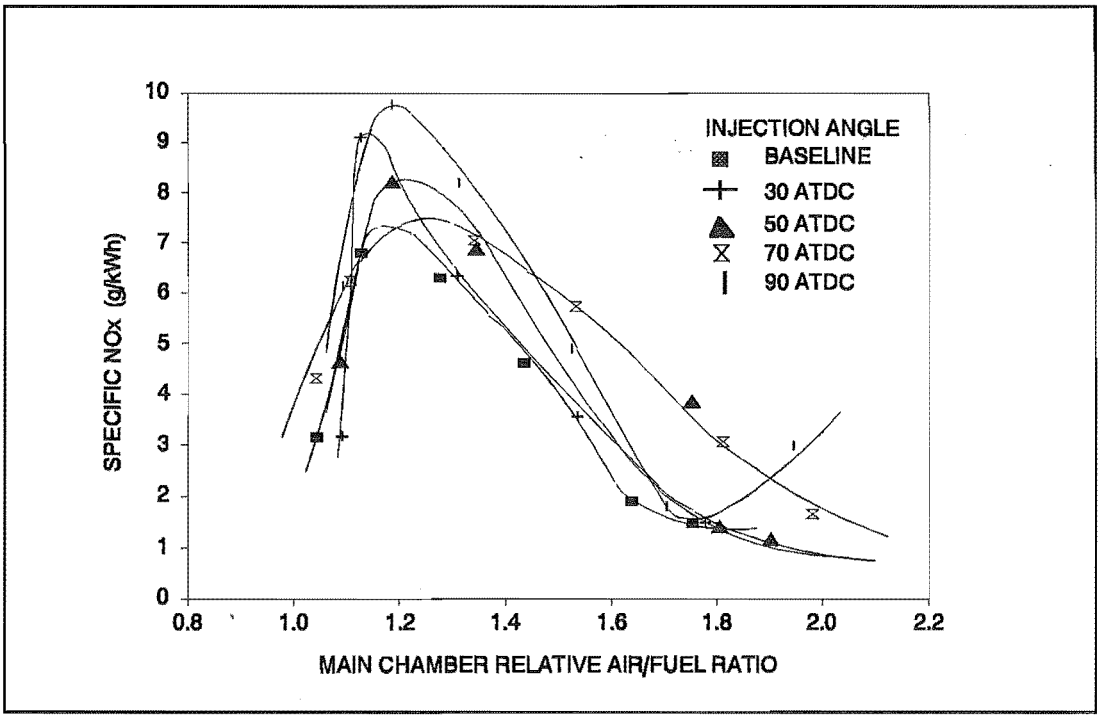

Figure 6,17 Specific NOx Emissions vs Main Chamber Relative Air/Fuel Ratio for various methane injection angles and baseline tests. 1500RPM, WOT, MBT, 100%IR, 0.0537kg/h.

6.4.3 Performance.

Performance characteristics of the charge stratification and baseline systems are compared in figures 6,18 → 6,20.

Figure 6,18 shows the corrected power output for both systems against the main chamber relative air/fuel ratio. It can be immediately seen that at stoichiometric air/fuel ratios up to $\lambda \approx 1.5$ the base line system has higher brake power. The reasons for the reduction in brake power and hence a reduction in brake thermal efficiency are believed to be as follows. Consideration of figure 6,19 shows that for the charge stratification system the ignition angle for MBT substantially retarded compared to the baseline tests over all equivalence ratios. One would assume that this would manifest itself as higher exhaust temperatures. Figure 6,20 shows however that the exhaust temperatures for the charge stratification tests are lower than the baseline tests over all equivalence ratios. From these two points it is postulated that the turbulence generated by the flows in and out of the pre-chamber are intensifying the combustion rate to such an extent as to reduce the overall burn time. However a combination of this intense turbulence, increased surface area of the combustion chamber due to the pre-chamber, and increased post-flame residence time of the combustion products is ing to increased rates of heat transfer from the combustion gases to the combustion chamber walls, reducing the available energy to produce useful work. Pischinger[66,80] concluded that thermal efficiency was highly dependent upon cooling losses for a pre-

chamber stratified charge engine.

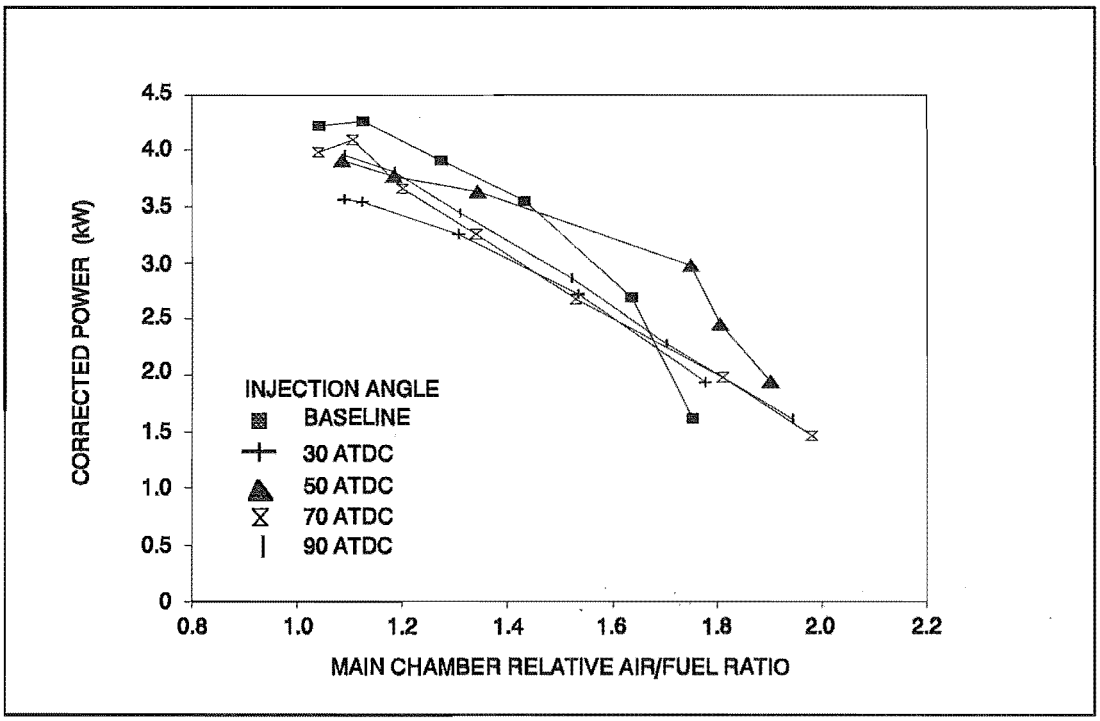

Figure 6,18 Corrected Brake Power vs Main Chamber Relative Air/Fuel Ratio for various methane injection angles and baseline tests. 1500RPM, WOT, MBT, 100%IR, 0.0537kg/h.

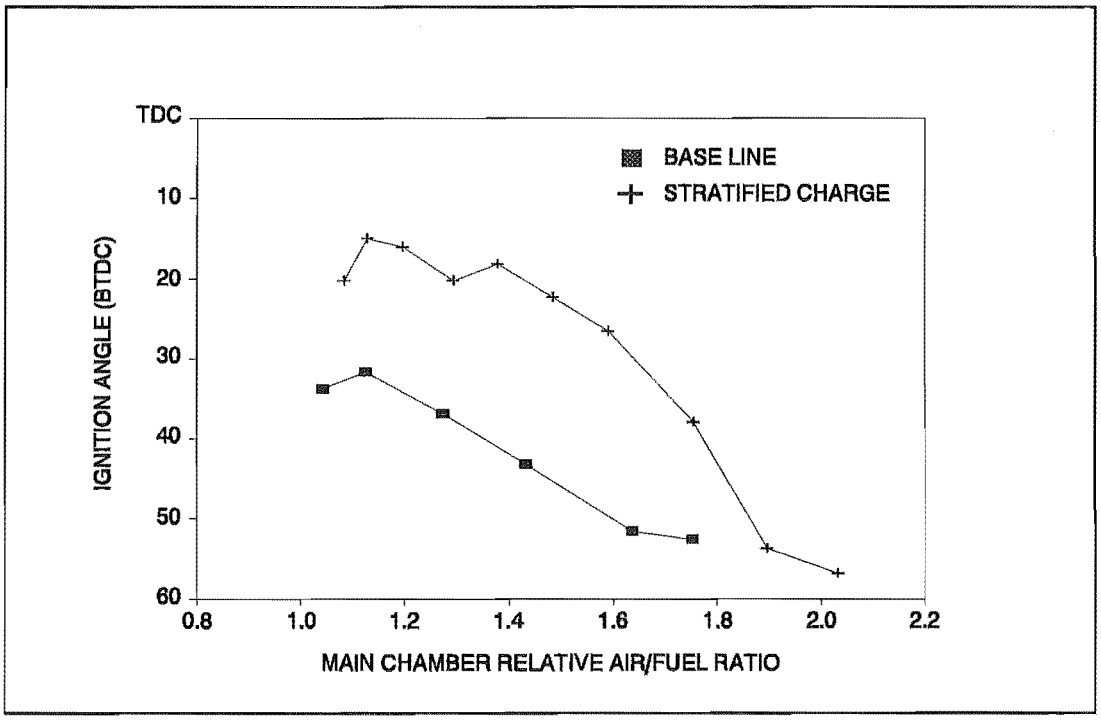

Figure 6,19 MBT Ignition Angle vs Main Chamber Relative Air/Fuel Ratio. 1500RPM, WOT, 100%IR, 0.0537kg/h

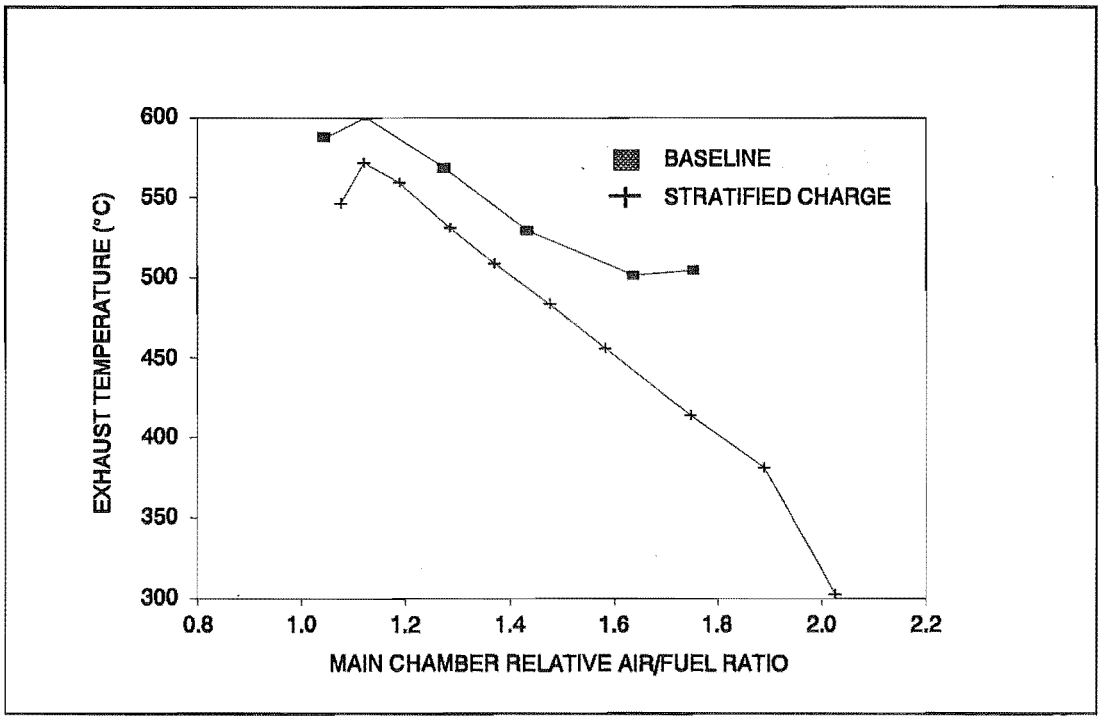

Figure 6,20 Exhaust Temperature vs Main Chamber Relative Air/Fuel Ratio. 1500RPM, MBT, WOT, 100%IR, 0.0537kg/h.

6.4.4 IMEP Variations.

Figure 6,21 shows the variations in IMEP for both the charge stratification system and the baseline system. This data was obtained from the analysis of the pressure data in the combustion chamber. Ten consecutive cycles, each of 1000 data points, were captured for each test and used as the basis for this analysis. Although 10 cycles are not strictly statistically a representative sample of the system, the limitations placed on the size of the data array by the data capture system restricted a larger sample size without effecting the resolution of each cycle.

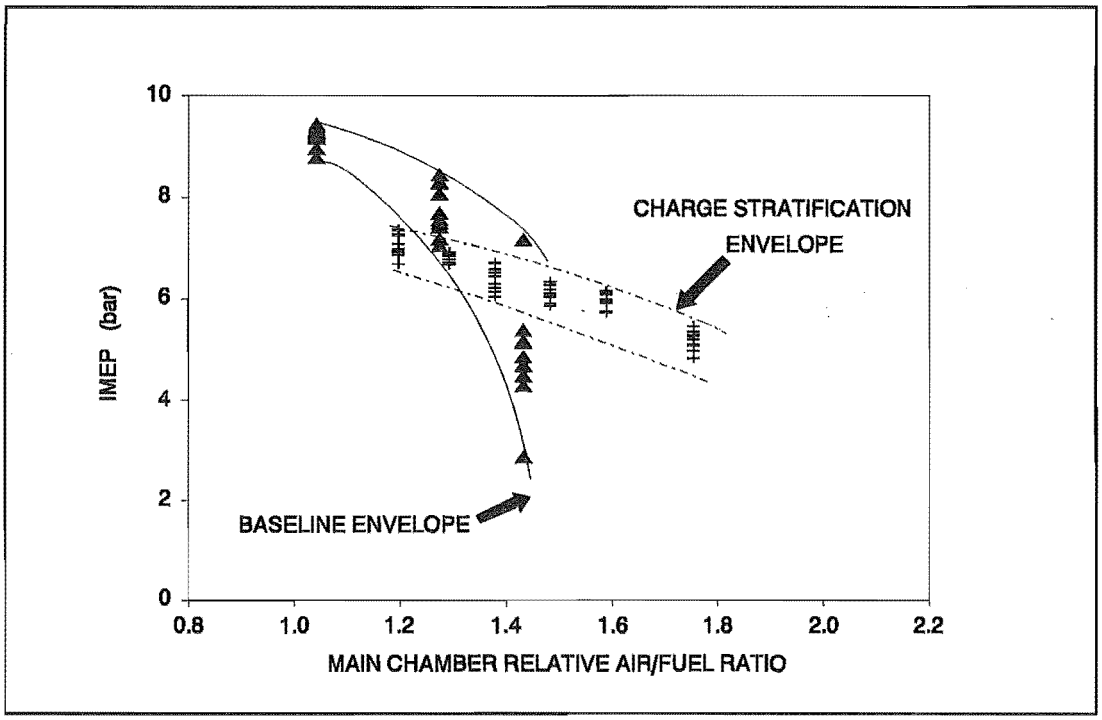

Figure 6,21 IMEP vs Main Chamber Relative Air/Fuel Ratio for baseline and charge stratification systems. 1000RPM, WOT, MBT.

An immediate improvement in the cyclic variability of the data can be seen for

the charge stratification system. The lower mean IMEP leding to a lower brake power is also evident. This reduction in the cyclic variability of the IMEP gives support to the hypothesis of improved ignition characteristics of the charge stratification combustion system. It should be noted that the limitations placed on the spike generator by the ignition pick up are the prime reason for the limited IMEP data. This limitation prevents any investigation into the misfire mechanisms from a point of view of analysis of the pressure traces near the misfire limit.

6.4.5 Part Load Operation.

The majority of an internal combustion engines working life is spent in the part load regime, hence the part load characteristics of the charge stratification system were also investigated. Throughout this section the terms 1/4 and 1/2 throttle will refer to 1/4 and 1/2 the full load of the engine under wide open throttle conditions. Figures 6,22 $\rightarrow$ 6,24 give a representative set of data which will the discussion centre around.

Figure 6,22 gives similar results to the WOT case, in that the equipment lean limit of combustion is extended for the charge stratification system, and that the BTE of the baseline system is higher around stoichiometric conditions. Again this difference can be attributed to the increased heat transfer reducing the power available due to the points raised in section 6.4.3. The higher BTE

values for the charge stratification system at the leaner air/fuel ratios can be attributed to the improved ignition characteristics discussed earlier.

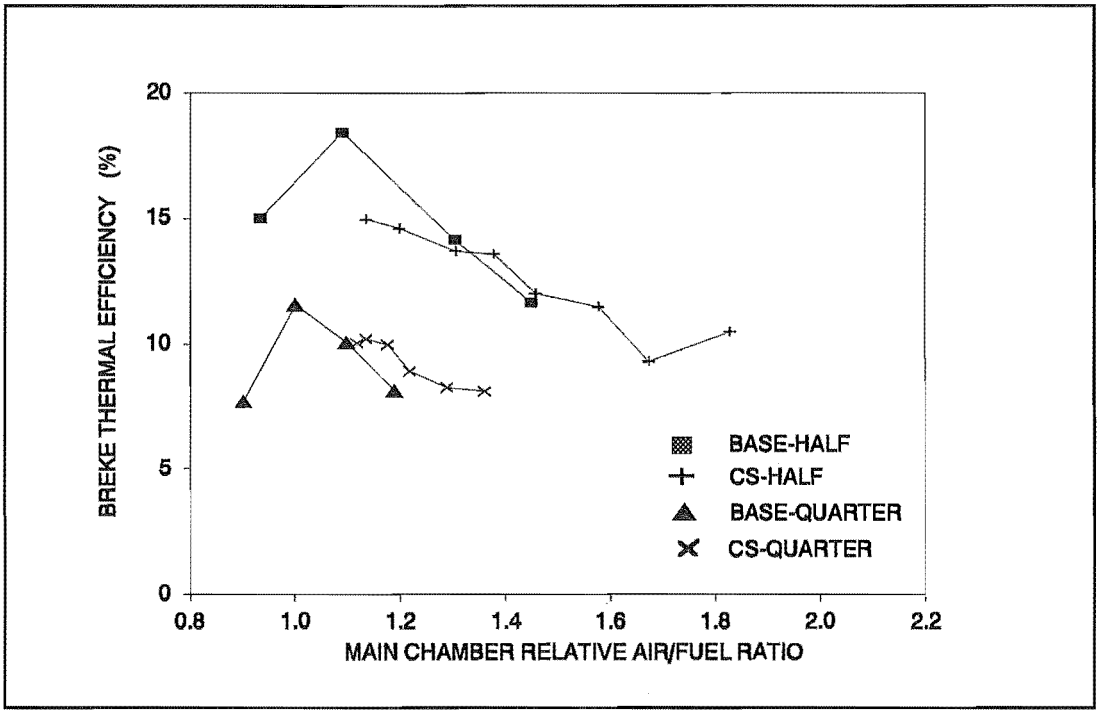

Figure 6,22 Brake Thermal Efficiency vs Main Chamber Relative Air/Fuel ratio for 1500RPM, 1/2 and 1/4 part load conditions. MBT, 100%IR 0.0537kg/h.

Emission characteristics of the part load tests are shown in figures 6,23 and 6,24. Hydrocarbon emissions for the 1/4 and 1/2 load tests show substantially higher values for the charge stratification system. The similarity between the 1/2 and 1/4 charge stratification levels suggest that the increased quench volumes of the pre-chamber and the ancillary equipment play an important role at reduced loads.

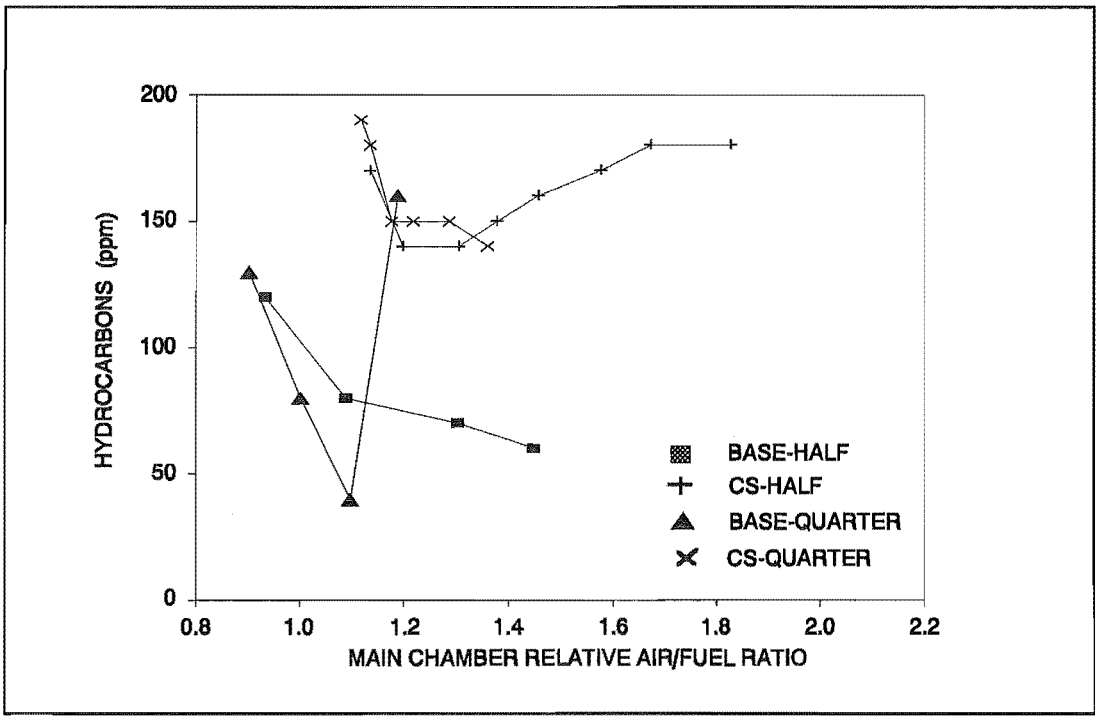

Figure 6,23 Hydrocarbon Emissions vs Main Chamber Relative Air/Fuel Ratio for 1/2 and 1/4 part load tests. 1500 RPM, MBT, 100%IR, 0.0537kg/h.

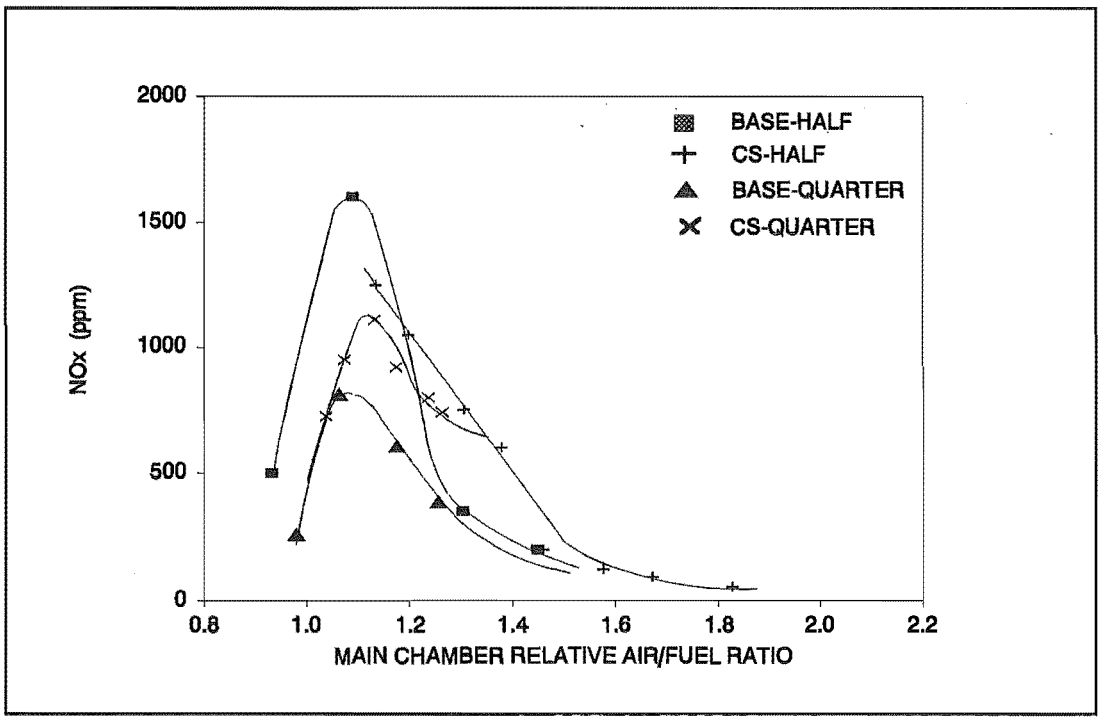

Figure 6,24 NOx Emissions vs Main Chamber Relative Air/Fuel Ratio for 1/4 and 1/2 part load tests. 1500RPM, MBT, 100%IR, 0.0537kg/h.

NOx emissions are shown in figure 6,24 for the part load tests. The 1/2 throttle tests show fairly similar levels of NOx emissions, indicating similar temperatures within the combustion chamber. The 1/4 throttle tests show increased levels for the charge stratification system. This could be explained by the following argument. Although the amount of air and fuel admitted through the main inlet valve has been reduced the flow into the pre-chamber has been kept constant. Therefore, for the same main chamber relative air/fuel ratio the charge stratification system will contain a larger amount of fuel, hence a potentially higher source of energy. This would increase the pressure and temperature of the resultant burned mixture and hence increase the formation of NOx.

6.4.5 Pre-chamber Combustion Characteristics.

The pressure-volume diagrams obtained from the engine testing gave some insight into the nature of the combustion processes. Figures 6,25 and 6,26 give two examples of pressure-volume diagrams obtained. Figure 6,25 shows a baseline test, and figure 6,26 shows a charge stratification test, both of which are for 1500RPM, WOT, MBT conditions.

Comparison of the two diagrams gives the following observations. The smaller area of the charge stratification diagram confirms the lower brake power, BTE and IMEP results. The charge stratification diagram shows a higher rate of

pressure rise around TDC than for the baseline test. This factor along with the retarded ignition angles shown in figure 6,19 indicate a rapid rate of combustion. It is believed that a pressure differential (as mentioned in section 6.4.2) is developed within the pre-chamber relative to the main chamber, this forces the hot combustion products out from the pre-chamber and into the main chamber where they are widely dispersed. These hot pockets of gas act as centres of ignition throughout the combustion chamber. As there are many centres of ignition the time for each flame to propagate is substantionally less than the single flame associated with a normal spark ignition combustion system. Hence the mass of fuel and air is burned at a higher overall combustion rate than compared with a normal single spark ignition source.

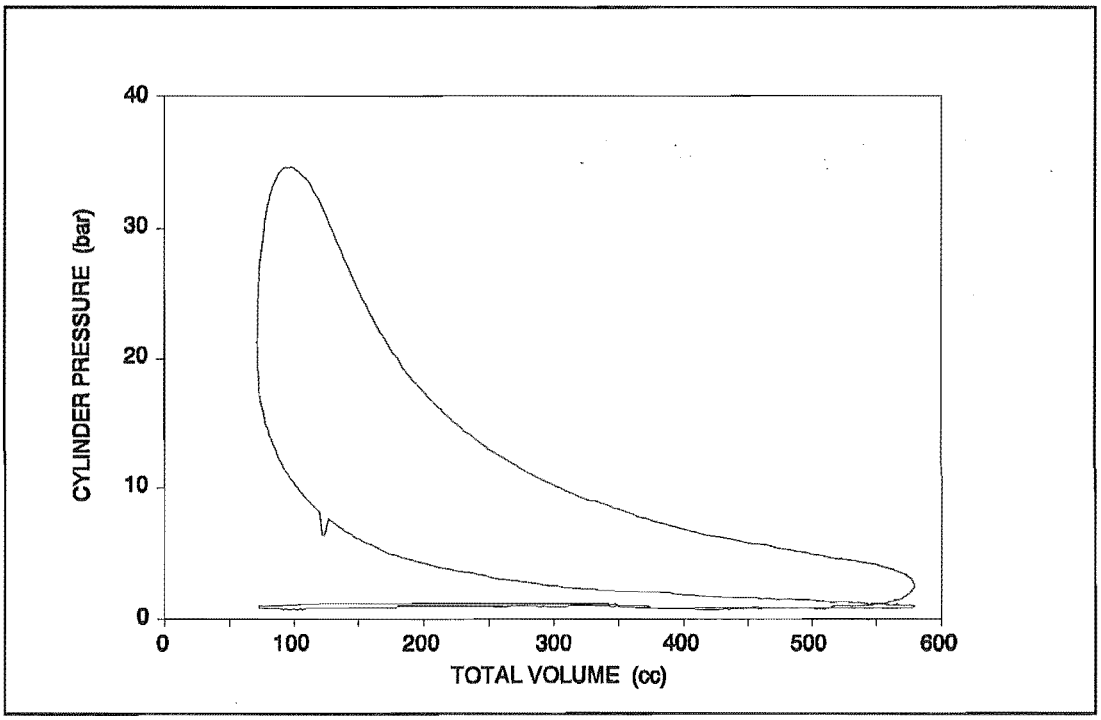

Figure 6,25 Pressure Volume diagram for baseline test. 1500RPM, WOT, MBT.

However, it is believed that the jet of hot gases issuing from the pre-chamber is intense enough to penetrate the boundary layers surrounding the combustion chamber and hence increase the rate of heat transfer. This would manifest itself as lower peak pressures, lower IMEP and hence a lower amount of brake power available.

Further evidence of the high rates of heat transfer can be resolved from an observation made during engine testing. Whilst operating in the stoichiometric region backfiring would sporadically occur, showing the presence of hot spots from within the combustion chamber. As methane is the most stable of hydrocarbon fuels the temperature of the hot spot would have to be in the vicinity of 650°C.[124]

Figure 6,26 shows relatively large pressure fluctuations, which are signs of knock occurring. However at no stage was any audible knock heard, and it is believed that with consideration of the above argument knock could not occur. Knock requires that the end gas be heated to the auto-ignition temperature by the process of adiabatic compression, before the propagating flame can engulf the end gas. With multiple centres of ignition it is very unlikely that the end gas could reach this temperature before being consumed by one of the many flames developed.

An explanation for the appearance of these pressure vibrations is believed to

be connected to one, or both of the following points. Firstly, referring back to the theory of multiple centres of ignition. Associated with each flame would be a pressure wave (the temperature of the burned gas would be higher than the unburned gas, hence a pressure differential) each of these pressure waves would propagate through the combustion chamber and at some point would come into contact with the pressure transducer, hence giving the appearance of the pressure fluctuations caused by end gas knock.

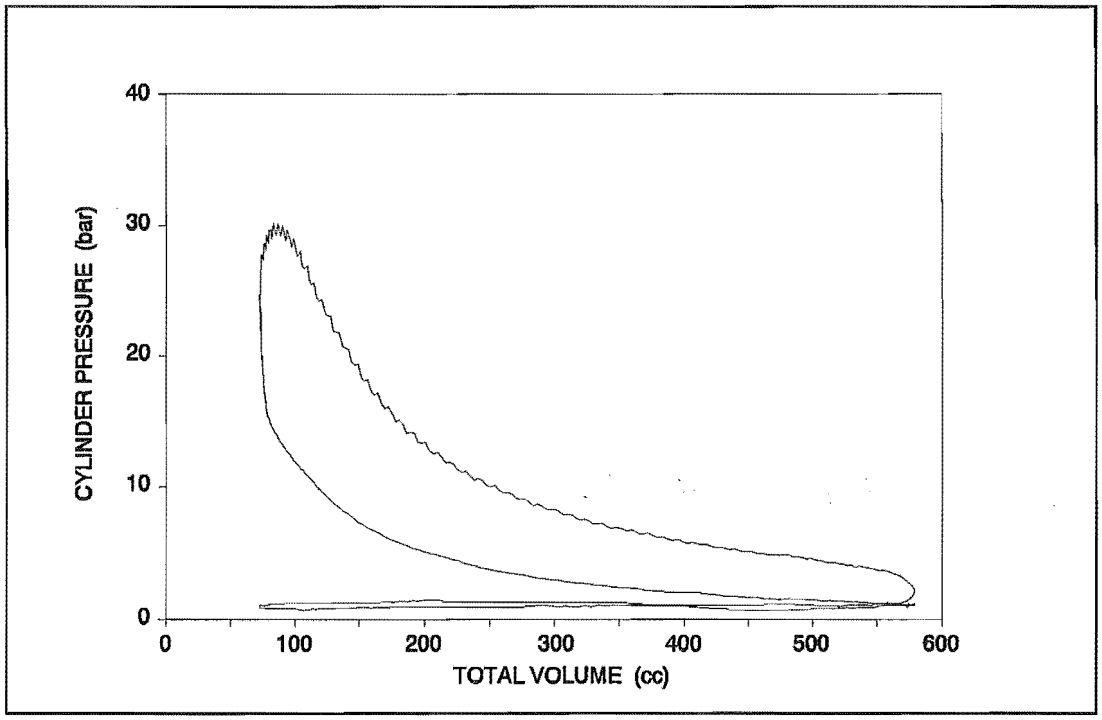

Figure 6,26 Pressure Volume diagram for the Pre-Chamber Stratified Charge Combustion engine. 1500RPM, WOT, MBT, 100%IR, 0.0537kg/h.

Upon closer examination of the pressure traces (figure 6,27) it can be seen that the pressure fluctuations seem to have a specific frequency.

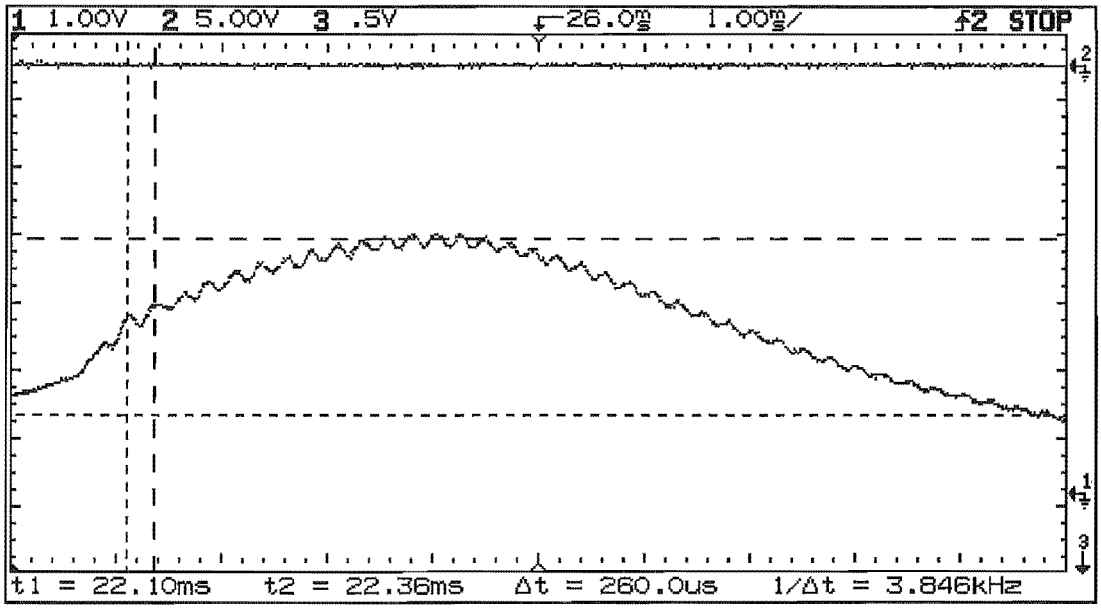

Figure 6,27 Pressure fluctuations on the crest of a pressure trace for the charge stratification process.

This regularity of the fluctuations led to the second hypothesis. Gas dynamics tells us that if a pressure wave propagating down a tube reaches a change in section, a second pressure wave of opposite form is reflected back along the tube. Within the pre-chamber connecting nozzle this reflection could occur at both ends and conceivably continue for some time. Within the main combustion chamber this would be observed as a pressure pulse emerging at regular intervals and showing up on the cylinder pressure trace as a vibration of the main pressure trace. Davis et al[82] observed such gas dynamic effects when measuring the pressure at the end of a pre-chamber connecting nozzle.

CHAPTER 7

CONCLUSIONS

The following conclusions have been drawn from the engine combustion test work undertaken.

1, Pre-chamber charge stratification combustion has been shown to be effective in extending the equipment lean limit of combustion.(ELLC)

2, The ELLC for the pre-chamber stratified charge engine is increased with an increase in engine speed, while the baseline spark ignition engine has a relatively constant ELLC. This observation leds to the conclusion that the ELLC for the pre-charnber stratified charge combustion is related to the flame propagation mechanisms, whereas the baseline ELLC is related to ignition and flame development mechanisms.

3, Pre-chamber stratified charge combustion in an engine is inherently stable due to the enhanced ignition characteristics associated with the system.

4, Pre-chamber charge stratification combustion reduces the combustion duration time due to:

Increased levels of turbulence within both the pre-chamber and main chamber caused by gas flow in and out of the pre-chamber.

The ejection of active species from the pre-chamber into the main chamber which provide multiple centres of ignition within the lean charge,forming flames which burn independently, thereby reducing the overall burn time.

5, Brake thermal efficiency of the pre-chamber stratified charge system is reduced relative to the baseline system around the stoichiometric region. This is believed to be due to increased heat transfer from both the main and pre-chambers caused by the increased turbulence levels, and the issuing jet from the pre-chamber.

6, Brake thermal efficiency of the pre-chamber stratified charge system is increased relative to the baseline system in the leaner air/fuel regions. This is due to the improved ignition and burning characteristics of the pre-chamber stratified charge system.

7, Combustion vibrations within the pre-chamber stratified charge engine are believed to be due to either multiple pressure waves forming within the main chamber due to the issuing jet from the pre-chamber creating multiple flame fronts, or by resonant gas dynamic effects associated the

interaction of the pre-chamber geometry and the gas flow in and out of the pre-chamber.

8, Hydrocarbon levels are reduced relative to Zavier's work, but are still higher than the baseline tests. Reductions relative to Zavier's work are believed to be due to:

Minimisation of additional quench volumes due to the hypodermic tube connecting the injector to the pre-chamber.

Improved control of the ignition mixture within the pre-chamber.

The higher levels of hydrocarbons relative to the baseline tests are believed to be due to:

Lower exhaust gas temperatures resulting in reduced post-flame oxidation rates of the hydrocarbons.

Increased surface area/volume ratio and other quench volumes of the combustion chambers relative to the baseline chamber. The increase in surface area/volume ratio was only 3%, however this would contribute to the overall increase. It is believed that the quench volumes associated with the hypodermic connection

between the methane injector and the pre-chamber still play a significant role.

Turbulent vortices created by the issuing flame front out of the connecting passage would stretch the flame locally around the edges of the passage exit causing some localised extinction of the flame, and hence increased hydrocarbon levels.

9, Carbon monoxide levels did not vary significantly between the pre-chamber stratified charge engine and the baseline engine.

10, NOx measurements were reduced slightly for optimum injection timings, however on a specific basis were increased due to the reduction in brake power.

11, Under part load conditions the ELLC of the pre-chamber engine is extended relative to the part load baseline tests. However the part load ELLC relative to the WOT ELLC tests for the pre-chamber engine is reduced due to increased levels of residual exhaust gas in the combustion chamber. The extension of the pre-chamber engine part load ELLC relative to the part load baseline engine tests is due to the points listed earlier.

12, Hydrocarbon emissions for the part load tests were higher than the baseline tests. This can be attributed to the points listed above for the WOT case.

13, NOx levels for the 1/4 throttle case are increased slightly due to the relative increase in the amount of fuel within the pre-chamber resulting in relatively higher temperatures within the pre-chamber than the main chamber.

CHAPTER 8

RECOMMENDATIONS FOR FUTURE WORK

An initial attempt has been made to reduce the hydrocarbon emissions experienced by Zavier. This was achieved by the minimisation of possible quench volumes within budgetary restraints, and by improvements in the mixture formation around the spark plug at the point of ignition. Further improvements into the minimisation of quench volumes could be obtained with the re-design of the pre-chamber combustion system to incorporate the fuel injector directly within the pre-chamber and to include the pre-chamber as part of the cylinder head. In this respect the pre-chamber location could also be optimised.

The pre-chamber air supply system suffered from a low inertial response of the check valve, and hence reduced flow characteristics. A suitable mechanically or electrically actuated system could be designed to improve the performance of the air system and hence reduce the necessity to pressurise the incoming air.

Pressure-volume diagrams of the pre-chamber combustion characteristics showed vibrations caused by either combustion or gas dynamic phenomenon. A study into the cause of these vibrations would be most beneficial in further understanding of the combustion system.

REFERENCES

1, **PERKINS H.C**
"Air Pollution"
McGraw Hill Book Co
1974.

2, **ATKINS P.R**
"The natural removal of lead pollutants from a suburban atmosphere."
Dissertation 1968,
Stanford University.

3, **CONCAWE**
"Motorvehicle emission regulations and fuel specifications."
1991-update.

4, **BOWMAN C.T**
"Kinetics of pollutant formation and destruction in combustion."
Prog energy, combust sci 1975
Vol 1, pp33-45.

5, **CHIGIER N.A**
"Polutant formation and destruction in flames."
Prog energy combust sci 1975
Vol 1, pp3-15.

6, **HEYWOOD J.B**
"Pollutant formation and control in spark ignition engines."
Prog energy combust sci 1976

Vol 1 pp135-164.

7, **NEWHALL H.K**

"Kinetics of engine generated nitrogen oxides and carbon monoxide."
12th Symposium on combustion 1969.

8, **STARKMAN E.S**

"Theory, experiment and rationale in the generation of pollutants by combustion."
12th Symposium on combustion 1969.

9, **PISCHINGER F. KLEINSCHIMDT W.**

"Study of NO, NO_2 and CO formation in spark ignition engines by using extended reaction kinetics."
Combstion institute (European) symposium 1973
pp 457-462

10, **WATFA M. DANESHYAR B.**

"Formation of nitric oxide(NO), carbon monoxide(CO) and unburnt hydrocarbons(HC) in spark ignition engines."
Combustion Engines.
Imech E 1975.

11, **NEWHALL H.K, ELMESSIRI I.A**

"A combustion chamber designed for minimum engine exhaust emmissions."
SAE 700491.

12, **VARDE K.S LUCAS C.G**

"Effects of pressure variations and combustion duration on the emission of hydrocarbons and nitric oxide."

SAE 760142.

13, **DANIEL W.A**
"Engine variable effects on exhaust hydrocarbon composition. (A single cylinder engine study with propane as the fuel.)"
SAE 670124.

14, **DANIEL W.A**
"Why engine variables affect exhaust hydrocarbon emissions."
SAE 700108.

15, **TOMANY J.P**
"Air pollution: the emissions, the regulations and the controls."
American elsevier publishers,
1975.

16, **SPRINGER G.S, PATTERSON D.J**
"Engine emissions, pollutant formation and measurements."
Plenum Press ltd
1973.

17, **MA T.H, WOODS W.A, PANESAR A, BROWN P, DENT J.C, LAMBERT N,** "Tracing the sources of hydrocarbon emissions in engines- a review of several research programmes made over the past five years."
Vehicle emissions and their impact on the European air quality.
Imech E 1987-8.

18, **PANESAR A, BROWN P.G, WOODS W.A**
"The results of recent experiments on unburnt hydrocarbons."
Imech E

1988.

19, **LORUSSO J.A, KAISER E.W, LAVOIE G.A**
"In cyliner measurments of wall layer hydrocarbons in a spark ignition engine."
Combustion science and technology.
Vol 33 pp75-112
1983

20, **KAISER E.W, ROTHSCHILD W.G, LAVOIE G.A**
"Storage and partial oxidation of unburnt hydrocarbons in spark ignition engines- effect of compression ratio and spark timing."
Combustion science and technology.
Vol 36 pp171-189.
1984.

21, **ADAMCZYK A.A, KACH R.A,**
"The effect of oil layers on hydrocarbon emissions: Low solubility oils."
Combustion science and technology.
Vol 36 pp227-234.
1984.

22, **ADAMCZYK A.A, ROTHSCHILD W.G, KAISER E.W,**
"The effect of fuel and oil structure on hydrocarbon emissions from oil layers during closed vessel combustion."
Combustion science and technology.
Vol44 pp113-124.
1985.

23, **CROUSE W.H**
"Automotive emission control."
McGraw Hill publishers.
1971.

24, **STRAUSS W MAINWARING S.J**
"Air Pollution"
Edward Arnold publishers.
1984.

25, **MATHAVI, J.N. GROFF, G. MATEKUNAS, F.A.**
"Turbulence flame motion and combustion chamber geometry - their interactions in a lean combustion engine."
C100/79 IMechE 1979

26, **PETERS, B.D.**
"Mass burning rates in a spark ignition engine operating in the partial burn engine."
C92/79 IMechE 1979

27, **QUADER, A.A.**
"What limits leans operation in spark ignition engines - flame initiation or propagation?"
SAE 760760

28, **KALGHATGI, G.T.**
"Spark ignition, early flame development and cyclic variation in I.C. engines."
SAE 870163

29, **PATTERSON, D.J.**
"Cylinder pressure variations, a fundamental combustion problem."
SAE 660129

30, **BOLT, J.A. HARRINGTON, D.L.**
"The effects of mixture motion upon the lean limit and combustion of spark ignited mixture."
SAE 670467

31, **QUADER, A.A.**
"Lean combustion and the misfire limit in spark ignition engines."
SAE 741055

32, **TANUMA, T. SASAKI, K. KANEKO, T. KAWASAKI, H.**
"Ignition, combustion and exhaust emissions of lean mixtures in automotive spark ignition engines."
SAE 710159

33, **FISHER, P.D. PITT, P.L. RIDLEY, J.D. CLEMENTS, R.M.**
"Puff-jet ignition of methane in an internal combustion engine."
Combustion Science and Technology.
Vol 46 pp137-143
1986

34, **PITT, P.L. CLEMENTS, R.M.**
"The effects of plasma jet ignition on a methane fuelled internal combustion engine."
Combustion Science and Technology.
Vol 30 pp327-333
1983

35, **PITT, P.L. RIDLEY, J.D. CLEMENTS, R.M.**
"Low energy ignition of an ultra lean methane fuelled internal combustion engine."
Combustion Science and Technology.
Vol 38 pp217-225
1984

36, **YAMAMOTO, H. MISUMI, M.**
"Analysis of cyclic combustion variation in a lean operating S.I. engine."
SAE 870547

37, **DAILY, J.W.**
"Cycle to cycle variations: a chaotic process?"
SAE 870165

38, **GRUDEN, D. HAHN, R.**
"Performance, exhaust emissions and fuel consumption of an I.C. engine operating with lean mixtures."
C111/79 IMechE 1979

39, **HANSEL, J.G.**
"Lean automotive engine operation - hydrocarbon exhaust emissions and combustion characteristics."
SAE 710164

40, **BALLAL, D.R. and LeFEBVRE, A.H.**
"Effect of electrode spacing on spark ignition of flowing mixtures."
Combustion Institute European Symposium, pp236-241
1973

41, **BARTON, R.K., KENEMUTH, D.K., LESTZ, S.S. MEYER, W.E.**
"Cycle by cycle variation of a spark ignition engine - a statistical analysis."
SAE 700488

42, **BOLT, J.A. HOLKENBEOR, D.H.**
"Lean fuel/mixtures for high-compression spark ignition engines."
SAE Trans., 70: 195-202, 1962.

43, **BURT, R., ROBERTS, D.D. WOODWORTH, J.A.**
"A comparison of fuel - economy, exhaust emissions and performance of three European cars operating on homogeneous fuel-air mixtures."
C148/79, Fuel economy and emissions of lean burn engines,
IMechE Conference Publications, 1979.

44, **CLARKE, J.S.**
"Ignition and some controlling parameters of combustion in the automobile engine."
SAE Trans., 70: 240-261, 1962.

45, **COLE, D.E. MIRSKY, W.**
"Mixture motion- its effect on pressure rise in a combustion bomb; a new look at cyclic variation."
SAE 680766

46, **CRAVER, R.J., PODIAK, R.S. MILLER, R.D.**
"Spark plug design factors and their effect on engine performance."
SAE 700081

47, **CURRY, S.**
"A three-dimensional study of flame propagation in a spark ignition

engine."
SAE Trans, 71: 628-650, 1963.

48, **HARROW, G.A. CLARKE, P.H.**
"Mixture strength control of engine power: fuel economy and specific emissions from gasoline engines running in fully vaporized fuel/air mixtures."
C90/79, Fuel economy and emissions of lean burn engines,
IMechE Conference Publications, 39-50. 1979.

49, **HATTORI, T. GOTTO, K. OHIGASHI, S.**
"Study of spark ignition in flowing lean mixtures."
C101/79, Fuel economy and emissions of lean burn engines,
IMechE Conference Publications, 153-163. 1979.

50, **HUGHES, D.W. GOULBURN, J.R.**
"Fuel vaporisation - economy with reduced exhaust emission."
Proc.Inst. of Mech.Engrs.,
190: 1-11. 1976.

51, **KOMIYAMA, K. HEYWOOD, J.B.**
"Predicting NO emissions and effects of EGR in spark ignited engines."
SAE 730475

52, **MA, T.H.**
"Effect of cylinder charge motion on combustion"
C81/75, Combustion of Engines,
IMechE Conference Publications, 1-12. 1975.

53, **MATSUOKA, S. YAMAGUCHI, T. UMEMUKI, Y.**
"Factors influencing the cyclic variation of combustion of spark ignition engine."
SAE 710586

54, **MAY, M.G.**
"The high compression lean burn spark ignited 4-stroke engine."
C97/79, Fuel economy and emissions of lean burn engines,
IMechE Conference Publication, 107-116. 1979.

55, **MAYO, J.**
"The effect of engine design parameters on combustion rate in spark ignited engines."
SAE 750355

56, **OBLANDER, K. ABTHOFF, J. FRICKER, L.**
"From engine testbench to vehicle - an approach to lean burn by dual ignition."
Fuel economy and emissions of lean burn engines,
IMechE Conference Publications, 19-24. 1979.

57, **SCHWARZ, H.**
"Ignition systems for lean burn engines."
Fuel economy and emissions of lean burn engines,
IMechE Conference Publications, 87-96. 1979.

58, **ZIEGLER, G.F.W. MALAY, R.R. WAGNER, E.P.**
"Effects of ignition system design on flammability requirements in ultra-lean turbulent mixtures."
C47/83, Combustion in Engineering,
IMechE Conference Publications, 1:81-92. 1983.

59, **KOWALEWICZ, A.**
"Combustion systems of high speed piston I.C engines."
Elsevier science publishing Co.
1984.

60, **HASLETT R.A MONAGHAN M.L McFADDEN J.J**
"Stratified charge engines."
SAE 760755

61, **NEWHALL H.K**
"Combustion process fundamentals and combustion chamber design for loe emissions."
SAE 751001

62, **ALPERSTEIN M SCHAFER G.H VILLFORTH F.J**
"Texacos stratified charge engine - multifuel, efficient, clean and practical."
SAE 740563

63, **CHMELA F.**
"High compression stratifiedcharge engines and their suitability for conventional and alternative fuels."
C400/80 Stratified charge automotive engines.
IMechE 1980.

64, **MEURER J.S URLAUB A.C**
"Development and operational results of the MAN-FM combustion system."
SAE 690255

65, **GRUDEN D MARKOVAC U LORCHER H**
"Development of the Porsche SKS engine."
IMechE 1976

66, **PISCHINGER F.F KLOCKER K.J**
"Single-cylinder study of stratified charge process with pre-chamber injection."
SAE 741162

67, **KUCK H.A BRANDSTETTER W.R**
"Investigations on a single cylinder stratified charge engine with a scavenged pre-chamber."
C92/75
IMechE 1975

68, **BRANDSTETTER W.R**
"Experimental results from a Volkswagen's pre-chamber stratified charge engines."
C249/76
IMechE 1976

69, **DATE T YAGI S ISHIZUYA A FUJII I.**
"Research and devlopment of the Honda CVCC engine."
SAE 740605

70, **YAGI S FUJII I NISHIKAWA M SHIRAI H.**
"A new combustion system in the three-valve stratified charge engine."
SAE 790439

71, **YAGI S FUJII I AJIKI Y TSUADA T.**
"The anti-knock quality in the stratified charge engine with an auxiliary

combstion chamber."
C395/80
IMechE 1980

72, **GUSSAK L.A**
"High chemical activity of incomplete combustion products and a method of pre-chamber torch ignition for avalanche activation of combustion in internal combustion engines."
SAE 750890

73, **GUSSAK L.A TURKISH M.C**
"LAG-Process of combustion and its application in automobile engines."
C257/76
IMechE 1976.

74, **GUSSAK L.A KARPOV V.P TIKHONOV Y.V**
"The application of LAG-Process in pre-chamber engines."
SAE 790692.

75, **WYCZALEK F.A HARNED J.L MAKSYMIAK S BLEVINS J.R**
"EFI pre-chamber torch ignition of lean mixtures."
SAE 750351.

76, **VARDE K.S LUBIN M.J**
"The roll of connecting nozzle and the flame initiation point in the performance of a dual chamber stratified charge engine."
SAE 741161

77, **RYU H CHTSU A ASANUMA T.**
"Effect of torch jet direction on combustion and performance of a pre-

chamber spark ignition engine."
SAE 870167.

78, **SAKAI Y KUNII K TSUTSUMI S NAKAGAWA** Y
"Combustion characteristics of the torch ignited engine."
SAE 741167.

79, **PURINS E.A**
"Pre-chamber stratified charge engine combustion studies."
SAE 741159.

80, **PISCHINGER F ADAMS F**
"Influence of intake swirl on the characteristics of a stratified charge engine with pre-chamber injection."
C391/80
IMechE 1980

81, **SAKAI Y KUNII K SASAKI M KAKUTA N AIHARA H**
"Combustion characteristics of a torch ignited engine:- analytical measurements of gas temperature and mixture formation."
C247/76
IMechE 1976

82, **DAVIS G.C KRIEGER R.B TABACZYNSKI R.J**
"Analysis of the flow and combustion processes of a three valve stratified charge engine with a small pre-chamber."
SAE 741170.

83, **KRIEGER R.B DAVIS G.C**
"The influence of the degree of stratification on jet ignition engine emissions and fuel consumption."
C254/76

IMechE 1976.

84, **AL-MAMAR F.N.A.A HYNES J SHEPPARD C.G.W**
"Combustion rate in a dual chamber SI engine."
Combustion Science and Technology.
Vol 45
1986.

85, **BRADSHAW P,**
"An introduction to turbulence and its measurements."
Pergamon Press ltd.
1st ed
1971.

86, **TABACZYNSKI R.J, FERGUSSON C.R, RADHAKRISHNAN K.**
"A turbulent entrianment model for spark ignition engine combustion."
SAE 770647.

87, **FENTON J.**
"Gasoline engine analysis"
Mechanical engineering publications ltd
1986

88, **QUADER A.A**
"The axially stratified stratified charge engine."
SAE 820131.

89, **FULLER D.F**
"Mixture motion in an engine cylinder"
Phd Thesis,
Cambridge University

1975.

90, **SEMENOV E.S**
"Studies of turbulent gas flow in piston engines."
NASA technical translation F97
1963.

91, **ARCOUMANIS C. WHITELAW J.H**
"In cylinder flow measurement in motored internal combustion engines."
IMechE 1991.

92, **LANCASTER D.R**
"Effects of engine variables on turbulence in a spark ignition engine."
SAE 760159.

93, **DENT J.C SALAMA N.S**
"The measurement of the turbulence characteristics in an internal combustion engine cylinder."
SAE 750896.

94, **COLE J.B SWORDS M.D**
"Optical studies of the flow field in a motored E6 engine" Fuel economy and emissions of lean burn engines.
IMechE 1979.

95, **BOPP S. VAFIDIS C. WHITELAW J.H**
"The effect of engine speed on the TDC flowfield in a motored reciprocating engine."
SAE 860023.

96, **FRASER R.A FELTON P.G BRACCO F.V SANTAVICCA D.A**
"Preliminary turbulence length scale measurements in a motored IC engine."
SAE 860021.

97, **GRASSO F. WEY M.J BRACCO F.V ABRAHAM J.**
"3D computations of flows in a stratified charge rotary engine."
SAE 870409.

98, **GLASSMAN I.**
"Combustion"
Academic Press.
1977.

99, **LEWIS B. vonELBE G.**
"Combustion, flames and explosions."
3rd edition.
Academic Press
1987.

100, **GAYDON A.G WOLFHARD H.G**
"Flames: their structure, radiation and temperature." 3rd edition
Chapman Hall ltd
1970.

101, **SPENCER R.B**
"Adaptive control of th ignition timing of spark ignition engines utilising the combustion flame light emissions."
M.E Thesis
University of Canterbury.
1985.

102, **BARNARD J.A BRADLEY J.N**
"Flames and combustion."
2nd edition.
Chapman and Hall Publishers.
1985.

103, **BRACCO F.V**
"Structure of flames in premixed charge internal combustion engines."
Combustion science and technology.
1988.

104, **ABRAHAM J. WILLIAMS F.A BRACCO F.V**
"A discussion of turbulent flame structure in premixed charges."
SAE 850345.

105, **FLANAGAN R.C SEINFELD J.H**
"Fundamentals of air pollution engineering."
Prentice Hall
1988

106, **CHOMIAK J. JAROSINSKI J.**
"Flame quench by turbulence."
Combustion and Flame.

107, **LOCKWOOD F.C MEGAHED I.E.A**
"Extinction in turbulent reaction flows."
Short communication.
Combustion science and technology.
1978.

108, **DANESHYAR H. MENDESLOPES J.M.C LUDFORD G.S.S**
"Effect of strain fields on burning rate."
19th Symposium on combustion.
1982.

109, **DANESHYAR H. MENDESLOPES J.M.C LUDFORD G.S.S TROMANS P.S**
"The influence of straining on a premixed flame and its relevance to combustion in SI engines."
IMechE 1983.

110, **BARITAUD T.A GREEN R.M**
"A 2-D flame visualisation technique applied to the IC engine."
SAE 860025

111, **KECK J.C HEYWOOD J.B NOSKE G.**
"Early flame development and burning rates in SIE's and their cyclic variability."
SAE 870164

112, **STONE R.**
"Introduction to internal combustion engines."
2nd edition.
MacMillian Press ltd.
1992.

113, **ELLIS A.**
"Gas phase quenching in combustion processes."
Bachelor of Engineering report No21
Mechanical Engineering department.
University of Canterbury.

1986.

114, **LENZ H.P**
"Mixture formation in spark ignition engines."
Society of Automotive Engineers.
Springer Verlag publishers.
1992.

115, **LOM W.L**
"Liquified natural Gas."
Applied sciences publishers.
1974.

116, **WEST J.P BROWN L.G**
"Compressed natural gas."
Wellington gas company
New Zealand energy research and development committee.
1979.

117, **KARIM G.A ALI I.A**
"Combustion, knock and emission characteristics of a natural gas fuelled spark ignition engine with particular reference to low intake temperature conditions."
IMechE
1975.

118, **CAMPBELL A.R**
"Development and use of a test rig for monitoring the combustion of fuels in a spark ignition engine with particular reference to the use of methanol in transport vehicles."
Master of Engineering Thesis.

University of Canterbury.
1983.

119, **DAMIANO L.F**
"The effect of charge stratification on the combustion of lean methane-oxygen mixtures under constant volume conditions."
Master of Engineering Thesis.
University of Canterbury.
1993.

120, **MELVIN A**
"Natural gas:-basic science and technology."
British gas plc.
1988.

121, **GLASSON N**
"Hydrogen fuelling of an internal combustion engine."
Ph.d Thesis.
University of Canterbury.
1992.

122, **ZAVIER C.C**
"Charge stratification of an internal engine."
Master of Engineering Thesis.
University of Canterbury.
1991.

123, **GREEN R.K ZAVIER C.C**
"Charge stratification in a spark ignition engine."
A01491
IMechE 1992.

124, **BOSCH R**
"Automotive handbook."
2nd edition.
Robert Bosch Gmbh.
1986.

125, **BOND J**
"Sources of igntion"
Butterworth Heinemann London.
1991.

126, Personal Communication,
Christchurch city drainage board,
1986.

APPENDICIES

The following appendicies are contained within this section:

1, Computer programs.

2, NOx meter, gas system operating instructions.

3, Equations of state for accurate gas mixtures.

4, NO/N_2 gas mixture preparation procedure.

APPENDIX 1

COMPUTER PROGRAMS

The following computer programs were developed to analyse the large amount of data generated by the combustion tests. All programs were written in Microsoft QuickBASIC version 4.5.

PRESANAL.BAS is a program to analyse the pressure data captured from the piezo-electric pressure transducer. The program calculates the IMEP, Peak Pressure and IP for each of the cycles captured.

RICPC.BAS is a program to analyse the engine performance and emission data collected during the engine test schedule. The program calculates Power output, BSFC, BTE, Fuel consumption rates, Relative Air/Fuel ratios and Specific emissions.

PRESANAL.BAS

```
' Program origionally written in March 1992 by N.Glasson and extensively
' modified in May 1993 by I. Calvert for the analysis of combustion
' chamber pressure.  The program reads data from the {filename}.PIZ files
' written from RICARDO.BAS and displays the data graphically on screen.
' The data point numbers corresponding to probable ignition timing spikes
' on the pressure trace are then presented for user verification.
' The program computes the crank angle associated with each data point.
' This information is used to calculate pressure-volume data which is
' displayed on screen and written to a data file.(.PVD) The pressure-volume
' data is also used to calculate the indicated mean effective pressure,
' peak pressure and related information. This data is written to a
' separate data file.(.IPD)

    DECLARE FUNCTION ASIN! (ANG!) ' declare the inverse sine function
    DIM PIZ!(1 TO 10000), IGNPOINT%(1 TO 100)
    DIM RADCA!(1 TO 10000), RADDEG!(1 TO 10000), VOLUME!(1 TO
       10000)
    DIM WORK!(1 TO 20), PEAK!(1 TO 20), IMEP!(1 TO 20), IP!(1 TO 20)

    SCREEN 0          'sets screen type, text only
    CLS              'input information on the engine test
    WIDTH 40, 25      'Sets text format to 40 columns, 25 lines
    COLOR 3           'sets text colour to cyan
    PRINT
    PRINT
    PRINT
    PRINT " WELCOME TO THE RICARDO ENGINE DATA"
    PRINT "         ANALYSIS PROGRAM."
    PRINT
    PRINT
    PRINT "PLEASE ENTER THE DATA REQUESTED BELOW."
    COLOR 14          'sets text colour to light yellow
    PRINT
    PRINT
    PRINT
    INPUT "ENTER THE ENGINE TEST FILE NAME "; RUNNO$
    INPUT "ENTER THE ENGINE SPEED IN RPS   "; RPS!
    INPUT "ENTER THE IGNITION TIMING BTDC  "; BTDC!
    INPUT "ENTER THE COMPRESSION RATIO     "; CR!
    INPUT "ENTER THE PIEZO CONSTANT (BAR/V)"; PCAL!
    COLOR 21
    PRINT
    PRINT "      PLEASE WAIT, LOADING FILE!"
```

```
    OPEN "C:\IAN\RAW\" + RUNNO$ + ".PIZ" FOR INPUT AS #1
    DATANO% = 1
    DO WHILE NOT EOF(1) AND DATANO% <= 10000
      INPUT #1, PIZ!(DATANO%)
      DATANO% = DATANO% + 1
    LOOP
    CLOSE #1
    REM SCREEN 9                          ' this setup for EGA screen
    SCREEN 9                             ' this setup for HERC screen
                        ' View port sized to proper scale for graph:
    REM VIEW (0,0)-(740,200), , 1          ' this setup for EGA screen
    VIEW (20, 2)-(600, 200)               ' this setup for HERC screen
    WINDOW (0, -1)-(3000, 8)
    VIEW PRINT 16 TO 24                    ' Scroll printed output in
    REM COLOR 14, 9                       ' rows 16 to 24

    CLS
    FOR I% = 0 TO 6
      LINE (I% * 500, -1)-(I% * 500, 8)
      REM ,4
    NEXT I%

    FOR J% = 1 TO DATANO%                  'displays pressure trace
       LINE (J%, PIZ!(J%))-(J% + 1, PIZ!(J% + 1))
    NEXT J%

50  LOCATE 16, 1
    ' test for spikes in the pressure trace
    CLS 2
    PRINT "NOTE:   EACH VERTICAL LINE ON THE GRID REPRESENTS
500 DATA POINTS!"
    PRINT
    PRINT "      TAKE CARE IN SELECTING THE IGNITION POINTS!!!!!!"
    PRINT
    PRINT "        ENTER IGNITION POINT TOLERANCE (Volts/data)"
    INPUT "  (A TOLERANCE OF 0.2 Volts/Data IS A GOOD RANGE.) ";
             TOL!
    J% = 0
    FOR I% = 2 TO 10000
     IF (PIZ!(I% - 1) - PIZ!(I%)) > TOL! THEN J% = J% + 1:
                              IGNPOINT%(J%) =I%
      IF J% = 99 GOTO 100
    NEXT I%

    CLS 2
100  FOR I% = 1 TO J%
```

```
    PRINT I%, IGNPOINT%(I%)
    IF I% MOD 5 = 0 THEN INPUT "PRESS A KEY TO VIEW FURTHER
                DATA POINTS"; A$
  NEXT I%


150  LOCATE 24, 1
  INPUT "PRESS 'S' TO SELECT DATA POINTS OR 'R' TO RESET
        TOLERANCE"; REPLY$
  IF REPLY$ = "S" OR REPLY$ = "s" THEN GOTO 200
  IF REPLY$ = "R" OR REPLY$ = "r" THEN GOTO 50
  GOTO 150
  ' prompt user for input of ignition spike location

200  CLS 2
  INPUT "              ENTER THE FIRST  IGNITION DATA NUMBER";
        FST%
  INPUT "             ENTER THE SECOND IGNITION DATA NUMBER";
        SEC%
  CLS 2
  PRINT "                PLEASE WAIT, CALCULATING P-V DATA"
  FSTPNT% = IGNPOINT%(FST%)
  SECPNT% = IGNPOINT%(SEC%)

  CLS
  PI# = 3.1415927#
  CYCL% = SECPNT% - FSTPNT%                'determines cycle length
  NOCYC% = 0

  DO UNTIL DATANO% <= NOCYC% * CYCL%  'determines number of
                                cycles
        NOCYC% = NOCYC% + 1
  LOOP
  IF DATANO% < NOCYC% * CYCL% THEN
        NOCYC% = NOCYC% - 1
        ELSE GOTO 300
  END IF

300  INCR# = (4 * PI#) / CYCL%          ' crank angle increment in
                                    radians
  BTDCRAD! = (BTDC! * (2 * PI#)) / 360      ' data capture start angle
  RADCA!(1) = 2 * PI# - INCR# * FSTPNT% - BTDCRAD!
  DO WHILE RADCA!(1) < 0             'sets start of radca to start
    RADCA!(1) = RADCA!(1) + (4 * PI#)
  LOOP
```

```
    FOR I% = 1 TO DATANO%
      VC# = .000507# / (CR! - 1)                'gives clearance volume
      A# = PI# * (.0762# * .0762#) / 4          'piston area
      rl# = .1199677686#                        'stroke to conrod length
      VOLUME!(I%) = 1000000! * (VC# + A# * (.2965625# - .241 *
            SIN(PI# - (ASIN!(.0555625# * SIN(RADCA!(I%)) /
            .241)) - RADCA!(I%)) / SIN(RADCA(I%))))
            'volume in cc
      IF RADCA!(I%) > 4 * PI# THEN RADCA!(I%) = RADCA!(I%) - 4 * PI#
      RADDEG!(I%) = RADCA!(I%) * 360 / (2 * PI#)
      RADCA!(I% + 1) = RADCA!(I%) + INCR#
    NEXT I%

    DIVNO% = 0
    SUM! = 0
    FOR I% = 1 TO DATANO%
      IF ((0 < RADCA!(I%)) AND (RADCA!(I%) < PI#)) OR ((3.1 * PI# < RA
DCA!(I%)) AND (RADCA!(I%) < 4 * PI#)) THEN SUM! = SUM! + PIZ!(I%) *
PCAL!: DIVNO% = DIVNO% + 1
    NEXT I%
    POFFSET! = (SUM! / DIVNO%) - 1     'removes drift voltage

    FOR I% = 2 TO DATANO%                'removes spikes from pressure
                                        data
      IF ABS(PIZ!(I%) - PIZ!(I% - 1)) > .4 THEN
            PIZ!(I%) = PIZ!(I% - 1) + (PIZ!(I% - 1) - PIZ!(I% - 2))
      END IF
    NEXT I%

    FOR I% = 1 TO DATANO%
      PIZ!(I%) = PIZ!(I%) * PCAL! - POFFSET!
    NEXT I%                              'converts voltage to pressure
                                          'in bar
    VIEW (20, 2)-(600, 200)
    WINDOW (0, 0)-(600, 80)
    VIEW PRINT 16 TO 24          ' Scroll printed output in
                                ' rows 23 and 24.
    CLS
    CLS 2
    LOCATE 16, 1
    PRINT "                          PLOTTING P-V DIAGRAMS"
    FOR I% = 1 TO DATANO% - 1  ' display P-V diagram
      LINE (VOLUME!(I%), PIZ!(I%))-(VOLUME!(I% + 1), PIZ!(I% + 1))
    NEXT I%           'plots PV diagrams
    CLS 2
    PRINT "                          PLEASE WAIT!!!!!"
```

```
PRINT
PRINT    " WRITING OUTPUT FILES TO C:\IAN\CALC\"; RUNNO$; "
         .IPD AND .PVD"

' Calculate area of P-V diagram and find peak pressures
PEAKMAX! = 0: IMEPMAX! = 0: IPMAX! = 0
IMEPMEAN! = 0: WORKMEAN! = 0: PEAKMEAN! = 0: IPMEAN! = 0
IMEPSUM! = 0: WORKSUM! = 0: PEAKSUM! = 0: IPSUM! = 0:
DATACYC% =      0

FOR J% = 1 TO 20
  WORK!(J%) = 0: PEAK!(J%) = 0: IMEP!(J%) = 0: IP!(J%) = 0
NEXT J%

I% = 1
FOR J% = 1 TO NOCYC%
FOR I% = (I% + 1) TO (J% * CYCL%)
  IF 0 <= RADCA!(I%) AND RADCA!(I%) <= PI# THEN SIGN! = .1
  IF PI# < RADCA!(I%) AND RADCA!(I%) <= 2 * PI# THEN SIGN! =
   -.1
  IF 2 * PI# < RADCA!(I%) AND RADCA!(I%) <= 3 * PI# THEN SIGN!
   = .1
  IF 3 * PI# < RADCA!(I%) AND RADCA!(I%) < 4 * PI# THEN SIGN!
   = -.1
  WORK!(J%) = WORK!(J%) + SIGN! * ABS(VOLUME(I%)
   VOLUME(I% - 1)) * (PIZ!(I%) + PIZ(I% - 1)) / 2
  IF PIZ!(I%) > PEAK!(J%) THEN PEAK!(J%) = PIZ!(I%)
  IMEP!(J%) = .00001 * WORK!(J%) / .000507#
  IP!(J%) = .001 * (RPS / 2) * WORK!(J%)
  NEXT I%
NEXT J%

FOR J% = 1 TO NOCYC%
  PEAKSUM! = PEAK!(J%) + PEAKSUM!
  WORKSUM! = WORK!(J%) + WORKSUM!
  IMEPSUM! = IMEP!(J%) + IMEPSUM!
  IPSUM! = IP!(J%) + IPSUM!
NEXT J%

PEAKMEAN! = PEAKSUM! / NOCYC%
WORKMEAN! = WORKSUM! / NOCYC%
IMEPMEAN! = IMEPSUM! / NOCYC%
IPMEAN! = IPSUM / NOCYC%
DATACYC% = CYCL% * NOCYC%
PVNO% = (NOCYC% / 2) * CYCL%
```

```
FOR J% = 1 TO NOCYC%
  IF IMEP!(J%) > IMEPMAX! THEN IMEPMAX! = IMEP!(J%)
  IF IP!(J%) > IPMAX! THEN IPMAX! = IP!(J%)
  IF PEAK!(J%) > PEAKMAX! THEN PEAKMAX! = PEAK!(J%)
NEXT J%

OPEN "C:\IAN\CALC\" + RUNNO$ + ".IPD" FOR OUTPUT AS #2
PRINT #2, "OUTPUT DATA FOR ENGINE TEST "; RUNNO$
PRINT #2, "RPS= "; RPS!
PRINT #2, "IGNITION TIMING = "; BTDC!; "deg BTDC"
PRINT #2, "COMPRESSION RATIO = "; CR!
PRINT #2, "PIEZO CONSTANT (Bar/volt) = "; PCAL!
PRINT #2,

FOR J% = 1 TO NOCYC%
PRINT #2, IMEP!(J%); TAB(12); "IMEP of cycle "; J%
PRINT #2, IP!(J%); TAB(12); "Indicated power of cycle "; J%
PRINT #2, PEAK!(J%); TAB(12); "Peak pressure obtained in cycle "; J%
PRINT #2,
NEXT J%

PRINT #2,
PRINT #2, IMEPMAX!; TAB(12); "Maximum IMEP."
PRINT #2, IMEPMEAN!; TAB(12); "Mean IMEP."
PRINT #2, IPMAX!; TAB(12); "Maximum indicated power."
PRINT #2, IPMEAN!; TAB(12); "Mean indicated power."
PRINT #2, PEAKMAX!; TAB(12); "Maximum peak pressure."
PRINT #2, PEAKMEAN!; TAB(12); "Mean peak pressure."
PRINT #2,
PRINT #2, FSTPNT%; TAB(12); "First ignition data point."
PRINT #2, SECPNT%; TAB(12); "Second ignition data point."
PRINT #2, NOCYC%; TAB(12); "Number of cycles"
PRINT #2, CYCL%; TAB(12); "Cycle length in data points"
PRINT #2, DATACYC%; TAB(12); "Number of data points analysed in
                                cycles."
PRINT #2, DATANO%; TAB(12); "Total number of data points."
CLOSE #2

'write PV data to file(s) and indicate ignition spikes

IF DATANO% > 8000 THEN          'splits data into two files if longer
  IF NOCYC% > 1 THEN             'than 8000 data points
  OPEN "C:\IAN\CALC\" + RUNNO$ + ".PV1" FOR OUTPUT AS #3
  PRINT #3, "FIRST PV DATA FOR ENGINE TEST "; RUNNO$
  PRINT #3, " PRESSURE     VOLUME"
  PRINT #3, "   Bar          cc  "
```

```
      FOR I% = 1 TO PVNO%
            IF I% = FSTPNT% THEN PRINT #3, PIZ!(I%), VOLUME!(I%),
                  PIZ!(I%): GOTO 1000
            IF I% = SECPNT% THEN PRINT #3, PIZ!(I%), VOLUME!(I%),
                  PIZ!(I%): GOTO 1000
            PRINT #3, PIZ!(I%), VOLUME!(I%)
1000    NEXT I%
      CLOSE #3
      OPEN "C:\IAN\CALC\" + RUNNO$ + ".PV2" FOR OUTPUT AS #4
      PRINT #4, "SECOND PV DATA FOR ENGINE TEST "; RUNNO$
      PRINT #4, " PRESSURE       VOLUME"
      PRINT #4, "   Bar            cc  "
      FOR I% = (PVNO% + 1) TO DATACYC%
            IF I% = FSTPNT% THEN PRINT #4, PIZ!(I%), VOLUME!(I%),
                  PIZ!(I%): GOTO 2000
            IF I% = SECPNT% THEN PRINT #4, PIZ!(I%), VOLUME!(I%),
                  PIZ!(I%): GOTO 2000
            PRINT #4, PIZ!(I%), VOLUME!(I%)
2000    NEXT I%
      CLOSE #4

   ELSE OPEN "C:\IAN\CALC\" + RUNNO$ + ".PVD" FOR OUTPUT AS
#5
      PRINT #5, "PV DATA FOR ENGINE TEST "; RUNNO$
      PRINT #5, " PRESSURE       VOLUME"
      PRINT #5, "    Bar            cc  "
      FOR I% = 1 TO DATACYC%
      IF I% = FSTPNT% THEN PRINT #5, PIZ!(I%), VOLUME!(I%),
                           PIZ!(I%): GOTO 3000
      IF I% = SECPNT% THEN PRINT #5, PIZ!(I%), VOLUME!(I%),
                           PIZ!(I%): GOTO 3000
      PRINT #5, PIZ!(I%), VOLUME!(I%)
3000    NEXT I%
      CLOSE #5
   END IF
   END IF

9999

REM $DYNAMIC
   FUNCTION ASIN! (ANG!)
     ASIN! = ATN(ANG! / (SQR(-ANG! * ANG! + 1)))
   END FUNCTION
```

RICPC.BAS

```
'A program written in june 1993 by I.Calvert to analyse the Ricardo engine
'prechamber stratified charge data. The program requests the information
'required and outputs the results to a file under the c:\work\ directory.
'Output includes an analysis of the emission data into a specific output
'format. Also air/fuel ratios are calculated for both the main chamber and
'the prechamber based on the amounts of each constituant induced into
each
'chamber.

    DIM POWER!(1 TO 20), WGTNO!(1 TO 20), CO2!(1 TO 20)
    DIM AIRVOL!(1 TO 20), RPS!(1 TO 20), SPRING!(1 TO 20)
    DIM AIRMAN!(1 TO 20), TEMPCOR!(1 TO 20), AIRMASS!(1 TO 20)
    DIM AIRTEMP!(1 TO 20), CARBFLT!(1 TO 20), INJFLT!(1 TO 20)
    DIM CARBMASS!(1 TO 20), INJMASS!(1 TO 20), LAMMAIN!(1 TO 20)
    DIM LAMPC!(1 TO 20), LAMALL!(1 TO 20), NOX!(1 TO 20), HC!(1 TO
  20)
    DIM CO!(1 TO 20), SFNOX!(1 TO 20), SFHC!(1 TO 20), SFCO!(1 TO
    20)
    DIM INJSTART!(1 TO 20), INJEND!(1 TO 20), APCMASS!(1 TO 20)
    DIM THROTTLE!(1 TO 20), IGNTIME!(1 TO 20), EXTEMP!(1 TO 20)
    DIM AIRFLT!(1 TO 20), INJDURAT!(1 TO 20), CORPWER!(1 TO 20)
    DIM SFC!(1 TO 20), BTE!(1 TO 20), MAPC!(1 TO 20), MFPC!(1 TO
    20)
    DIM MOLFUEL!(1 TO 20), OXYGEN!(1 TO 20), CR!(1 TO 20)

    LCV = 50020        'LCV of methane,kJ/kg
    PI# = 3.141592654#
    CGRADG! = .0125#: CZERO! = .11548#      'kg/hmm
    IGRADG! = .00068181818#: IZERO! = .002580645#      'kg/hmm
    AIRGRAD! = 1.241667#: AIRZERO! = .75       'l/min scale

    SCREEN 0
    CLS
    WIDTH 40, 25
    LOCATE 3, 9
    COLOR 14
    PRINT "RICARDO STRATIFIED CHARGE"
    LOCATE 4, 13
    PRINT "ANALYSIS PROGRAM"
    PRINT : PRINT : COLOR 3
    PRINT " PLEASE ENTER THE DATA REQUESTED BELOW!"
    PRINT : PRINT : PRINT : COLOR 15
    INPUT "1. TEST DATE,(eg 31/5/93)  "; DAT$
    INPUT "2. ATMOSPHERIC PRESSURE,(mmHg)"; PATM!
```

```
    INPUT "3. ENTER THE FILE NAME.       "; FILE$
    INPUT "3. NUMBER OF RUNS. (Max 20)   "; RUNNO!
    IF RUNNO! > 20 THEN
     COLOR 14: PRINT
     PRINT "MAXIMUM NUMBER OF RUNS IS 20."
     INPUT "PLEASE RE-ENTER NUMBER OF RUNS"; RUNNO!
    END IF

    PATP! = (PATM! / 760) * 101.3
    SCREEN 9

    FOR I% = 1 TO RUNNO!
100    CLS
      PRINT "RUN NUMBER "; I%: PRINT
      INPUT "ENGINE SPEED IN RPS.                "; RPS!(I%)
      INPUT "ENTER THE COMPRESSION RATIO,        "; CR!(I%)
      INPUT "ENTER THE THROTTLE SETTING,(0-20)
";THROTTLE!(I%)
      INPUT "AIR MANOMETER LEVEL, mm             "; AIRMAN!(I%)
      INPUT "AIR TEMPERATURE,(Degrees Celcius)   "; AIRTEMP!(I%)
      INPUT "TEMP CORRECTION FACTOR,             "; TEMPCOR!(I%)
      INPUT "GAS CARB FLOAT LEVEL, mm GLASS FLOAT
                          ;CARBFLT!(I%)
      INPUT "INJECTOR FLOAT LEVEL, mm GLASS FLOAT ";
INJFLT!(I%)
      INPUT "PRECHAMBER AIR FLOAT LEVEL,(0-10)   "; AIRFLT!(I%)
      INPUT "NUMBER OF DYNO WEIGHTS,             "; WGTNO!(I%)
      INPUT "SPRING BALANCE READING,             "; SPRING!(I%)
      INPUT "IGNITION TIMING, Degrees CA         "; IGNTIME!(I%)
      INPUT "EXHAUST TEMP (Deg Celcius)          "; EXTEMP!(I%)
      INPUT "NOx LEVEL IN PPM,                   "; NOX!(I%)
      INPUT "CARBON MONOXIDE (CO) LEVEL IN %Vol  "; CO!(I%)
      INPUT "CARBON DIOXIDE (CO2) LEVEL IN %Vol  "; CO2!(I%)
      INPUT "HYDROCARBON LEVEL IN PPM,           "; HC!(I%)
      INPUT "OXYGEN (O2) LEVEL IN %Vol           "; OXYGEN!(I%)
      INPUT "INJECTOR START ANGLE,               "; INJSTART!(I%)
      INPUT "INJECTOR END ANGLE,                 "; INJEND!(I%)
      INPUT "INJECTOR DURATION SETTING (0-1000)  ";
INJDURAT!(I%)
      PRINT : INPUT "ARE THESE ENTRIES CORRECT ?????"; ENTRY$
      IF ENTRY$ = "N" OR ENTRY$ = "n" THEN 100
     NEXT I%

    CLS
    PRINT "                    PLEASE WAIT !!!!!!!!": PRINT
    PRINT "  WRITING OUPUT TO FILES C:\WORK\"; FILE$; " .POW and
```

```
        .INP!!!"

FOR I% = 1 TO RUNNO!
 POWER!(I%) = (((WGTNO!(I%) * 20.15) - SPRING!(I%)) * RPS!(I%))
              /348.1
 CORPWER!(I%) = POWER!(I%) * (101.3 / PATP!) * SQR((273 +
                AIRTEMP!(I%)) / 293)
 AIRVOL!(I%) = .000077 * AIRMAN!(I%) * TEMPCOR!(I%) * 3600
 AIRMASS!(I%) = (AIRVOL!(I%) * PATP) / (.287 * (AIRTEMP!(I%) +
              273))

 IF CARBFLT!(I%) <= 0 THEN       'carburated mass of methane
      CARBMASS!(I%) = 0       'kg/hr
 ELSE CARBMASS!(I%) = CGRADG! * CARBFLT!(I%) + CZERO!
 END IF

 IF INJFLT!(I%) <= 0 THEN        'injected mass of methane
      INJMASS!(I%) = 0        'kg/hr
 ELSE INJMASS!(I%) = IGRADG! * INJFLT!(I%) + IZERO!
 END IF

 IF AIRFLT!(I%) <= 0 THEN        'induced mass of air into PC
       APCMASS!(I%) = 0       'kg/hr
 ELSE APCMASS!(I%) = (AIRGRAD! * AIRFLT!(I%) + AIRZERO!) *
                     .06 * PATP! / (.287 * (AIRTEMP!(I%) + 273))
 END IF

 LAMMAIN!(I%) = (AIRMASS!(I%) / CARBMASS!(I%)) / 17.2

 IF APCMASS!(I%) > 0 THEN
      IF INJMASS!(I%) > 0 THEN
       LAMPC!(I%) = (APCMASS!(I%) / INJMASS!(I%)) / 17.2
      END IF
 END IF

 IF APCMASS!(I%) = 0 THEN
      IF INJMASS!(I%) > 0 THEN
       MAPC!(I%) = .011 * AIRMASS!(I%)
       MFPC!(I%) = .011 * CARBMASS!(I%)
       LAMPC!(I%) = (MAPC!(I%) / (MFPC!(I%) + INJMASS!(I%))) /
                    17.2
      END IF
 END IF

 IF APCMASS!(I%) = 0 THEN
      IF INJMASS!(I%) = 0 THEN
```

```
        LAMPC!(I%) = LAMMAIN!(I%)
       END IF
  END IF

  MOLFUEL!(I%) = CO2!(I%) + CO!(I%) + (HC!(I%) * 6 / 10000)
  LAMALL!(I%) = ((AIRMASS!(I%) + APCMASS!(I%)) /
                (CARBMASS!(I%) + INJMASS!(I%))) / 17.2
  SFC!(I%) = (CARBMASS!(I%) + INJMASS!(I%)) / POWER!(I%)
  BTE!(I%) = 100 * (3600 * POWER!(I%)) / ((CARBMASS!(I%) +
                INJMASS!(I%)) * LCV!)
  SFCO!(I%) = CO!(I%) * 28000 * SFC!(I%) / (MOLFUEL!(I%) * 16)
  SFNOX!(I%) = NOX!(I%) * 30000 * SFC!(I%) / (MOLFUEL!(I%) *
                160000)
  SFHC!(I%) = HC!(I%) * 96000 * SFC!(I%) / (MOLFUEL!(I%) * 160000)
NEXT I%

OPEN "C:\IAN\POW\" + FILE$ + ".INP" FOR OUTPUT AS #1
PRINT #1, "INPUT DATA FOR FILE "; FILE$
PRINT #1, "DATE "; DAT$
PRINT #1, "ATMOSPHERIC PRESSURE "; PATP!; " (kPa)"
PRINT #1, "NUMBER OF DATA RUNS"; RUNNO!
PRINT #1, "COMPRESSION RATIO"; CR!(1)
PRINT #1, "ENGINE SPEED"; RPS!(1); " RPS"
PRINT #1,
PRINT #1, "RUN  RPS  THROT  AIRTEMP  AIRMAN  CARB  INJ
        PCAIR  DYNO  SPRING  IGN"
PRINT #1, " No      0-20     C       mm     mm     mm   1-10  No
         N   Deg CA"
PRINT #1,
FOR I% = 1 TO RUNNO!
  PRINT #1,     I%; TAB(6); RPS!(I%); TAB(13); THROTTLE!(I%);
                TAB(22); AIRTEMP!(I%); TAB(32); AIRMAN!(I%);
                TAB(39); CARBFLT!(I%); TAB(47); INJFLT!(I%);
                TAB(54); AIRFLT!(I%); TAB(60); WGTNO!(I%);
                TAB(67); SPRING!(I%); TAB(75); IGNTIME!(I%)
NEXT I%
PRINT #1,
PRINT #1,
PRINT #1, "RUN  EXTEMP   NOx   CO2   CO   HC   O2   INJST
        INJEND  INJSET"
PRINT #1, " No   C      ppm    %Vol  %Vol  ppm  %Vol  BTDC
        BTDC   0-1000"
PRINT #1,
FOR I% = 1 TO RUNNO!
  PRINT #1,     I%; TAB(6); EXTEMP!(I%); TAB(15); NOX!(I%);
                TAB(22); CO2!(I%); TAB(29); CO!(I%); TAB(35);
```

```
                HC!(I%); TAB(41); OXYGEN!(I%); TAB(50);
                INJSTART!(I%); TAB(59); INJEND!(I%); TAB(65);
                INJDURAT!(I%)
NEXT I%

CLOSE #1

OPEN "C:\IAN\POW\" + FILE$ + ".POW" FOR OUTPUT AS #2
PRINT #2, "OUTPUT DATA FILE "; FILE$
PRINT #2, "DATE "; DAT$
PRINT #2, "ATMOSPHERIC PRESSURE "; PATP; " (kPa)"
PRINT #2, "NUMBER OF DATA RUNS "; RUNNO!
PRINT #2, "COMPRESSION RATIO "; CR!(1)
PRINT #2, "ENGINE SPEED "; RPS!(1); " RPS"
PRINT #2,
PRINT #2, "RUN  POWER     CORRECTED     SFC          BTE
          FUEL MASS       FUEL MASS"
PRINT #2, "No    kW          kW          kg/kWh        %          CARB
          kg/hr      INJ kg/hr"
PRINT #2,

FOR I% = 1 TO RUNNO!
  PRINT #2, I%; POWER!(I%), CORPWER!(I%), SFC!(I%), BTE!(I%),
                CARBMASS!(I%), INJMASS!(I%)
NEXT I%
PRINT #2,
PRINT #2,
PRINT #2, "RUN  LAMBDA    LAMBDA        LAMBDA        SNO
           SCO          SHC"
PRINT #2, " No    ALL       PC           MAIN          g/kWh          g/kWh
          g/kWh"
PRINT #2,
FOR I% = 1 TO RUNNO!
  PRINT #2, I%; LAMALL!(I%), LAMPC!(I%), LAMMAIN!(I%),
          SFNOX!(I%), SFCO!(I%), SFHC!(I%)
NEXT I%

CLOSE #2
```

APPENDIX 2

NOx METER, GAS SYSTEM OPERATING INSTRUCTIONS.

The following pages are a listing of the Operating Instructions for the gas supply system developed for use with the Beckman 951A NO/NOx analyser, when being used in a portable mode.

INSTRUCTIONS FOR THE USE OF THE NOx GAS SYSTEM

1. Connect sample hose to both the pump inlet and the sample point connections. NOTE: the pump requires 240Vac and the analyzer requires 110Vac.

2. Connect the exhaust hose to the exhaust outlet and place the other end in a well ventilated area, preferably outside. If in the Ricardo test cell 1, connect to outlet below fan.

3. Start up NOx meter as per Beckman operating instructions.

4. Oxygen flow to the analyzer is automatic when the oxygen supply pressure is set at 40 PSIG.

5. To set zero gas flow to the analyzer, turn right valve to the **ZERO** position and the left valve to **SAMPLE**. Set the sample regulator to approximately 12-13 PSIG, as this will supply a sufficient quantity of gas to the analyzer. Do not change the regulator outlet pressure for either the zero gas or sample gas to be analyzed as this will vary the mass flow rate and will give erroneous results.

6. To set span gas flow set the left valve to **SPAN** and adjust the span gas regulator to the same pressure as the sample regulator.

7. To analyze sample gas set both valves to **SAMPLE** and ensure pressure to analyzer is the same as that for the zero and span gases.

APPENDIX 3

EQUATIONS OF STATE FOR ACCURATE GAS MIXTURES

The most desirable means of mixing accurate gas mixtures would be on a mass basis. For this work a set of scales with the required accuracy was not available. Therefore the method of partial pressures was employed to produce the mixtures. Accurate knowledge of the mixture composition requires a good understanding of the state of the mixture. There are a vast number of equations of state of varying accuracy and application which describe the behaviour of real gases.

Ideal gas behaviour.

A first approximation of the behaviour of gases can be obtained from the ideal gas equation;

$$PV = nRT$$

where; n = Number of moles,

R = universal gas constant.

This equation is based upon two major assumptions.

-The molecules/atoms occupying the space are point masses,

-There are no intermolecular forces between the molecules/atoms.

These assumptions brake down as the pressure is increased and/or the specific volume decreases. Hence the equations application is prone to error.

Van der Waals equation of state.

An attempt to account for these assumptions within the ideal gas equation is given in the Van der Waals equation;

$$\left(P + \frac{a}{v^2}\right)(v - b) = RT$$

The term a/v^2 takes into account the intermolecular forces between the molecule/atoms, and the (v-b) term considers the volume occupied by the molecules/atoms. The Van der Waals equations allows a more accurate approximation of the state of the gas composition and was used throughout the mixture preparation of the span gas for the NOx analyser. Equations with increased accuracy are available for use, but a lack of data for the constants within these equations for nitric oxide (NO) prevented their use.

Calculation procedure.

As mentioned earlier the final mixture was prepared using the method of partial pressures utilising the Van der Waals equation of state. Before this

could be utilised to calculate the partial pressures of the mixture, an indication of the number of moles required for an approximate final filling pressure was needed.

The required gas composition was known (in ppm) and an approximate final filling pressure of 20bar was selected. (This was the linear limit of the pressure transducer used in the mixing process.) Application of the ideal gas equation to the partial pressure equation gave the number of moles of nitric oxide and nitrogen required. These values were then re-applied to the partial pressure equation, but utilising the Van der Waals equation to calculate the final filling pressure of the mixture and hence the partial pressures of each constituent. These equations were used in a spread sheet to calculate the partial pressures for a range of temperatures that were experience within the laboratory.

The constants for both nitric oxide and nitrogen are listed below.(**REFhsieh)**

$a_{NO} = 1.438$ $\{(litres)^2(atm)/(mole)^2\}$

$b_{NO} = 0.02885$ {litres/mole}

$a_{Nitrogen} = 1.438$ $\{(litres)^2(atm)/(mole)^2\}$

$b_{Nitrogen} = 0.03864$ {litres/mole}

$R = 0.08205$ {(atm)(litre)/(mole)(K)}

APPENDIX 4

NO/N_2 GAS MIXTURE PREPARATION PROCEDURE

The following pages give a listing of the procedure for the mixing of Nitric Oxide/Nitrogen mixtures for use with the Beckman 951A NO/NOx analyser.

OPERATING PROCEDURE FOR THE MIXING

OF NITRIC OXIDE/NITROGEN MIXTURES

CAUTION!!!: Nitric Oxide in the presence of air quickly forms Nitrogen dioxide, a brown gas which is **HIGHLY TOXIC!!!!** Extreme caution and care must be used when preparing Nitric Oxide mixtures.

EQUIPMENT.

The following equipment is necessary for the preparation of the mixtures:

1, NOx mixture panel.

2, 1x cylinder of 99.0% Nitric oxide and connection adaptor.

3, 2x NZIG D size cylinders for the mixture storage.

4, 1x cylinder of Dry Nitrogen, preferably Oxygen Free Grade.

5, 1x Matherson 3500 regulator and adaptor.

6, 1x Victor SR4F high pressure regulator (0-60 bar output).

7, 1x digital thermometer.

8, 1x SS flexible hose with swagelok connections.

9, 1x filling adaptor.

10, Pressure transducer and data acquisition system from combustion rig.

11, Vacuum pump and connecting hose.

PROCEDURE.††††

1. Gas mixtures are to be prepared in the boiler house utilising the data acquisition system on the combustion rig to measure the cylinder pressure.

2. Open boiler house roller door and all doors into the boiler house to provide sufficient ventilation. The vacuum pump must be placed as far as possible from the filling area, preferably outside the roller door.

3. In an open area blow down the contents of the mixture cylinder to be filled.

4. Connect filling hose, vacuum line, pressure transducer, Nitric oxide line and Nitrogen line to their appropriate connections on the mixture panel. Connect the filling hose to the cylinder to be filled with the vent valve at the cylinder end of the hose. Place the vent hose outside the boiler hose door. Also connect the digital thermometer.

---

†††† All filling pressures stated are absolute and given in bar unless otherwise stated.

5. Switch on the pressure transducer and the associated PC and enter the pressure program "PTMIX". Set the gain to 50 and the number of samples to 2000. Switch on digital thermometer.

6. Open nitrogen cylinder valve, set the regulator to 25 bar, then open the panel Nitrogen valve 1/2 a turn and vent valve, and allow nitrogen to purge the mixture panel for a few seconds, then close the nitrogen panel valve. Leave the vent valve open.

7. Open the Nitric Oxide cylinder valve and set the regulator pressure to 20psig. Briefly open the regulator valve and metering valve to purge the NO regulator. Close the regulator valve THEN the metering valve.

8. Open the Nitrogen panel valve and vent the filling system. Close the Nitrogen valve then the vent valve.

9. Switch vacuum pump on. Open the vacuum valve and evacuate the mixture panel.

10. Open the mixture cylinder valve and evacuate the cylinder to -100kPa. Read vacuum off vacuum gauge as the pressure transducer output in this range is non-linear. Close vacuum valve .

11. Open the nitrogen valve and break the vacuum (ie to atmospheric). Close the Nitrogen valve and open the vacuum valve and evacuate the mixture cylinder again to -100kPa gauge. Close the vacuum valve.

12. Open the nitrogen valve and break the vacuum until cylinder pressure is approximately 2 bar absolute.(Read pressure off transducer output). Close nitrogen valve.

13. Allow temperature and pressure to stabilise (approximately 10 mins). Note the pressure and temperature. From the tables determine the partial pressure of NO to be added for the relevant ambient temperature. Check the metering valve is closed and open the NO regulator valve 1/2 a turn.

14. Open the metering valve a full turn and note the rate of pressure increase. Adjust the metering valve accordingly to obtain an accurate pressure reading without quickly overshooting the target pressure. When approaching the target pressure close the metering valve and allow the pressure to stabilise. NOTE: if the settled target pressure is significantly overshot then the cylinder must be blown down and evacuated and the filing process restarted.

15. Open and close the metering valve until the required settled partial

pressure is obtained, then close the metering valve and regulator valve.

16. Open the Nitrogen fill valve a full turn and allow cylinder to approach the target pressure. Close the Nitrogen valve. NOTE: the Nitrogen target pressures given are the final absolute filling pressures of the mixture and not the partial pressure of the Nitrogen.

17. Allow the cylinder pressure and temperature to stabilise before topping up to obtain the settled target pressure.

18. Once the settled target pressure is obtained then close the mixture cylinder valve and open the vent valve.

19. Close the Nitric oxide cylinder valve and open the metering and regulator valves and allow pressure in regulator to dissipate. Reset the regulator then close the regulator valve.

20. Close the Nitrogen cylinder valve and open the nitrogen panel valve and allow nitrogen pressure to dissipate. Reset the regulator and close the nitrogen fill valve and the NO metering valve.

21. Disconnect the filling hose from the mixture cylinder. The mixture is

now ready for use.

22. Disconnect the nitrogen and Nitric oxide cylinders from the filling panel. Switch the vacuum pump off and disconnect. Turn off computer and disconnect pressure transducer from filling panel.